CHARACTERIZATION OF SOLID DISPERSIONS OF HYDROXYPROPYL CELLULOSE FILMS WITH GRISEOFULVIN VIA HOT-MELT EXTRUSION

By

Marianela Cora Laó

A thesis submitted in partial fulfillment of the requirements for the degree of

MASTER OF SCIENCE
in
CHEMICAL ENGINEERING

UNIVERSITY OF PUERTO RICO
MAYAGÜEZ CAMPUS
2012

Approved by:

_____	_____
Aldo Acevedo-Rullan, PhD President, Graduate Committee	Date
_____	_____
Carlos Rinaldi, PhD Member, Graduate Committee	Date
_____	_____
Rafael Mendez, PhD Member, Graduate Committee	Date
_____	_____
Mercedes Ferrer, PhD Representative of Graduate Studies	Date
_____	_____
Aldo Acevedo, PhD Chairperson of the Department	Date

ABSTRACT

Hot-melt extrusion has gained significance in the pharmaceutical industry to formulate solid dispersions. In a solid dispersion, poorly-water soluble drugs can be dispersed in an inert hydrophilic polymer matrix, improving the stability and bioavailability of the drug. In this work, solid dispersions of hydroxypropyl cellulose (HPC) and griseofulvin were formulated *via* this method and the effects of HPC molecular weight, type of plasticizer, griseofulvin concentration, and processing temperature on the thermal, mechanical and rheological properties was evaluated.

Films showed Young's moduli in the following ascending order: glycerol, d-dorbitol, and PEG, which shows a proportional relationship to plasticizer miscibility. On the other hand, griseofulvin loading has a plasticizing effect in Young's moduli. Griseofulvin loading also showed a plasticizing effect in melting peak temperature, except at certain concentrations when glycerol and d-sorbitol are used as plasticizers. This deviation can be attributed to stronger intra molecular interactions of griseofulvin with glycerol and d-sorbitol as demonstrated by calculated strengths of interaction parameters. In addition, melt viscosity demonstrated that griseofulvin has a plasticizing effect in HPC, decreasing melt viscosity by one order of magnitude with the addition of 0.20 volume fraction. Once a plasticizer is added to the solid dispersion, griseofulvin has an antiplasticizing effect, i.e. melt viscosity increases.

Flory-Huggins solubility parameters indicate partial miscibility, of lower molecular weight additives in HPC and, therefore, have better plasticizing effects, including griseofulvin. But once a third component, such as a plasticizer, is added to a solid dispersion the properties depend of the concentrations, miscibility, and molecular interactions of the specific components of the formulation. Calculation of the solubility and interaction

parameters can be used as *a priori* method to screen for suitable solid dispersion formulations.

RESUMEN

Extrusión de fundido en caliente ha ganado auge en la industria farmacéutica para la formulación de dispersiones solidas. Una dispersión solida es un sistema en el cual una droga poco soluble en agua se dispersa en una matriz polimérica inerte e hidrofílica, resultando en mejor estabilidad y biodisponibilidad de la droga. En este trabajo, se formularon dispersiones sólidas de hidróxipropil celulosa (HPC) y griseofulvin mediante este método y se evaluaron los efectos de peso molecular del HPC, tipo de plastificante, concentración de griseofulvin y temperatura de procesamiento en las propiedades termales, mecánicas y reológicas.

Las dispersiones solidas mostraron valores de módulo de Young en el siguiente orden ascendente: glicerol, d-sorbitol y PEG, lo cual indica una relación proporcional a la miscibilidad del plastificante en HPC. Por otro lado, se determinó que la adición de griseofulvin tiene un efecto plastificante en el módulo de Young. La adición de griseofulvin también mostro un efecto plastificante en la temperatura de fusión, excepto a ciertas concentraciones cuando glicerina y sorbitol se utilizan como plastificantes. Esta desviación se le puede atribuir a fuerzas intermoleculares más fuertes de griseofulvin con glicerina y sorbitol según lo indican las fuerzas de interacción calculadas. En adición, las medidas de viscosidad probaron que el griseofulvin tiene un efecto plastificante en HPC, disminuyendo la viscosidad por un orden de magnitud al añadir una fracción volumétrica de 0.2 griseofulvin. Al incorporar plastificante a las dispersiones sólidas griseofulvin tiene un afecto antiplastificante, i.e. viscosidad aumenta.

Los parámetros de solubilidad de Flory-Huggins calculados, indican miscibilidad parcial de los aditivos de menor peso molecular en HPC, por tal razón tienen mejores efectos

plastificantes, incluyendo griseofulvin. En general, las propiedades mecánicas, termales y reológicas de una dispersión sólida van a depender de las concentraciones, miscibilidad e interacciones moleculares de los componentes específicos de la formulación. Cálculo de los parámetros de solubilidad e interacción pueden ser utilizados como un método *a priori* para la exanimación de formulaciones adecuadas de dispersiones sólidas.

Acknowledgements

First of all I want to thank Good for giving me the health and strength to pursue my professional goals. I also want to thank my family for always being there for me and giving me their support and advice. INDUNIV for providing the funds for the project. I appreciate the collaboration of my undergrad student Luis Colón and Dr. Barbara Calcagno for providing guidance and validating the extensional tests. Finally, I want to thank my advisor doctor Aldo Acevedo, the institution, and the Chemical Engineering faculty for providing me all the knowledge, guidance, and tools needed to conclude this work.

Table of Contents

Figure List

Figures **Page**

Table List

Tables **Page**

1 INTRODUCTION

Hot-melt extrusion processes have numerous applications. Extrusion can be simply defined as the process of forming a new material (the extrudate) by forcing it through an orifice or die under controlled conditions, such as temperature, mixing, feed-rate and pressure [1]. In this specific case it will be used to produce films with drug delivery purposes. Over the last decade interest in hot-melt extrusion with pharmaceutical applications has increased with over more than 100 papers being published [2]. Previous studies have demonstrated that hot-melt extrusion can be used as a formulation method for poorly soluble drugs, increasing their bioavailability because of increased wettability. In addition, hot-melt extrusion has advantages over traditional formulation methods, making it appealing in the pharmaceutical industry. Some of those advantages include: efficient manufacturing process that may enhance the quality and efficacy of manufactured products, solvents are not required, which makes the process more environmentally friendly and cost effective; fewer unit batch operations are required than in traditional methods; and improved content uniformity because intense mixing and agitation can be achieved [1]. But more importantly, the polymeric components used in the extrusion process may function as thermal binders, drug stabilizers, drug solubilizers and/or drug release controlling excipients with no compressibility requirements resulting in the formation of solid dispersions or solid solutions, enhancing drug dissolution rate *in vivo* [1]. These characteristics make hot-melt extrusion an appealing method for delivery of poorly water soluble drugs.

Thin films of hydroxypropyl cellulose will be produced via hot-melt extrusion under various conditions and the poorly soluble model drug that will be used for this purpose is griseofulvin. In this project the variables that will be considered are HPC molecular weight,

plasticizer type, griseofulvin concentration, and processing temperature. Several levels for each variable will be used and their effects on viscosity, thermal and mechanical properties will be evaluated using the techniques discussed in Chapter 4. The effect of drug loading changes on the thermophysical and rheological parameters of formulations have been analyzed by Chokshi [3]. In their work, the Cross model was used to quantify the shear thinning effect of their melt. Using different molecular weights of the same polymer and different plasticizers will also affect the thermal, rheological and mechanical properties of the films as has been reported [4].

In the following chapters previous research on the subject and theoretical background are explained in more details.

1.1 Motivation

Thin films for drug delivery devices and wound care applications are frequently produced utilizing cast films but this requires long processing times and high costs. It has been demonstrated that thermally stable drugs, could be hot-melted extrude into pellets or other forms without significant drug degradation [4]. It is known that drugs that have poor water solubility have restricted absorption and dissolution rates. For improvement of solubility and dissolution rate of poorly soluble drugs, numerous commercially viable techniques have been proposed [5]. Solid dispersion is the most promising method to formulators because of its ease of preparation, ease of optimization, and reproducibility [5]. In a solid dispersion a poorly soluble drug is dispersed in an inert hydrophilic polymer or matrix by melting, solution formation, or solvent melting to yield solid dispersion. Melt-extrusion could be a new continuous formulation process for the production of tablets, granules, implants, pellets or films. Thus, it is desired to have a

better understanding of different processing and formulation parameters on the mechanical, thermal, and rheological properties of solid dispersions.

During the last 5 years, there has been a significant increase in the use of hot-melt extrusion for the manufacture of drug delivery systems and molecular solid dispersions. Nifedipine, nimodipine and itraconazole have been successfully produced by this method [1]. There are several companies that specialize in the use of hot-melt extrusion as a drug delivery technology including PharmaForm (TX, USA) and SOLIQS (Germany) [1].

1.2 Literature Review

Poor bioavailability of lipophilic drugs meant to be used via oral administration is a problem that the pharmaceutical industry is actually facing. The solubility, and therefore bioavailability, of a drug varies with the physicochemical properties of the drug itself, as well as the method of preparing the pharmaceutical formulation [6]. In the last few years, new formulation methods for poorly soluble drugs have been developed in order to improve bioavailability. Some of the formulation methods to improve bioavailability that have been suggested include techniques such as liquisolid, in which a drug in solution state or dissolved is adsorbed over insoluble carriers; nanomorph, a patented technology for controlled crystallization of drug; and, coprecipitation using antisolvent [5]. Surfactants can also be used in formulations to improve wettability and solubility of many lipophilic substances [5]. Others have attempted to increase the surface area of a compound, either by spraying the amorphous compound onto an inert carrier or by micronizing the compound [7]. Some other methods include salt formation, pH adjustment, complexation, prodrug, nanomization, preparation of liposome, and formation of

solid solutions or solid dispersions (SD) [8]. The difference between a solid solution and a solid dispersion is that in a solid solution the drug is characterized by the lack of a melting point peak at the melting point of the drug indicating the absence of the solid state of the drug. The amount of drug present in the form of a solid state solution to the amount present as a solid dispersion can be determined by the use of thermal analysis techniques, such as differential scanning calorimetry (DSC), thermal gravimetric analysis (TGA), and differential scanning microcalorimetry [9]. The crystallinity of the drug can be determined by x-ray diffraction. All of the afore mentioned techniques still require to dissolve the drug either in amorphous or in crystalline form.

Of all the available formulation techniques, solid dispersion is one of the most promising methods to formulators because of its ease of preparation, ease of optimization, and reproducibility. Solid dispersions have been extensively used because they are a viable and economic method to enhance bioavailability of poorly water soluble drugs and it also overcomes the limitations of other approaches [8]. The term solid dispersion is used to describe any system in which the lipophilic compound is dispersed within or in an inert carrier in solid state. The formulation method for solid dispersions encompasses a poorly soluble drug to be dispersed usually in an inert hydrophilic polymer by melting, solution formation, or solvent melting.

Previous studies have demonstrated that hydrophilic polymer/drug solid dispersions increase drug dissolution [5]. It is known that drugs that have poor water solubility restrict absorption and dissolution rates [5]. Thus, the bioavailability of a drug can be improved by increasing the solubility and dissolution rate of the drug. A possible explanation for the increase in dissolution is that usually in solid dispersions, the drug is partially dissolved in melted or dissolved polymer. After drying of these solid dispersions, the drug will not nucleate to form

firm crystals resulting in formation of microcrystals [5]. It has been proved that the transformation of crystalline drug to amorphous state upon solid solution formulation increases the dissolution rate, since no lattice structure has to be broken down for dissolution to take place [8]. Thus, the drug microcrystals that are embedded in the water-soluble matrix, where hydrophilic polymers present the ability of rapid wetting, will present higher dissolution rates than the original drug crystal in solid dispersions [5]. The overall mechanisms involved in improving bioavailability include increased wettability, solubilization of drug by carrier at diffusion layer and reduction or absence of aggregation and agglomeration. The bioavailability of the drug will be increased if there is an easy and rapid dispersibility in aqueous dissolution fluids.

The polymer used as matrix is supposed to hold the drug in intimate contact with water because of its water retention potential and increase its wettability [5]. Therefore, the polymers used for these applications need to be water soluble low melting point polymer capable of forming a solid dispersion of a poorly soluble drug. Some polymers that have the required qualities to form solid dispersions and increase bioavailability include polyvinylpyrrolidone, copolymers of vinyl acetate/vinylpyrrolidone, methylcellulose, hydroxypropyl cellulose, hydroxypropyl methylcellulose, acetate succianate, polyethylene oxide, polyethylene glycol, and cyclodextrin among others [6]. In some cases, it is necessary to add other excipients such as: flavoring agents, coloring agents, taste-masking agents, pH-adjusting agents, buffering agents, preservatives, stabilizing agents, anti-oxidants, wetting agents, humidity-adjusting agents, surface active agents, suspending agents, absorption enhancing agents, or agents for modified release [6]. Previous studies have demonstrated that polymers, such as polyvinylpyrrolidone (PVP), mannitol, or polyethylene glycols (PEGs) show superior results in drug dissolution

enhancement, but the amount of polymer required is relatively large, around 1:2 to 1:8 drug/polymer ratio [5]. In a solid dispersion, the poor soluble drug must be maintained substantially as a molecular dispersion or in amorphous form during storage, transportation and commercial distribution of the composition containing the solid dispersion of the solubility-enhancing polymer and poorly soluble drug [6]. Researchers have observed that in some cases PVP and PEG get dissolved first in dissolution media due to their high water solubility, leaving the drug back in undissolved state [5]. In such case, the drug is in a controlled crystallization state or amorphous state. Thus, the polymers are unable to provide wetting ability to the drug particles. There is the possibility that there is a rapid reversion of amorphous drug to the more stable crystalline state in presence of small amounts of plasticizers, such as water [5]. On the other hand, solid dispersions of hydrophilic swellable polymers, such as CMC and HPMC, become gelatinized in the dissolution medium. Being water retentive, gelled dispersions also increase wetting of the drug, which increases dissolution. However, the gelled dispersion can act as a barrier for drug diffusion, due to its viscosity [5]. Overall, it has been extensively proven that dispersed drug particles that are surrounded by a matrix core of a water soluble polymer, such as HPMC and by amphiphilic additives, have a better wetting of the drug particles by the dissolution medium [10].

As mentioned before, one of the determining factors for the bioavailability of a drug is the dissolution rate. The dissolution energy of the drug, is given by the sum of the sublimation energy, of the transfer energy, of the sublimated molecules into free volumes formed in the solvent, and eventually of the solvation energy, as shown in Figure 1.1 [11]. For poorly soluble drugs, the dissolution energy is rather low. The energies of the alternative routes, however, are significantly higher.

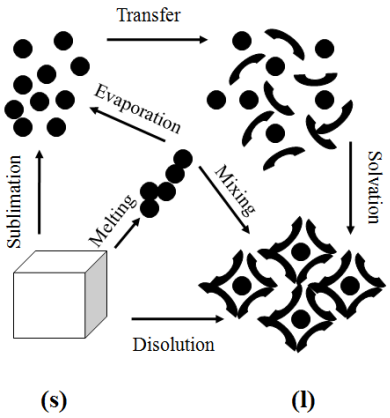

Figure 1:1: Paths that describe dissolution process [11].

It has been demonstrated that when a polymer is in the rubbery state, diffusion of small molecules within the polymer and, hence, recrystallization is possible, under such conditions the polymer would not be able to form stable solid solutions [11]. Researchers believe that the improvement in solubility of griseofulvin observed with solid dispersions in PEG 6000 is due to an improvement of the solvent properties of water by the presence of PEG 6000 [11]. The solubilities obtained in previous studies with griseofulvin and PEG 6000 in aqueous solutions are as shown in Figure 1.2.

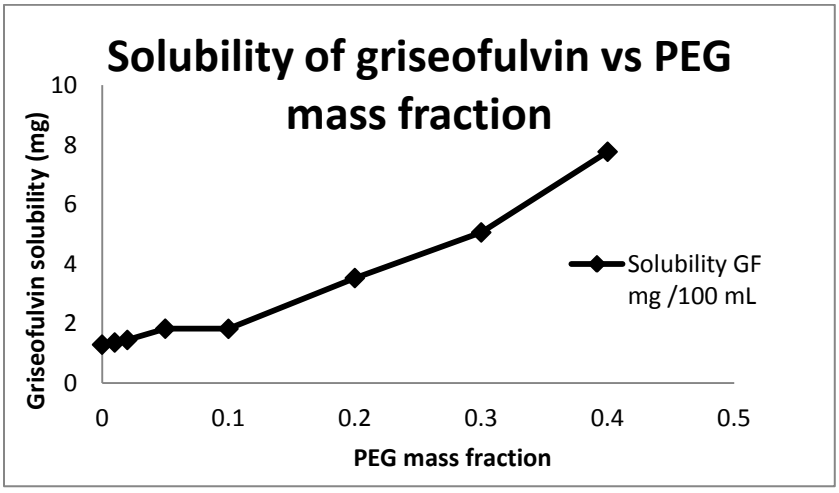

Figure 1:2: Solubility of griseofulvin (GF) in aqueous solutions containing various amounts of PEG 6000 at T = 22 °C [11].

One of the theories of the dissolution mechanism of griseofulvin in PEG is that some of the poly(ethane-1,2-diol) chains are able to solvate griseofulvin [11]. In the same study, researchers observed that the improvement in solubility increases with decreasing PEG molar mass. When solid dispersions of PEG 6000 and griseofulvin are dissolved in water, the water solubility of griseofulvin increases [11]. The increased dissolution is attributed to the formation of solid solutions of griseofulvin in PEG. It is possible for small molecules, such as griseofulvin, to diffuse in PEG of molar weights with glass transition temperatures below room temperature. Thus, solid solutions of griseofulvin in low molecular weight PEG are not stable. Solid dispersions that are prepared by dissolving griseofulvin in a melt of PEG 6000 and were cooled to liquid nitrogen temperatures contain fine crystals [11]. The crystals that are formed are smaller than the crystals used for the preparation of mixtures of griseofulvin with PEG 6000, therefore the dissolution rate of the solid dispersion is higher [11].

The rheological properties of a polymer/drug solid dispersion are important for selecting the processing conditions [12]. It has been observed that the presence and the distribution of the fillers greatly affect the viscoelasticity of a polymer matrix [13]. The rheological properties of polymer composites filled with particles strongly depend, on one hand, on the morphology of these particles, and on the other hand, on the character of their interaction with the polymer. Neither factor can be regarded as independent, since the morphology of particles substantially affects the accessibility of functional groups interacting with the matrix macromolecules. An understanding of the rheological characteristics of filled polymer systems is beneficial to the design of polymer processing equipment, with the ability for predicting the energy requirement, optimizing the processing conditions, and correlating to its structural development. In polymer processing, the properties of the end products are dependent not only on the materials used, but

also on the design of the processing equipment, such as the geometry of the screw and die in an extruder [14]. In rheological studies of fluid polymeric materials, extrusion experiments have been used extensively for the measurement of flow properties, such as the apparent viscosity and flow curves. The most common technique used to study rheological properties of polymer melts is capillary rheometry [15]. In capillary flow, the melt not only experiences shear, but also elongational deformation, when it flows through a restricted die (i.e., converging flow) [16]. Thus, rheological measurements in a capillary rheometer provide shear information of a polymeric melt. In the case of hot-melt extruded hydroxypropyl cellulose films, researchers have reported a large increase in percent of elongation when testing the films in a direction perpendicular to flow versus parallel to flow [4]. Due to geometrical constraints and force interactions with the wall, the material adjacent to the wall behaves differently from those in the bulk. During capillary extrusion of molten polymers, shearing takes place throughout the extrudate with a distribution of velocities and it is generally assumed that there is no slip at the capillary wall. In a capillary extrusion, the quantities actually measured are the extrusion pressure and the screw velocity.

The extrusion pressure P, is the pressure drop in the capillary P_{cap} plus the pressure drop at the entrance to the capillary P_{ent}, with the assumption of neglecting the exit pressure drop. When the polymer flow is forced to enter a capillary from a larger diameter barrel as observed in Figure 1.3, the velocity profile starts to develop and continues to change until the flow is fully developed. The finite length of the capillary required for attaining a fully developed flow profile is called “entrance length” and its magnitude depends on the velocity of the flow, the diameter of the capillary and the barrel, and the flow properties of the materials, including the elastic and viscous properties [16].

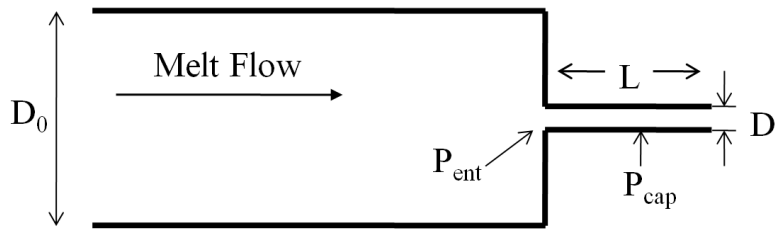

Figure 1:3: Schematic illustration of a capillary extrusion apparatus.

When deriving equations it is assumed that the flow of the material is fully developed throughout the capillary and that the pressure gradient is linear along the capillary extrusion axis. Generally, the feed barrel has a significantly larger diameter than the capillary. This is necessary to produce high flow velocities in the capillaries. Consequently, the material passes through the barrel at a relatively low velocity until it approaches the final capillary velocity. This change in flow velocity can result in an increased pressure gradient over this entrance region. In his work of 1957 Bagley considered that this large pressure drop at the entrance might be treated as an effect of an imaginary extension to the actual capillary length, which is generally called "Bagley's end correction" [12].

Another important factor that needs to be considered when determining the size and quality of the extrudate products is the die or extrudate swell. The extrudate swell can be used to assess the elasticity of the polymer upon melt extrusion. The mechanism and degree of swelling of the extrudate are usually explained in terms of elastic recovery or effect of applied residence time. During a converging flow through a die, polymer molecules tend to uncoil. The entanglements will, to some extent, prevent the molecules from slipping past one another, thus preventing total relaxation of the molecules. At the die exit, recoiling of the molecules occurs to some extent, causing the extrudate to swell [13].

In the past rheological measurements of HPC/water have been reported. Bu and Russo obtained shear viscosities of 60, 300, and 1000 kDa HPC in a cone-and-plate rheometer at shear rates of 2 to 40 Hz for 4.53 and 10.7 g/L solutions [17]. Shear thinning was negligible under these conditions. Phillies and Quinlan used capillary viscometry to measure the solution viscosities up to 3 x 10^5 cP for 300, 1000, and 1,150 kDa HPC samples [17]. The molecular weight and concentrations used on this study were too small for entanglement-based viscoelasticity [17]. In the other hand, Paradkar and coworkers capillary rheometer measurements for 65, 131, and 171 kDa HPC showed shear thinning behavior, with viscosities in the range of 10 to 10,000 Pa s at 140 to 150 °C [18].

It has been reported that the mechanical properties of hydroxypropyl cellulose films are dependent on the plasticizer/polymer composition of the extruded film [19]. Without the use of a plasticizing additive, HPC could not be processed into a film due to excessive stress that was placed on the material during processing [19]. Other papers reported that when polyethylene glycol is used as the plasticizer and the melting point is greatly exceeded, the mechanical properties of the PEG are altered. Repka and coworkers have reported that the percent elongation was lower for a PEG 8000 than a PEG 400 [4]. These findings are consistent with those of Heinamaki and co-workers, who found that ductility (percent elongation) was mainly attributed to the molecular weight of the plasticizer. In a hot-melt extrusion process, polymers are subjected to both thermal and shearing stresses. The temperature can contribute to depolymerization of polymer chains, whereas chain scission may result from shearing effects of the screw [20]. Tensile strengths reported by Repka for HME 1,150 kDa HPC films with 5 wt% PEG are of 14.6 and 9.76 MPa for 1,150 depending upon relative humidity [4]. Increasing the temperature is the

most common practice to facilitate a polymer extrusion process in the plastic industry. Melt viscosity decreases exponentially with respect to an increase in temperature [19].

Researchers such as Mididoddi formulated solid dispersion of HPC-PEO-ketoconazole (T_m = 146 °C) via hot-melt extrusion at processing temperatures of 150 to 160 °C, and determined thermal, and bioadhesive properties. They found that the melting temperature of the films decreased with drug loading and showed good adhesion to the human nail [21]. On the other hand, Repka and coworkers have formulated solid dispersion of HPC-lidocaine (T_m = 69 °C) via hot-melt extrusion at processing temperatures of 140 to 156 °C, and determined thermal properties and drug release mechanisms. In this case a decrease in melting temperature of hot-melt extruded films is also observed and films showed a diffusion drug release mechanism [22].

1.3 Hot-melt Extrusion for Pharmaceutical Applications

Hot-melt extrusion (HME) had its origins in the polymer and plastic industry and has been used in industrial applications for many years. The production of thin films is one of the most prominent examples but it has also found numerous applications in the pharmaceutical industry. Using melt extrusion, various dosage forms can be manufactured, ranging from pellets, to granules and tablets, such as sustained release tablets and transdermal drug delivery systems [21]. Compared to other pharmaceutical production processes, hot-melt extrusion has the benefit of being a solvent free, environmental friendly, and a cost-efficient technology [1]. Several research groups have demonstrated that the hot-melt extrusion technique is a viable method to prepare pharmaceutical dosage forms [23]. By the implementation of HME it is possible to

improve bioavailability of lipophilic drugs by the formation of solid dispersions and solid solutions. This is relevant for poorly-soluble pharmaceutically active ingredients, frequently encountered among novel active ingredients. Such benefits have led to an increased interest of HME technology in recent years [24].

1.4 Summary of Following Chapters

In chapter 2, the fundamentals of rheology, more specifically hot-melt extrusion and capillary rheometry, are discussed to understand the formulation of solid dispersions via hot-melt extrusion. The third chapter describes the materials that will be used in the formulation of the films, while the fourth chapter describes the characterization methods that will be used to characterize the melts or films. Chapter 5 summarizes the results obtained for mechanical, thermal and rheological properties of the solid dispersions, and chapter 6 contains the main conclusions and recommendations for the formulation of solid dispersions.

2 THEORETICAL BACKGROUND

2.1 Rheology

2.1.1 Fundamentals

A typical flow is fully described by the law of conservation of mass, momentum, and energy, as well as by the rheological and thermodynamic equations of state. The rheological state equation, often referred to as the material law, describes the correlation between the flow velocity field and the resulting stress field. The flow properties of the given polymer are described by this equation. The description, explanation and measurements of the flow properties is at the core of the science of deformation and flow called rheology [25].

In the simplest case, the viscous flow of a Newtonian fluid is described by Newton's law of viscosity given for shear flow as:

$$\tau = \mu\frac{d\gamma}{dt} \qquad \text{Eq. 2-1}$$

where τ is the shear stress, μ is the Newtonian viscosity coefficient, and $\dot{\gamma}$ is the shear rate. The viscosity of non-Newtonian fluids such as concentrated polymer solutions and polymer melts is a function of temperature, pressure and shear rate. In addition, the viscosity of polymer solutions and melts exhibits a strong dependence on molecular weight. Melts of high-molecular weight polymers and their concentrated solutions display three characteristic regions. At low shear rates, shear viscosity is independent of shear rate (i.e. Newtonian behavior) and approaches a limiting Newtonian plateau at very high shear rates. At low shear rates, the entanglements impede shear flow and, therefore, viscosity is high. As the shear rate increases, chains begin to orient in the

flow direction and disentangle from one another, thus the viscosity drops. The molecules become fully oriented in the flow direction at very high shear rates. In the molten state, polymers are primarily viscous but will be elastic to some extent. This behavior is generally referred to viscoelastic behavior. Non-linear viscoelastic behavior can arise from the orientation of chain segments and from the retraction of the entire chain in its tube. A shear-thinning (and shear-thickening) behavior is considered to be reversible providing no thermal or mechanical degradation has occurred [26].

2.1.2 Polymer molecules in the melt

The conformation of a molecule in a melt, where it is surrounded by other polymer molecules rather than solvent molecules, is very close to that in a theta solvent. Over a certain rather narrow range of molecular weights the dynamic interaction between polymer molecules starts to have a very marked effect on the dynamic behavior of the melt. This strong interaction is traditionally said to be due to entanglements, although it is now understood that it is not necessarily the result of the looping of one molecule around another but more simply the fact that the displacement of a molecule due to Brownian motion is highly constrained laterally by the other molecules, which cannot move out of the way as a solvent molecule does [15]. This phenomenon does not affect molecular dimensions in an unperturbed melt, but it has a very strong effect on the relationship between molecular structure and rheological properties.

2.2 Hot-melt Extrusion

Knowledge of the properties of the polymer melt is very important in the analysis of the extrusion process. The polymer melt flow properties determine to a large extent the characteristics of the extrusion process. Knowledge of the melt flow properties allows accurate optimization of the screw design and the process operating conditions [14]. There are two main classes of properties important in the extrusion process: the rheological properties and the thermal properties. The rheological properties describe how the material deforms when a certain stress is applied. The rheological properties of the *bulk* material are of importance in the feed hopper region of the extruder. The rheological properties of the polymer *melt* are important in the plasticating zone, the melt conveying zone, and the die forming region. Some of the most important properties of the bulk material are the bulk density (density of the polymeric particles, including the voids between the particles) the coefficient of friction, and particle size and shape. From these properties the transport behavior of the bulk material can be described with reasonable accuracy [14].

2.2.1 Capillary Rheometry

The quantity $\frac{4Q}{\pi R^3}$ is the shear rate at the wall for a Newtonian fluid, is also called the apparent shear rate when non-Newtonian fluids are studied and it represents what the shear rate at the wall would have been if the material had been Newtonian. To measure the viscosity for an unknown fluid believed to be a power-law generalized Newtonian fluid (GNF), pressure-drop and flow-rate data are collected on the fluid (the pressure drop is set, and the flow rate is measured, or vice versa). The pressure drop and flow rate data can be converted to viscosity [16].

The shear rate at the wall in capillary flow of a general fluid is represented by the following equation:

$$\gamma(\tau_R) \equiv \gamma_R = \gamma_a + \left[\frac{1}{4}\left(3 + \frac{d \ln \gamma_a}{d \ln \tau_R}\right)\right] \qquad \text{Eq. 2-2}$$

The quantity in the square brackets is called the Weissenberg-Rabinowitsch correction. For Newtonian fluids the correction becomes 1, and $\gamma_R = \gamma_a$ as before. This correction allows us to calculate the shear rate at the wall without assuming any form of the velocity profile. For a capillary flow system such as the one illustrated in Figure 2.1, the viscosity may be determined from measurements of Q (needed to calculate $\dot{\gamma}$), ΔP (to calculate τ_R) and the geometric constants R and L [16].

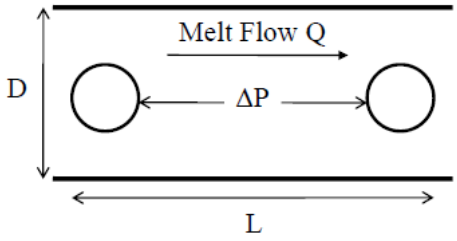

Figure 2:1: Schematic illustration of a capillary extrusion apparatus.

The expression derived for the viscosity is based on properties of the fluid near the wall. If the properties of the fluid at the wall are representative of the bulk (which they are believed to be for polymers melts and other similar systems), the viscosity measured in capillary flow may be relied upon. Yet, corrections may be needed in capillary rheometry to account for end effects and wall slip. For shear thinning fluids such as shown in Figure 2.2, the shear rate at the wall is higher than in a Newtonian fluid with the same average velocity [16].

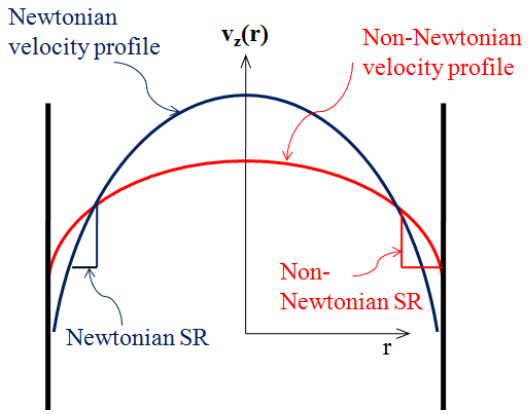

Figure 2:2: Schematic of the effect of material properties on the velocity profile shear rate in a capillary.

The analysis of many flow problems can be simplified by considering only one component of the equation of motion, the one in the direction of flow [14]. One of the assumptions in the derivation of τ_R in a capillary was that the capillary is long and therefore velocity variations in the z-direction may be neglected. In an actual capillary rheometer, however the flow takes some time to develop at the inlet, and for polymers, the flow at the exit is disturbed by die swell. These two effects induce some z-variation in the velocity. The z-variation is not a problem as long as $P_0 - P_L$ and L is only measured over the portion of the capillary where steady fully developed unidirectional flow occurs. The pressure at the top of the capillary P_0 is related to the force per unit area $\frac{F}{\pi R_b^2}$ that is required to move the piston at a steady rate [16]. The pressure drop across the wide barrel is neglected. The pressure at the bottom of the capillary P_L is atmospheric. The pressure drop over the entire capillary is then just the difference between these two pressures:

$$P_0 = P_{atm} + \frac{F}{\pi R_b^2} \qquad \text{Eq. 2-3}$$

$$P_L = P_{atm} \qquad \text{Eq. 2-4}$$

$$P_0 - P_L = \frac{F}{\pi R_b^2} \qquad \text{Eq. 2-5}$$

The effect of pressure drop in the barrel can be eliminated by measuring the pressure at the inlet of the capillary independently, that is by placing a transducer. The end effects can be accounted for by observing the effect of changing the ratio of capillary length to diameter at constant shear rate as observed in Figure 2.3.

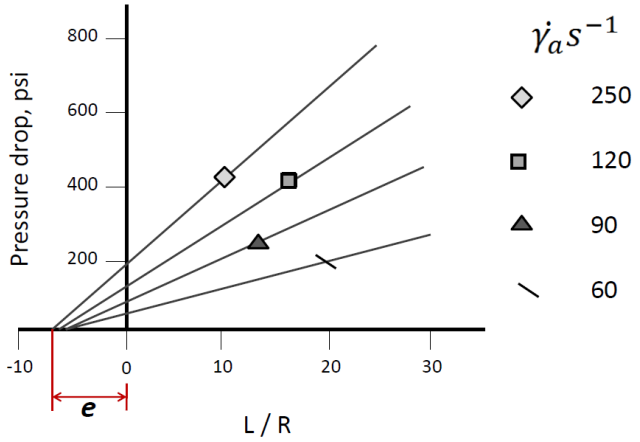

Figure 2:3: Pressure loss versus L/R at constant shear rate [16].

Capillary data may be corrected for end effects by subtracting the pressure-axis intercept of the ΔP versus L/R plot from the values of pressure used to calculate τ_R. Equivalently, the end effects can be corrected by adding *e* to the value of L/R used in calculating τ_R. This is called the Bagley correction [16].

To determine if there is wall slip, a slipping system has to be examined. The effect of slip is to reduce the deformation experienced by the fluid. In the case where slip is occurring as compared to the no-slip case, the shear rate is reduced throughout, but especially near the wall. To calculate viscosity in a situation where slip is occurring, one must calculate the true shear rate

near the wall; this analysis is due to Mooney. The first step is to correct the apparent shear rate for slip. The apparent shear rate is normally given by (no slip)

$$\dot{\gamma}_a = \frac{4Q}{\pi R^3} = \frac{4v_{z,av}}{R} \qquad \text{Eq. 2-6}$$

where $\frac{4v_{z,av}}{R}$ is the average fluid velocity in the tube. When slip occurs, this calculation of apparent shear rate is too large since much of $v_{z,av}$ goes into slip at the wall. A corrected value for apparent shear rate may be obtained by substituting $v_{z.av} - v_{z,slip}$ for $v_{z.av}$ in Eq. 6, where $v_{z,slip}$ is the wall slip velocity. The corrected shear rate is given as:

$$\dot{\gamma}_{a,silp-corrected} = \frac{4v_{z,av}}{R} - \frac{4v_{z,slip}}{R} \qquad \text{Eq. 2-7}$$

If the slip velocity $v_{z,slip}$ is only a function of wall shear stress τ_R then plots of $\frac{4v_{z,av}}{R} = \frac{4Q}{\pi R^3}$ versus $\frac{1}{R}$ at constant τ_R would give straight lines with a slope of $4v_{z,slip}$ and an intercept of $\dot{\gamma}_{a,silp-corrected}$ as observed in Figure 2.4 Conversely, if the plots of $\frac{4v_{z,av}}{R} = \frac{4Q}{\pi R^3}$ versus $\frac{1}{R}$ at constant τ_R have a slope of zero, no slip has been achieved in the experiments [16].

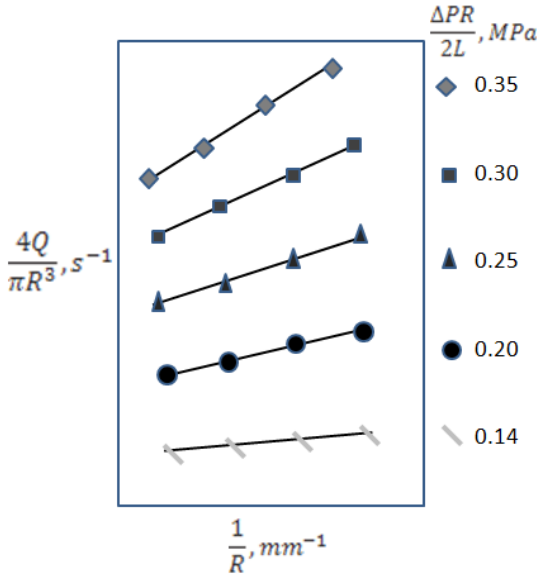

Figure 2:4: Apparent shear rate, uncorrected for slip, versus inverse capillary radius at different constant values of wall shear stress.

However, the Mooney technique is only an indirect measurement of $v_{z,slip}$, based on a postulate that slip is occurring. Other violations of the assumptions could be responsible for the measured nonzero slope, for instance, the possible contributions of entrance losses, instability, compressibility, or normal stresses. When appropriate attention is paid to end effects and slip effects, the measured viscosities can be very accurate.

Amongst advantages of capillary rheometer are:

ability to measure very high shear rates ($\approx 10^6 s^{-1}$);

ability to measure extrudate swell characteristics;

ability to measure melt fracture characteristics; and,

relatively easy to use.

Disadvantages of the capillary rheometer are:

the polymer is not exposed to a uniform shear rate;

various corrections have to be applied to the data;

it does not yield an accurate description of viscoelastic behavior; and,

it is unreliable at high shear rates (temperature effects) [1].

2.3 Power Law Fluid

The fact that the polymer melt viscosity reduces with shear rate is of great importance in the extrusion process. A fluid behaves as a Newtonian fluid at low shear rates but the range of shear rates encountered in most polymer processing operations varies from 1 to 10,000/s [14].

A viscosity-shear rate curve can be reasonably approximated with a straight line relationship. This is true for most polymers. A double logarithmic scale is convenient because

the viscosity changes about 4 to 5 orders of magnitude over more than 10 orders of magnitude change in shear rate. A straight-line relationship on a log-log plot indicates that the variables can be related by a power law equation. This is generally written as:

$$\eta = m\dot{\gamma}^{n-1} \text{ or } \tau = m\dot{\gamma}^{n} \qquad \text{Eq. 2-8}$$

where m is the consistency index and n the power law index. The power law index indicates how rapidly the viscosity reduces with shear rate and can be represented by the following equation:

$$n = \frac{\Delta \log \dot{\gamma}}{\Delta \log \tau_w} \qquad \text{Eq. 2-9}$$

For pseudoplastic fluids, the power law index ranges from 1 to 0. When the power law index is unity, the fluid is Newtonian and the consistency index becomes the Newtonian viscosity. The power law index indicates the degree of non-Newtonian behavior. A power law index of less than 0.5 is typical of shear thinning polymers [14].

Generally, the power law can be used to represent a flow or viscosity curve with an acceptable accuracy over only a certain range of shear rates. The size of this range depends on the curvature of the viscosity data. If a flow curve has to be described by the power law over a large range, it has to be divided into segments, each with its own values of m and n to be determined as in Figure 2.5. Therefore, in the collection of standard rheological material data there will be different values of m and n corresponding to different ranges of shear rates.

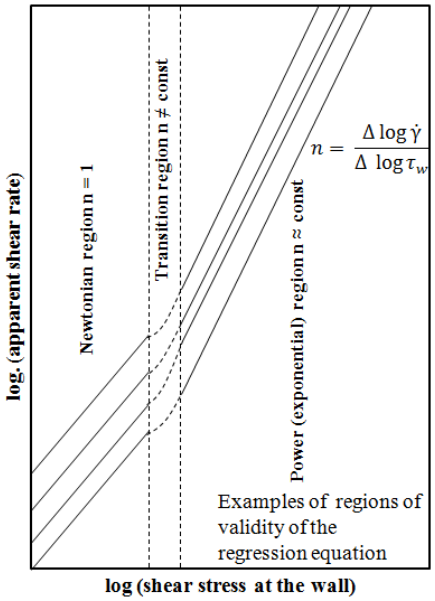

Figure 2:5: Approximation of the flow curve by a power law [25].

There is a very large difference in behavior between fluids of different power law index, therefore the power law index of a polymer melt, to a large extent, will determine its extrusion behavior [25].

2.4 Parameters that Influence Melt Rheology

Rheological properties govern the flow behavior of polymers when they are processed in the molten state. The structure of a polymer includes: size and shape of the molecules, and their corresponding distribution among the molecules. Thus, quantities of interest include: the molecular weight and its distribution, tacticity (when the monomer has a pseudochiral center), and branching (types, lengths and their distributions). For linear homopolymers, in which tacticity is not an issue, the molecular weight distribution contains complete information

regarding structure [15]. Other factors that affect the flow of melts are melting temperature, hydrostatic pressure, additives and their distribution, shear rate and shear stress among others.

2.4.1 Temperature

When the viscosity is plotted against shear rate at several temperatures, the curve generally lowers with increasing temperature. This is a result of the increased mobility of the polymer molecules. The effect of temperature on the viscosity is considerably more pronounced at low shear rates, particularly in the range of zero shear viscosity when compared to high shear rates [25]. For the time being, it is assumed that no irreversible changes occur as a result of degradation. However, whenever experiment or processes are conducted at elevated temperatures, the possible effects of degradation have to be taken into account.

For many polymers the effect of temperature is greater at lower temperature. The temperature sensitivity of the viscosity varies widely for different polymers. As a general rule, amorphous polymers have high temperature sensitivity, while semicrystalline polymers have relatively low temperature sensitivity. The closer a polymer is to its glass transition temperature, the larger the temperature sensitivity of the viscosity. In general, polymers that are processed considerably above their glass transition temperature (more than 150 °C above T_g) show a relatively small temperature sensitivity [14]. At lower temperatures in the vicinity of the glass transition temperature, viscosity increases much more rapidly with decreasing temperature than given by the Arrhenius expression.

2.4.2 Pressure

There is a shift in T_g when there is a shift in pressure, which can be determined directly from a P-V-T diagram. The pressure dependence of the glass transition temperature can be assumed to be linear up to pressures of about 1kbar. The resulting shifts in T_g are of the order of 15 to 30° C per kbar. At pressures higher than 1 kbar the glass transition temperature increases with increasing pressure at a much smaller rate [25].

Generally it is known that the pressure affects the flow properties of amorphous polymers stronger than the flow of semi-crystalline polymers. It has been found that, the effect of pressure in viscosity becomes quite significant at pressures substantially above 35 MPa [14].

2.4.3 Time

The rearrangement of the polymer structure takes a certain amount of time, depending on the polymer and the temperature. The polymer properties are, therefore, a function of time and depend on the deformation history of the polymer. The deformation history is often referred to as the shear history. However, it is not only shearing deformation that affects the polymer properties but elongational deformation as well. In fluids with time dependent behavior, the effects of time can be reversible or irreversible. If the time effects are reversible, the fluids are either thixotropic or rheopectic. Thixotropy is the continuous decrease of apparent viscosity with time under shear and the subsequent recovery of viscosity when the flow is discontinued. Rheopexy is the continuous increase of apparent viscosity with time under shear. Polymer melts do exhibit some thixotropy effects; however, thixotropy can also occur in inelastic fluids. The time scale of thixotropy is not necessarily associated with the time scale for viscoelastic relaxation. For a proper description of the flow of a polymer melt, the viscoelastic properties

have to be taken into account, including the dependence on deformation history. In the quantitative analysis of most extrusion problems, the polymer melt is generally considered to be a viscous, time-independent fluid. This assumption is a simplification, but it usually allows one to find a relatively straightforward solution to the problem.

2.4.4 Molecular Weight Distribution

The polydispersity index is a primitive measure of the breadth of the molecular weight distribution. Molecular weight and the critical molecular weight for entanglements, M_c, should significantly influence the rheological properties of polymers. It has been shown that the zero-shear viscosity is directly proportional to the weight-average molecular weight. The onset of shear-thinning behavior occurs at progressively lower shear rate as molecular weight increases.

Figure 2.6 is a sketch of viscosity curves for two polymers having the same weight average molecular weight but different molecular weight distributions. The upper curve is for a nearly monodisperse sample, while the lower one is for a sample with a moderately broad MWD. The broadening of the distribution stretches out the range of shear rates over which the transition from the zero-shear viscosity to the power law region occurs.

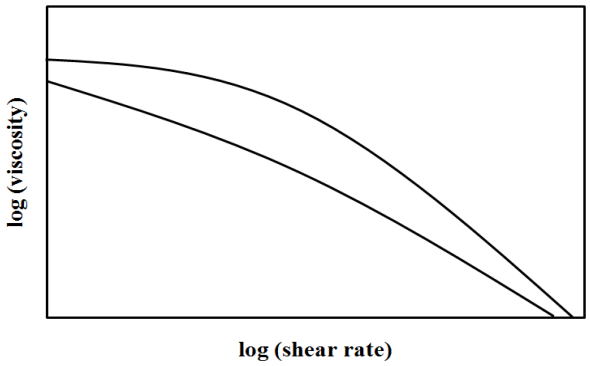

Figure 2:6: Sketch of viscosity versus shear rate curves for samples with narrow (upper curve) and broad (lower curve) molecular weight distributions; both have the same Mw [15].

2.4.5 Shear Rate

As in the case of Newtonian fluids, the viscosity of a polymer depends on temperature and pressure, but for polymeric fluids it also depends on shear rate, and this dependency is quite sensitive to molecular structure. Factors that enhance the shear rate dependency of viscosity are high solvent power, large molecular weight and broad molecular weight distribution. To avoid consideration of this parameter, measurements must be made at sufficiently low shear rates that the viscosity is essentially equal to its low-shear rate limiting viscosity. The curve of viscosity versus shear rate is of central importance in plastics processing, where it is directly related to the energy required to extrude a melt. At sufficiently high shear rates, the viscosity often approaches a power law relationship with the shear rate.

2.4.6 Mixing in Screw Extruders

Polymer solutions and melts may contain particulate or fiber fillers. Suspended particles affect the rheological properties of suspensions and therefore mixing is very important. Mixing can be broadly defined as a process to reduce the non-uniformity of a composition. The basic mechanism of mixing is to induce physical relative motion of the ingredients [16]. The types of motion that can occur are molecular diffusion, turbulent motion, and convective motion. Convective motion is the predominant motion in high viscosity liquids, such as polymer melts. The mixing action generally occurs by shear flow and elongational flow. If the components to be mixed are compatible fluids and do not exhibit a yield point, the mixing is distributive. If the mixture contains a component that exhibits a yield stress, then the actual stresses involved in the process become very important. A very important aspect of the study of mixing is the characterization of the mixture. A complete characterization requires specification of the size,

shape, orientation, and spatial location of every discrete element of the minor component, which is impossible. Mixing is an essential function of the screw extruder. It is assumed that significant mixing only takes place when the polymer is in the molten state. The mixing action is not uniformly applied to all elements of the polymer melt. As a result of the inherent transport process in a screw extruder there will be considerable non-uniformities in the intensity of the mixing action and its duration. Fluid elements in the center of the flow channel are exposed to a very low shear rate and their residence is short because the velocities are highest in the center. Fluid elements at the wall are exposed to high shear rates and their residence time is long because of the low velocities at the wall. Thus, even if a perfectly mixed fluid enters a die, non-uniformities can be expected as the fluid leaves the die [14]. Striation thickness is defined as the total volume divided by half the total interfacial surface. Mixing efficiency reduces with shear strain because the orientation of the striation changes with shear strain. The striation becomes more and more oriented in the direction of flow as the shear strain increases. As a result, mixing for a long time does not make much sense because most of the mixing is achieved within the first 20 units of shear strain. However, the distributive mixing efficiency can be improved dramatically by reorienting the striations during the mixing process [14]. Randomizing mixing sections greatly improve the generation of interfacial area, and thus the mixing performance. The distribution of the filler within the polymer matrix can also be improved by treating the matrix with an agent that could reduce the viscosity of the matrix and, to some extent, prevent the fillers from forming a network [13]. Such an agent could be a plasticizer which reduce the viscosity, lower thermal transitions and modify mechanical properties of the polymeric matrix [14].

3 MATERIALS

3.1 Hydroxypropyl Cellulose

HPC is an ether of cellulose in which some of the hydroxyl groups in the repeating glucose units have been hydroxypropylated forming -R groups using propylene oxide with the chemical structure shown in Figure 3.1. HPC is a 1,4-linked propyl-substituted neutral polysaccharide [17]. It is also a thermoplastic polymer (i.e. polymer that can be heat-softened in order to process into a desired form) showing liquid crystal properties with changes in temperature. HPC is soluble in water, it has a HPC-water Flory-Huggins solubility parameter of $\chi = 1.55$ at infinite dilution and 323.4 K [27]. HPC has a tetragonal unit cell structure with 6 monomers and 2 chains per unit cell, and cell dimensions of a = b = 11.3, and c = 15.0 Å. Persistence lengths that have been reported for HPC include 10 nm obtained by the Yamakawa-Fuji expression for intrinsic viscosity-molecular weight dependence for a wormlike chain [28], and 12 nm in a dilute solution at room temperature [15].

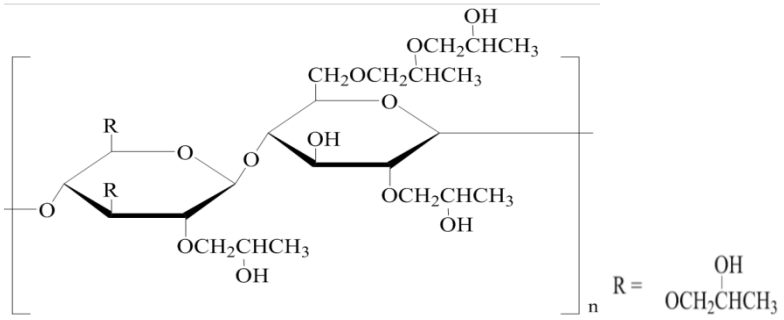

Figure 3:1: Hydroxypropyl cellulose chemical structure reproduced from reference [29].

Its major applications include: paints, coatings, inks, adhesives, cosmetics, papers, pharmaceuticals, and encapsulation, among others [27]. Medium to high HPC molecular weights are recommended for extrusion systems where more flexibility and higher tensile properties are desired [4]. Its low cost and pharmaceutical acceptability renders it suitable for this purpose.

In this work, molecular weights of 100, 370, and 1,000 kDa were purchased from Sigma-Aldrich (CAS 9004-64-2 Batch #: 17009PD, MKBC4098, and 05131JH). The melting peak temperatures (T_{mp}) obtained for pure HPC are as follows: 181, 212, and 216 °C for 100, 370, and 1,000 kDa HPC, respectively.

3.2 Griseofulvin

(2*S*,6′*R*)-7-Chloro-2′,4,6-trimethoxy-6′-methyl-3*H*,4′*H*-spiro[1-benzofuran-2,1′cyclohex[2]ene]-3,4′-dione, shown in Figure 3.2, is commonly known as griseofulvin [11]. Griseofulvin was the first available oral antibiotic and antifungal drug for the treatment of diseases such as dermatophytoses and has now been used for more than 40 years. It treats fungus infections caused by tinea organisms on the skin, hair, or nails. Presently, it is one of five available oral antifungal agents (ie. griseofulvin, ketoconazole, itraconazole, terbinafine, and fluconazole) in the treatment of onychomycosis. On the other hand, griseofulvin could be useful in the treatment of cancer [30]. It has a molecular formula of $C_{17}H_{17}ClO_6$, molecular weight of 352.770 g/mol, and a melting point near 225 - 226 °C. It is soluble in MeOH, dioxan, DMF, and Et_2O, fairly soluble in toluene, and poorly soluble in H_2O and hexane. It also has UV absorbances near [neutral] λ_{max} 211 (ε18000) ; 217 (ε18000) ; 236 (ε22400) ; 250 (ε14000) ; 291 (ε22000) ; 324 (ε15800) (MeOH).

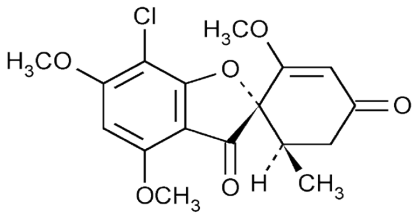

Figure 3:2: Griseofulvin absolute configuration.

Griseofulvin is a highly crystalline organic compound that shows x-ray signals at 10.78°,13.24°, 16.54°, and 28.53° [11]. It is produced by Penicillium aethiopicum, Penicillium griseofulvum and other Penicillium supplements. However, it has a very limited solubility in water (15 μg/ml at 37 °C), which results in a little absorption from the gastrointestinal tract resulting in low bioavailability [31]. Near its toxicity limits it can cause skin rashes and other adverse effects when used therapeutically and is a possible human carcinogen. The therapeutic dosage limit of griseofulvin is very close to the toxicity limit of the drug; because of this limitation, improvement of griseofulvin bioavailability by size reduction or by coformulation is desired [32].

Grsiseofulvin 97% pure was purchased from Alfa Aesar (Lot: G8629A).

3.3 Plasticizers

Plasticizers increase the workability, flexibility and distensibility of a polymer. Plasticization of a polymer will decrease the polymeric intermolecular attractions to provide greater freedom of movement for the polymeric molecules. Therefore, the film is more deformable [26]. When using a plasticizer the tensile strength may be decreased, and flexibility and elongation may be increased [4]. The plasticizer modifies the physical-mechanical properties,

by lowering the melt viscosity, glass transition temperature, and elastic modulus of a polymeric film [4]. The efficiency of a plasticizer is related to its chemical structure and the interaction between its functional groups with those of the polymer or polymers. In this work, PEG, d-sorbitol, and glycerol were used as plasticizers.

3.3.1 Polyethylene Glycol

Polyethylene glycol (PEG) has the following molecular formula: $(C_2H_4O)_{182}$ (depends on Mw used) as illustrated in Figure 3.3. Belongs to the polyalkylene ether type of polymer and is biodegradable [33]. It is available in a wide range of molecular weights up to several million ranging from 200-600 (clear, colourless, viscous liquids PEG), 8000 (partly crystalline), or 100000-1000000 Da (highly crystalline, thermoplastic solids). The structure can be linear or branched, amorphous, or crystalline [29].

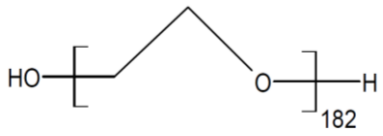

Figure 3:3: PEG chemical structure.

PEG melting temperature varies with molecular weight and crystallinity/crystallisation temperature. It is soluble in H_2O, chlorinated hydrocarbons, 2-butanone, 2-ethoxyethyl acetate, butyl acetate, cyclohexanone, esters, DMF, C_6H_6 (elevated temperature), and toluene (elevated temperature) [27]. Melt behavior is pseudoplastic, melt viscosity decreases significantly with an increase in shear rate. The effects of draw ratio on the tensile strength and modulus of PEO filaments, prepared by solid-state extrusion, have been reported. Both strength and modulus increase with the draw ratio. PEO is susceptible to oxidation. Degradation is also caused by

mechanical processing, such as high shear [29]. Pyrolysis studies on PEO (molecular weight 900,000 Da) show that degradation, by C-O and C-C bond scission, occurs in the range 235-255 °C [29]. Low molecular weight PEO is used as an intermediate in chemical manufacture (e.i. of surfactants and thickeners). Slightly higher MW (1000-2000 Da) polymers are used in pharmaceutical applications (i.e. ointments or suppositories) and in cosmetics (i.e. creams or lotions). Medium molecular weight polymers are used as adhesives, binders, plasticizers, lubricants, molding compounds or preservatives. Association complexes of PEO are used in medical applications such as controlled release formulations, microencapsulation and artificial kidney [27].

In this study a PEG of molecular weight 8000 Da purchased from Sigma Aldrich (Lot: 18F-0034) was used.

3.3.2 Glycerol

Synonyms include glycerin, glyceritol, amylac, and glyrol among others. Its linear chemical formula diagram looks as follows $HOCH_2CH(OH)CH_2OH$, while its structure is illustrated in Figure 3.4. It has a molecular formula of C_3H_8O with a molecular weight of 92 g/mol.

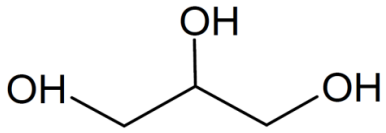

Figure 3:4: Glycerol chemical structure.

Glycerol can be obtained on large scale by alkaline hydrolisis of fats during soap manufacturing or from biological sources, where it can be extensively found in its esterified form in animal and plant glycerides. It is mainly used as an humectant, emollient, and solvent in

cosmetics and pharmaceutical products, foods, tobacco processing and in numerous industrial and domestic products. It is a component of alkyd resins and polyurethanes. It has also biological importance as a mild laxative and diuretic agent. It can be physically described as a syrup with sweet taste and has a melting point of 17.8 °C [29], and boiling point of 290 °C [34]. Glycerol is soluble in H_2O and EtOH but insoluble in C_6H_6, $CHCl_3$ and CCl_4 [35]. It has been previously demonstrated that glycerol has a highly hygroscopic nature [36].

3.3.3 D-Sorbitol

Synonyms of sorbitol, shown in Figure 3.5, include D-glucitol and L-gulitol, among others. It has a molecular formula of $C_6H_{14}O_6$ with molecular weight of 182.173 g/mol. Occurs widely in plants ranging from algae to the higher orders. D-sorbitol is used for manufacturing of sorbose, propylene glycol, ascorbic acid, resins, plasticizer and in antifreeze mixtures with glycerol or glycol [29]. It is also a tablet diluent, sweetening agent, and humectant. It has a sweet taste because it is 60% sucrose. Has a melting point of 97 °C (stable form), boiling point of 295 °C, and is freely soluble in H_2O, fairly soluble in hot EtOH and sparely soluble in cold ethanol, [37]. D-sorbitol was purchased from Sigma Aldrich (CAS 50-70-4 Batch #: MKBC8755).

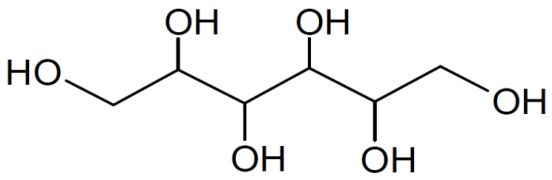

Figure 3:5: Sorbitol chemical structure.

4 EXPERIMENTAL METHODS

4.1 Film Sample Preparation

A 5 wt% mixture of HPC-plasticizer is used for the formulation of the films and griseofulvin concentration of 0, 5, 10 or 20 wt%. The pre-mixed, shown in Figure 4.1 is placed in the oven at 80 ^{0}C overnight to dry.

Figure 4:1: The image in the left is a blended mixture of HPC with plasticizer, the image to the right is the mixture at the extruder.

Two different processing temperatures were used: 180 and 190 °C. To use the extruder the temperature is set to the processing temperature and the HPC-plasticizer-GF blend is placed directly into the screws as illustrated in Figure 4.1. Once the temperature is reached the blend is processed for 100 minutes from 10 to 90 rpms. The film is extruded at the same processing temperatures (180 – 190 °C) at 50 rpms.

4.2 Polymer Melt Rheology

Measurements of viscosity as a function of shear rate were collected with Thermo Scientific Haake MiniLab II twin screw extruder. Data is collected at a capillary reflux, where measurements of ΔP and screw speed are used to calculate viscosity and shear stress using the Thermo Haake PolyLab software. To collect the data the mixture is fed into the extruder. Once the processing temperature has been reached, a mixing period of ten minutes at 10 rpms takes place. Once the mixing period is over, data is collected from 10 to 90 rpms at steps of 10 rpms every 10 minutes. Data collected provides information about the dependence of molecular weight, temperature, and filler concentration on viscosity.

4.2.1 Data Analysis

For a non-Newtonian fluid the terms apparent viscosity and apparent shear rate are used, because the actual value of the shear rate at the capillary wall will be different. With the data obtained from the HAAKE MiniLab II extruder the correction that can be applied is the Weissenberg-Rabinowitch correction. This correction allows calculating the shear rate at the wall without assuming any form for the velocity profile, accounting for differences in shear rates between the Newtonian case and the general case due to the fact that the velocity profiles for non-Newtonian fluids in capillary flow are non-parabolic.

$$\dot{\gamma}(\tau_R) \equiv \dot{\gamma}_R = \dot{\gamma}_a + \left[\frac{1}{4}\left(3 + \frac{d \ln \dot{\gamma}_a}{d \ln \tau_R}\right)\right] \qquad \text{Eq. 4-1}$$

The shear rate obtained from the Weissenberg-Rabinowitch correction is used to calculate the viscosity for a non-Newtonian fluid.

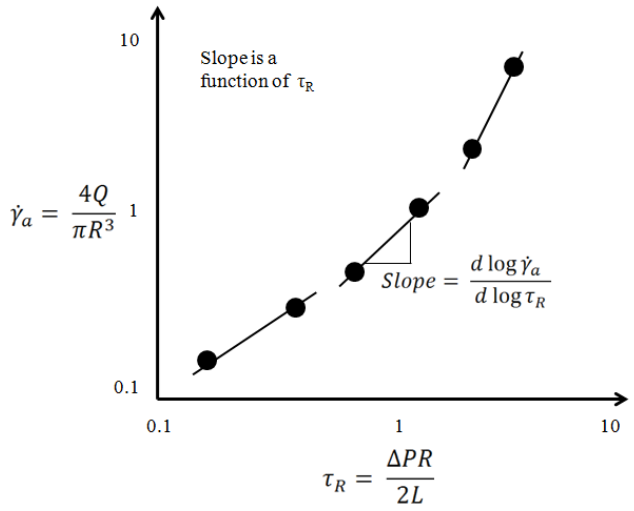

Figure 4:2: Schematic of how the derivative in the Weissenberg-Rabinowitsch correction is obtained from pressure-drop and flow-rate information for any type of fluid.

The slope $\frac{d \ln \dot{\gamma}_a}{d \ln \tau_R}$, obtained from the graph shown in Figure 4.2, is the value used to obtain the corrected shear rate, and viscosity will be obtained from the following equation:

$$\mu(\tau_R) = \frac{4\tau_R}{\dot{\gamma}_a}\left(3 + \frac{d \ln \dot{\gamma}_a}{d \ln \tau_R}\right)^{-1} \qquad \text{Eq. 4-2}$$

Corrections for wall slip, and entrance and exit effects (Bagley correction) cannot be applied because runs at different capillaries (changing R or L) are not available.

4.3 Differential Scanning Calorimetry

A Differential Scanning Calorimetry (DSC) measures the difference in heat flow rate (mW = mJ/sec) between a sample and inert reference as a function of time and temperature. The technique measures the temperatures and heat flows associated with transitions in materials as a

function of time and temperature in a controlled atmosphere. These measurements provide quantitative and qualitative information about physical and chemical changes that involve endothermic or exothermic process, or changes in heat capacity. DSC can provide direct measurement of the glass transitions, melting and boiling points, crystallization temperature, heats of fusion and reaction, and specific heats, among others. Heat flows into the sample (endothermic) as a result of heat capacity (heating), glass transition (T_g), melting, evaporation, and other endothermic process. Heat flows out of the sample as a result of heat capacity (cooling), crystallization, curing, oxidation and other exothermic processes.

DSC Q2000 and TA Instruments Universal Analysis 2000 were used to complete the experiments. Approximately 5-10 mg of sample was placed in a hermetic aluminum pan. All samples were analyzed from 30 to 300 °C at ramps of 10 °C per minute.

The melting of semicrystalline polymers is a very broad process because of the broad distribution of the crystallite sizes and the imperfection of these crystallites. The width of the melting peak is often 50°C or more; thus it was necessary to define melting point by convention [38]. The melting point is selected as the highest temperature of the melting endotherm. Nevertheless in many publications the melting is characterized by the peak temperature of melting (T_{mp}). This is an easy and simple method, but the peak temperature of melting simply indicates the temperature at which the melting proceeds with the maximum rate, and not the highest temperature at which crystals melt.

When reporting the melting data for crystalline polymers as the one shown in Figure 4.3, the following characteristic data should be reported:

- The starting point of melting (T_{st}). Often this is not easy to determine because this is a gradual process. The reproducibility is poor as it is a very subjective value, and considerable differences may arise because of slight changes in the instrumental baseline.
- The peak temperature of melting (T_{mp}), this temperature indicates the maximum rate of melting.
- The melting point (T_m), the highest temperature point of the melting endotherm. The sensitivity on the DSC trace must be increased considerably so that the determination procedure will be less subjective.

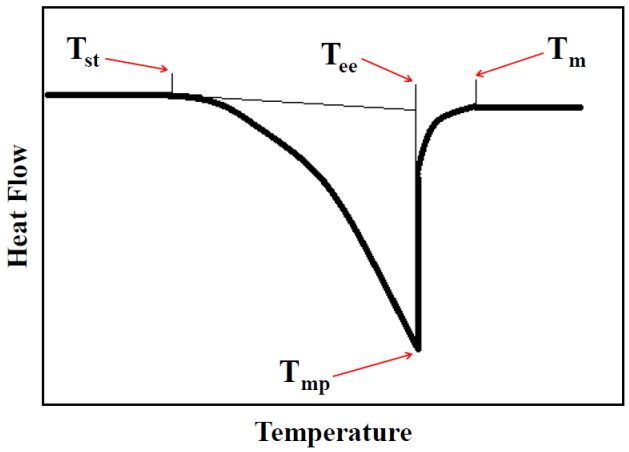

Figure 4:3: Characteristic temperatures of a polymer melting [38].

4.4 Tensile Strength Test

Tensile strength refers to the resistance to stretching. This property results from the characteristics of structure and morphology and the manner in which the polymeric matrix undergoes molecular reorientation in response to stress. Tensile strength is determined by

stretching a strip of polymer of uniform dimensions. The tensile stress (σ), is the force applied (F), divided by the cross sectional area (A) that is:

$$\sigma = \frac{F}{A} \qquad \text{Eq. 4-3}$$

The tensile strain, ε, is the change in sample length, *l* divided by the original length:

$$\varepsilon = \frac{\Delta l}{l_0} \qquad \text{Eq. 4-4}$$

The ratio of stress to strain is the tensile modulus, E:

$$E = \frac{\sigma}{\varepsilon} \qquad \text{Eq. 4-5}$$

which is a measure of the resistance to tensile stress. A distinction among fibers, plastics, and elastomers is often expressed in terms of stress-strain curves as shown in Figure 4.4.

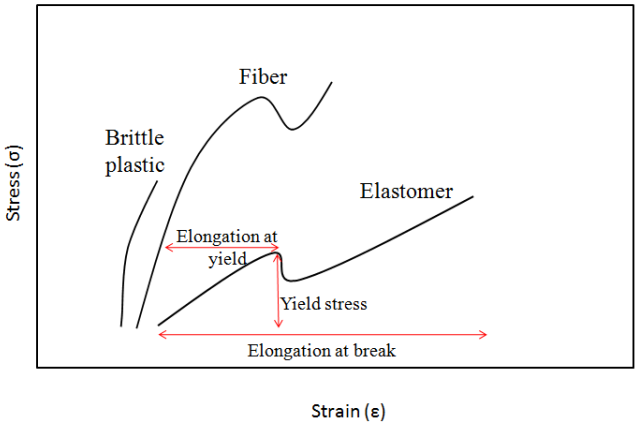

Figure 4:4: Characteristics of tensile stress-strain behavior and indications of a typical thermoplastic [24].

Both plastics and fibers exhibit a steep slope (high modulus), but fibers can sustain greater stress before breaking (end of curve). Elastomers have a low modulus initially, but once in the stretched state the modulus increases sharply. For a typical thermoplastic the initially the modulus is high, until a point is reached where the plastic yields or deforms. Prior to the yield point the elongation is reversible. At the yield point, enough stress has been applied to cause the

molecules to untangle and flow over one another, and further elongation is irreversible. Eventually the sample breaks. Mechanical properties are, however, very temperature dependent [26].

To measure tensile strength and elongation an Anton Paar MRC 301 extensional fixture SER2 as shown in Figure 4.5 was used. For the tests, specimens having a length of approximately 2.0 cm are clamped to the system. Once the sample is placed, a rotation (γ) of 1 to 100% is set the length, width and thickness of the sample are recorded, and the instrument measures elongational stress and strain automatically. With the data obtained the Young Modulus can be determined as indicated by ASTM D882 -10.

Figure 4:5 Anton Paar MRC 301 extensional fixture SER2.

5 RESULTS AND DISCUSSION

5.1 Mechanical Properties

5.1.1 Introduction

The results of mechanical tests completed for hot-melt extruded HPC films are shown in this section. Young modulus was determined as HPC molecular weight, type of plasticizer, griseofulvin concentration and processing temperature were varied. Three repetitions of the elongational tests were performed for each film and the relevance of the different factors (and their levels) was evaluated by means of a multiple linear regression model with a 5% significance level, as shown in Appendix G.

Information of physical properties such as mechanical properties of HPC hot-melt extruded films with different additives is limited. It is desired that films to be used as drug delivery devices have good mechanical properties to assure their integrity and their resistance during handling [39]. Films must be also capable of resisting considerable stress without fractures or appropriate elongation during the formulation process [39], thus the importance of determining how different formulation and processing parameters affect their mechanical properties.

5.1.2 Elongational Tests

As reported in literature, mechanical properties depend on intermolecular forces, molecular weight, and temperature among others [40]. Other factors that will also affect the

results are molecular weight distribution, morphology, method of sample preparation, and number and type of additives. Mechanical properties are dependent on molecular weight over a very broad range, although they tend to level off at the higher end of the molecular weight spectrum [40]. This will mainly depend on structure and morphology, and the manner in which the polymeric matrix undergoes molecular reorientation in response to stress. Anything that contributes to chain stiffening - bulky side groups, crystallinity - ought to increase mechanical properties at the expense of tensile elongation [40]. Semicrystalline thermoplastic polymers behave much like crosslinked polymers below the melting temperature, $T_{m,}$ because of the very strong intermolecular forces arising from close chain packing [40].

The persistence length of a polymer will determine if it is rigid, semi-flexible or flexible. Polymers that are rigid, have a contour length smaller than the persistence length, and behave like rigid rods. Semi-flexible polymers are those for which the persistence and contour lengths have the same order of magnitude. These polymers tend to bend and entangle. Flexible polymers are those for which the contour length is much larger than the persistence length. These polymers are elastic, entangle and coil into themselves [41].

The multiple linear regression model obtained with Minitab indicates that molecular weight, processing temperature, plasticizer and griseofulvin concentration make contributions to the model, as well as the interactions of molecular weight with drug concentration and processing temperature. The empirical model obtained is able to account for 40% of the variability in Young's moduli response as shown in Appendix G.

5.1.3 Effect of Processing Temperature

Figure 5.1 shows the results for 100 kDa films with glycerol at the two different processing temperatures. In this case, at all griseofulvin concentrations the lower processing temperature shows higher Young's moduli. It is believed that as temperature increases the average distance becomes longer, indicating active mobility of amorphous chain segments. Decrease in Young's moduli has also been attributed to thermal expansion of the average distance between amorphous chain segments [43]. The statistical analysis on the individual regressor coefficients, shown in Appendix G, states that processing temperature has a significant contribution to Young's moduli response with a P-value < 0.05.

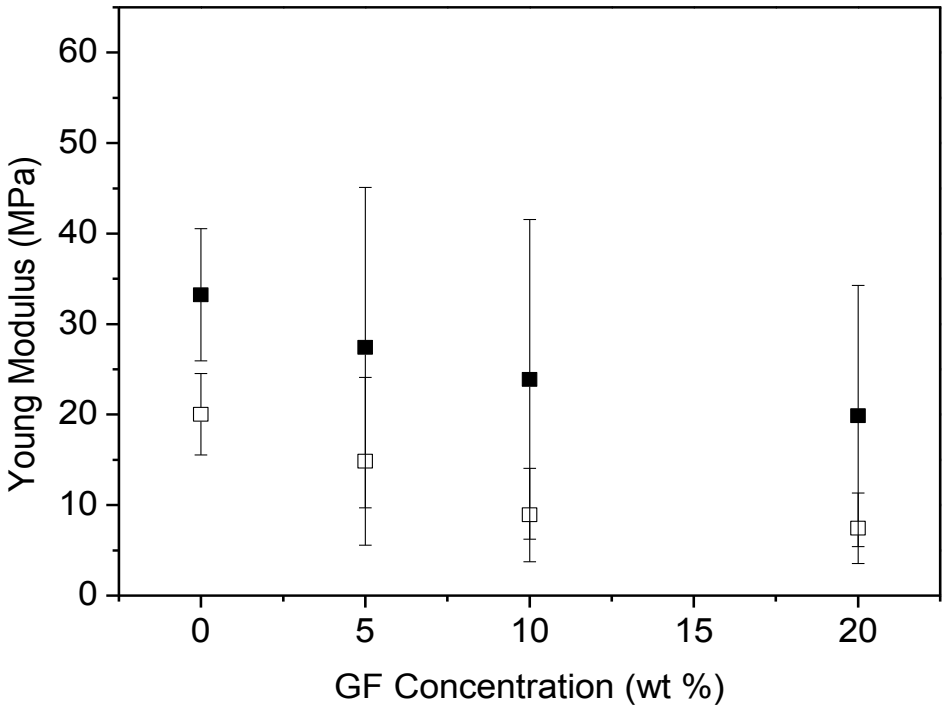

Figure 5:1: Young modulus as a function of griseofulvin concentration for 100 kDa glycerol hot-melt extruded HPC films at 180 (■) and 190 (□) °C.

5.1.4 Effect of HPC molecular weight

As stated in literature, mechanical properties of a polymeric film should increase as polymer molecular weight increases [40]. Young's moduli values reported for 95 and 1,195 kDa HPC cast films are of 600 MPa [39] and 703 MPa [42] , with tensile strengths of 14.6 MPa and 16 MPa, respectively. Films processed via hot-melt extrusion have tensile strengths between 14.95 to 9.76 MPa for 1,150 kDa HPC 5% PEG films [4], depending upon the relative humidity of the films. Matsuo and coworkers have reported that mechanical properties increase with increasing molecular weight, for 117, 192, and 1,195 kDa HPC cast films [33]. The reason for the proportional relationship between Young's moduli and molecular weight is that higher molecular weight polymers should have high intra and intermolecular forces. In the case of HPC, intra molecular hydrogen bonding of the poly(propylene oxide) side chains leads to a stiff rod-like molecule [43].

Figures 5.2, 5.3 and 5.4 show the results obtained for films processed at 190 °C. The dash lines represent the Young's moduli for films without additives. Each graph contains one molecular weight HPC with the different plasticizers and griseofulvin concentrations. The Young's moduli of 100, 370 and 1,000 kDa HPC matrixes without additives were 18.4, 21.7 and 13.1 MPa, respectively. These show a decrease in the modulus for the higher molecular weight polymer. For all experiments, the moduli fluctuates between 5 to 60 MPa for 100 and 370 kDa HPC and between 5 to 50 MPa for 1,000 kDa, reaffirming the slight tendency of a decrease in Young's moduli at higher molecular weights. In this case, the regressor coefficient for molecular weight has a P-value < 0.05. Therefore, as molecular weight increases there is a significant decrease in Young's moduli.

The absence of higher mechanical properties at higher molecular weights can be due to higher crystallization during the extrusion process for lower molecular weight polymers, which can induce higher Young's moduli. The difficulty is that crystallization process is too localized and only comparatively minor sections of a high molecular weight chains are incorporated in a crystal. When chain entanglements of the melt are thus not so much removed, they concentrate into regions between crystals where they give rise to low modulus, non-crystalline regions [44]. For optimal axial stiffness the molecules must be straight and aligned with the tensile axis, but also in their most extended conformation. Crystals preclude further rearrangement of the chains, the molecules are locked in the extended chain conformation, and held in perfect parallel alignment with each other [44]. Thus, in our case extrusion may be creating regions of crystals but if they are separated by non-crystalline regions overall stiffness will remain low for the higher molecular weight and more flexible HPC films. One more reason can be higher polydispersity (PDI) at higher molecular weight HPC, it has been previously demonstrated by several researchers as for example Wang and co-workers that polymers with narrower PDI's show higher mechanical properties [45]. In our case gel permeation chromatography measurements, shown in Appendix C, were inaccurate due to problems with the upper limit of the separation columns, consequently, this argument can not be proved or refuted.

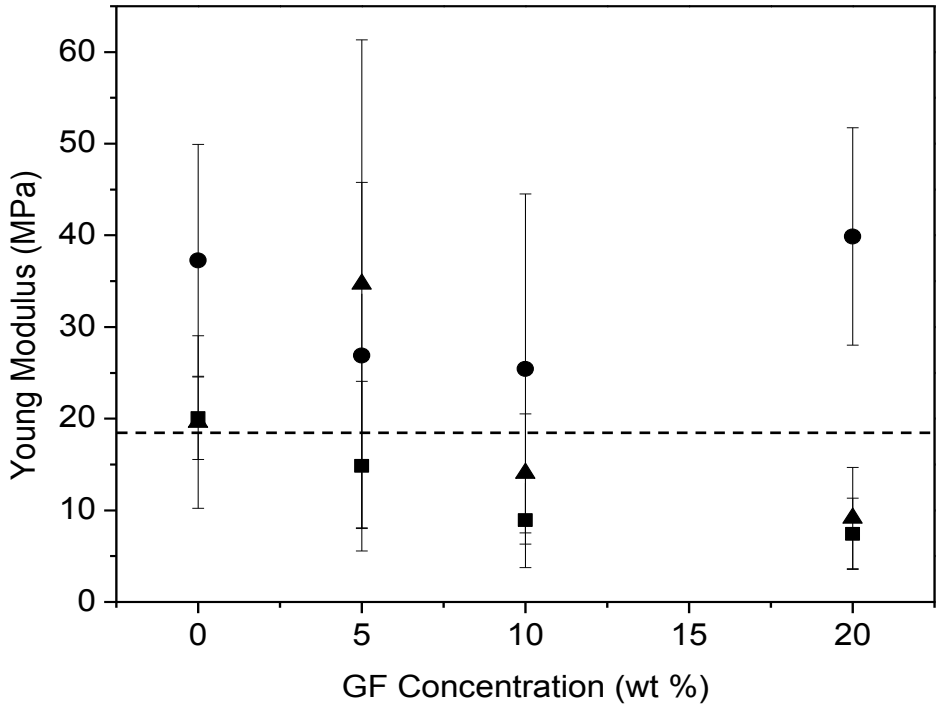

Figure 5:2: Young modulus as a function of griseofulvin concentration for 100 kDa HPC films processed at 190 °C with no aditives (– –), glycerol (■), PEG (●)and d-sorbitol (▲). Error bars represent standard deviation of three measurements.

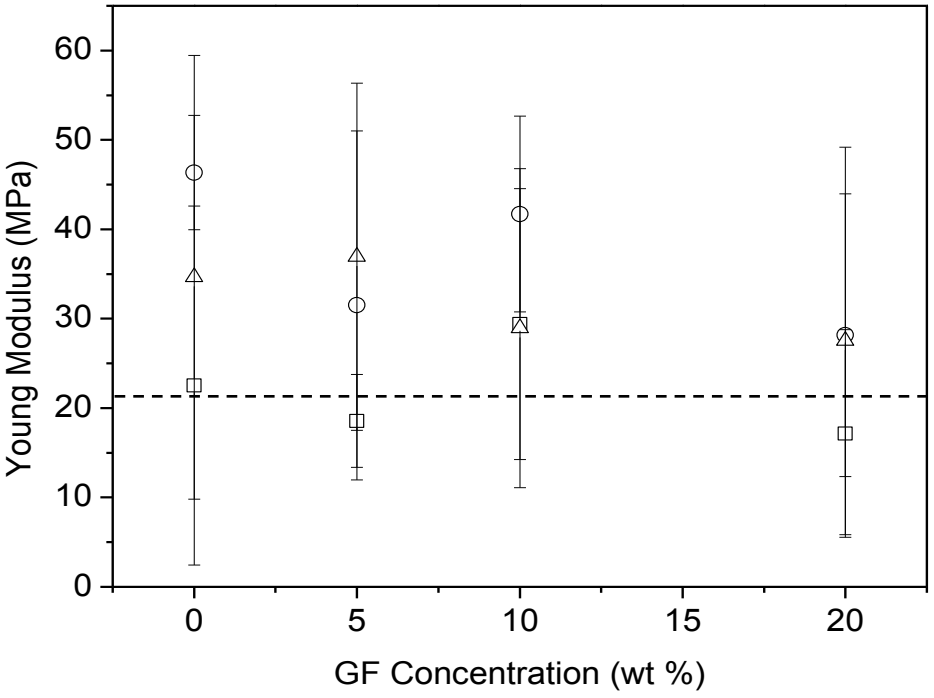

Figure 5:3: Young modulus as a function of griseofulvin concentration for 370 kDa HPC films processed at 190 °C with no aditives (– –), glycerol (□), PEG (○)and d-sorbitol (△). Error bars represent standard deviation of three measurements.

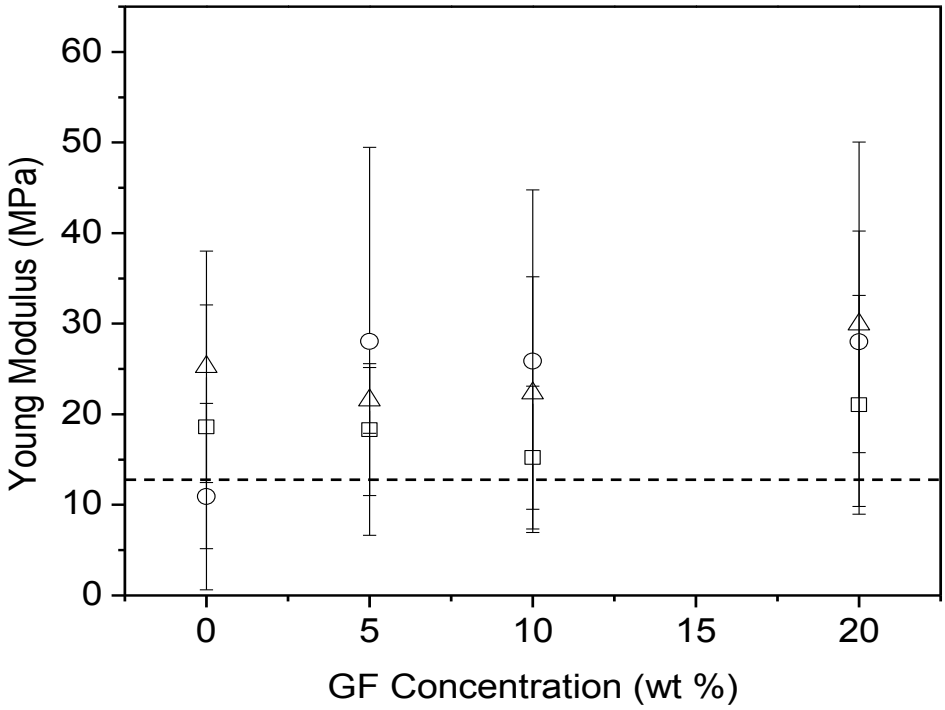

Figure 5:4: Young modulus as a function of griseofulvin concentration for 1000 kDa HPC films processed at 190 °C with no aditives (– –), glycerol (□), PEG (○)and d-sorbitol (△). Error bars represent standard deviation of three measurements.

5.1.5 Effect of Additive

5.1.5.1 Type of Plasticizer

Plasticizers modify mechanical properties by increasing flexibility. It is believed that the thermal motion of the low-molecular-weight plasticizers increase polymers free volume, allowing more "elbow room" for increased long-range segmental motion of the polymer molecules [26]. Criteria considered for evaluating plasticizer effectiveness should include compatibility. Solubility parameters for polymer solutions apply to plasticizers, except that now the polymer is the major constituent of the solution. Several researchers have used this method to access the polymer matrix/plasticizer compatibility, Mididoddi and co-workers obtained

Hildebrand solubility parameters between 21.27 to 23.58 for HPC, utilizing different methods [21].

In this case the addition of plasticizer causes an increase in Young's moduli as can be observed in Figures 5.2, 5.3, and 5.4 in the previous section. The regressor coefficient of the plasticizer has a P-value < 0.05, indicating that addition of plasticizer causes a significant increase in Youngs's moduli (in a range of 5 to 20 MPa). Films processed with glycerol have the smallest antiplasticizing effect. This behavior is in accordance with the lower Flory-Huggins solubility parameter ($\chi = 2.5$) for the HPC / glycerol system calculated in Appendix A. The plasticizers used do not seem to increase the flexibility of the polymer chains because they are not completely miscible with HPC, as determined by calculated Flory-Huggins parameters. The plasticizer is not uniformly distributed throughout the polymeric matrix, therefore it would not create long range segmental motion of the polymer chains. Previous studies have demonstrated that hydrogen bonding is required between HPC and inorganic ceramics in order to avoid phase separation [46].

Repka and co-workers have demonstrated that hot-melt extruded films of HPC 1,150 kDa with PEG 3350 and other plasticizers, have mechanical properties that depend on the composition of the films, and to the molecular weight of the plasticizer [4]. In our case glycerol and d-sorbitol have lower molecular weights than PEG and thus, smaller molar volumes; as a result they will diffuse more efficiently through the polymeric matrix decreasing polymeric intermolecular interactions.

5.1.5.2 Griseofulvin Concentration

At a processing temperature of 190 °C, 100 and 370 kDa films show a slight decrease in Young's modulus with increasing concentrations of griseofulvin, for most of the cases. A

possible explanation is that once griseofulvin is added it interrupts the polymeric interactions of HPC chains, and the ones with the plasticizer creating more chain freedom and therefore it has a plasticizing effect. Repka and co-workers found something similar, when Vitamin E TPGS is added to HPC / PEO hot-melt extruded films the tensile strength of the films decrease. They think that this behavior is due to a plasticization effect of Vitamin E TGPS, decreasing polymer intermolecular interactions to provide greater freedom of movement for the polymeric molecules [19]. As a consequence the tensile strength is decreased and flexibility and elongation are increased. In our case for 1,000 kDa this behavior is not observed, the inclusion of griseofulvin doesn't seem to have any effect. The multiple linear regression coefficient for griseofulvin concentration has a P-value < 0.05, therefore, it has significant contribution to Young's moduli.

5.2 Thermal properties

5.2.1 Introduction

To obtain full benefit of hot-melt extrusion in the formulation of solid dispersions it is necessary to understand how the physical properties of the films vary with the parameters under study. This way the optimum formulation conditions can be determined.

Thermal properties of polymeric films are dependent of chemical structure, molecular weight, stiffness and diluents, among others [47]. The effects that the different processing and formulations parameters used for the experiments caused in the melting peak temperature (T_{mp}) will be discussed in the following section.

Differential scanning calorimetry was used to perform thermal analysis of the films, with one repetition for each sample. This may give information about cristallinity, intra and intermolecular attractions, and thermal and mechanical history of the sample. Through a more in-depth understanding of the thermal properties of the films it may be possible to formulate an adequate drug delivery system, able to comply with processing and solid dispersion requirements.

The multiple linear regression model obtained with Minitab indicates that only molecular weight, and griseofulvin concentration have significant contributions in melting peak temperature response. The empirical model obtained is able to account for 23% of the variability in melting peak temperature response as shown in Appendix G.

5.2.2 Effect of Processing Temperature

It is known that the higher the temperature of crystallization, the higher the melting point of the crystals that are obtained. The forces of attraction between the chains in the well ordered depths of the crystal are greater at the surface so that ticker crystals have higher melting point. Crystalline domains that grow at higher temperatures are thicker (have longer "fold period") and therefore also melt at higher temperature [26].

In our case, Figures 5.6 and 5.7 shows T_{mp} as a function of GF concentration at different processing temperatures. Results demonstrate that in most of the cases there is a tendency for T_{mp} to increase with increasing processing temperature as expected. This behavior is more pronounced for films processed with PEG as the plasticizer. Higher melting temperatures are indicative of greater crystalline domains for 190 °C HME films. DSC analyses were performed for all the samples at the two different processing temperatures, and all the samples showed the same type of behavior. The multiple linear regression coefficient for processing temperature has

a P-value > 0.05, therefore, at a 5% significance level an increase of 10 °C in processing temperature does not have a significant influence in T_{mp}.

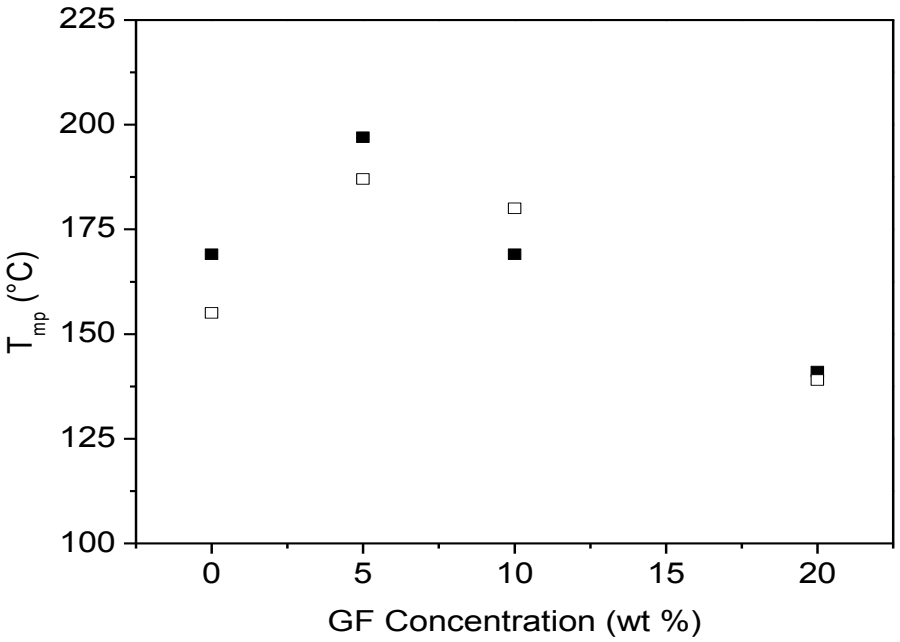

Figure 5:5: Melting peak temperature as a function of griseofulvin concentration for 100 kDa HPC-glycerol HME films at processing temperatures of 180 (□) and 190 (■) °C.

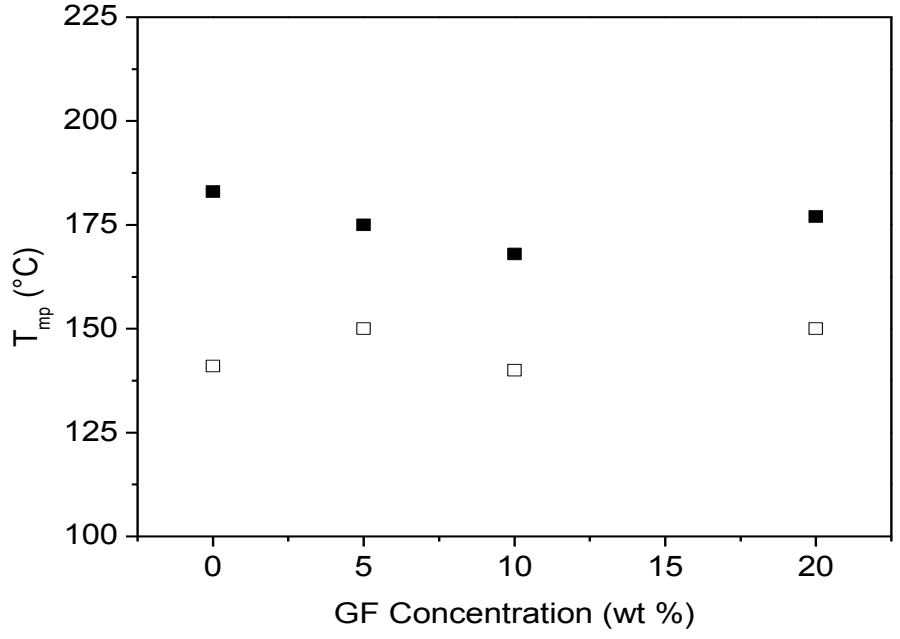

Figure 5:6: Melting peak temperature as a function of griseofulvin concentration for 100 kDa HPC-PEG HME films at processing temperatures of 180 (□) and 190 (■) °C.

5.2.3 Effect of molecular weight

End units on a chain are chemically different. They are usually bulkier than the repeating segments and therefore excluded from the lattice. As the chain length and therefore molecular weight is increased, the number of end-groups is proportionally decreased and the melting temperature increases [47].

Flory established a mathematical equation that describes the relationship of melting temperature (T_m) to number average molecular weight (M_n), as follows [47]:

$$\left[\frac{1}{T_m} - \frac{1}{T_m^0}\right] \propto \frac{1}{\overline{M_n}} \qquad \text{Eq. 5.1}$$

where T_m^0 is the melting point of a pure infinite chain length polymer.

On the other hand, increase in glass transition temperature (T_g) with molecular weight is due to the "extra" free volume contributions associated with polymer chain ends [48]. The same intermolecular forces are responsible for the magnitude of T_g and T_m, thus it follows that, these properties should parallel one another to an extent [26].

A decrease in T_{mp} was observed, for HPC HME films even when no plasticizer is used to process the film, as shown in Table 5-1. This implies that the processing method by itself reduces the thermal transitions of HPC films. Extrusion of HPC films without additives at 180 °C was unfeasible.

HPC MW	HPC powder T_{mp} °C	HPC HME film T_{mp} °C
100 kDa	181	165
370 kDa	212	158
1,000 kDa	216	183

Table 5-1: Peak melting temperatures of powder HPC and HPC HME films processed at 190 °C without additives, obtained from DSC analysis.

Results show that HME films with the different PZ's and GF concentrations have T_{mp}'s in the ranges specified in Table 5-2.

HPC MW	T_{mp} °C of films HME at 180 °C	T_{mp} °C of films HME at 190 °C
100 kDa	139 - 187	141 - 197
370 kDa	151 - 207	139 - 197
1,000 kDa	151 - 201	148 - 203

Table 5-2: Ranges of melting temperatures of HPC HME films with different PZ's and GF concentrations, obtained from DSC analysis.

Figure 5.7 illustrate melting peak temperatures (T_{mp}) obtained from DSC for the different molecular weight HPC, and hot-melt extruded films with plasticizers processed at 190 °C. It is observed that there is an increase in T_{mp} with increase in molecular weight from 100 to 370 kDa for HPC powder and HME films with PEG, but it tends to remain constant from 370 to 1,000 kDa. It might be that in some instances 370 kDa HPC has favorable conditions to accommodate and crystallize at a greater extent, resulting in higher melting temperatures. In this case, the multiple regression coefficient for molecular weight has a P-value < 0.05, hence molecular weight significantly affects T_{mp}.

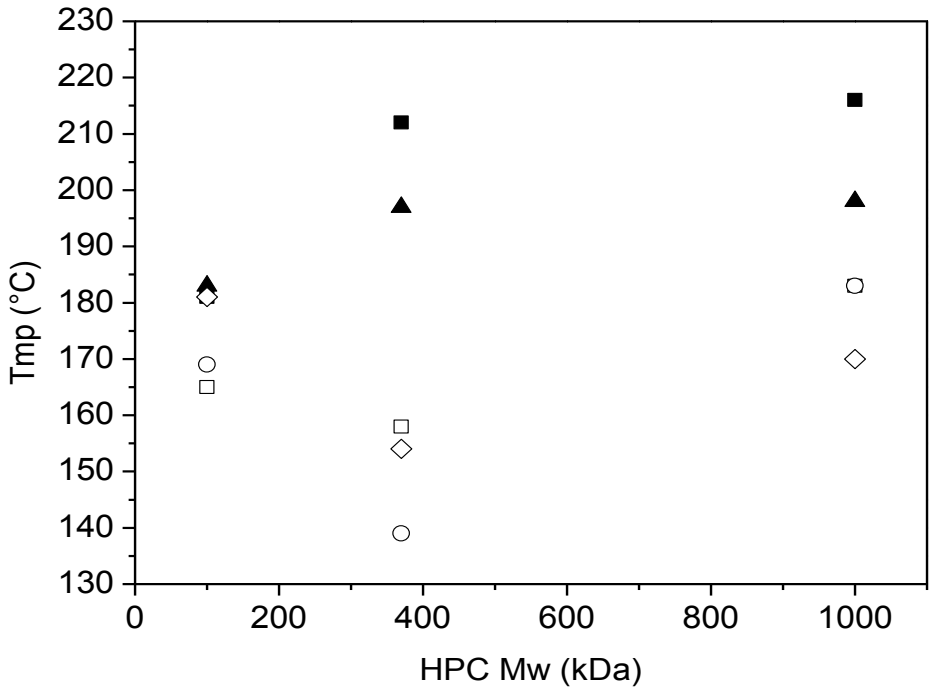

Figure 5:7: Melting point temperature (T_{mp}) as a function of HPC molecular weight for powder (■), hot-melt extruded powder (□) and hot-melt extruded films with PEG (▲), d-sorbitol (◊), or glycerol (○) processed at 190 °C.

5.2.4 Effect of additive

5.2.4.1 Plasticizer

Plasticizers (PZ) are usually used to lower rigidity and decrease glass transition. Plasticizers work by dissolving in the polymer and separating chains from each other to facilitate chain movement [48]. This effect will be more pronounced at higher solubility of the plasticizer on the polymer. If there is a diluent present (good solvent) then the liquid state is a solution, rather than a melt. A solution of a polymer and solvent has larger entropy than a pure polymer and T_m is lowered [47]. Penetration of the plasticizer through the polymeric matrix will also cause partial relaxation of the polymeric chains by reducing intermolecular forces of attraction producing greater freedom of movement across macromolecules [49]. When an additive does not fit onto the crystalline lattice it is excluded from the crystal domains.

Thermodynamic miscibility means that there is only one phase present. In the other hand, the term compatibility is used to denote a mixture or polymer blend that is homogeneous to the eye, remains homogeneous during a time scale, and has enhanced or desirable properties. In our case phase separation of HPC-plasticizer due to incompatibility may be occurring, but it is possible for miscibility regions to occur due to intimate mixing that maximizes surface interaction and favors intermolecular interactions. Mixing in an extruder end result is that component particle size must be reduced so that there is intimate mixing that allows particle surfaces and molecular groups to freely interact. Flory-Huggins interaction parameters calculated as shown in Appendix A, suggest that the mixtures are not completely miscible, therefore there has to be phase separation to some extent. Glycerol and d-sorbitol have χ of 2.5 and 4.1 in that order with respect to HPC, while PEG has a χ of 153. This proves that the lower molecular weight plasticizers are more miscible and as a result should be more effective when reducing thermal transitions. Several researchers such as Rowe and coworkers demonstrated that as molecular weight and size of PEG is decreased, the mole fraction of available hydroxyl groups to interact with the hydroxyl groups of the polymer will increase [50]. That explains why in our case glycerol and d-sorbitol, the lower molecular weight PZ's at a fixed concentration of 5 wt% decrease to a greater extent T_{mp} and therefore are better plasticizers than PEG.

Figure 5.7 illustrated in the previous section, shows that in some instances the plasticizers and the concentration used for the formulations had an antiplasticization effect. PEG causes an antiplasticization effect at all molecular weights whereas for 100 kDa HPC all plasticizers had an antiplasticization effect. Antiplasticization may occur, when small amounts of plasticizer are used. Small amounts of plasticizer (below a certain amount) provide enough additional free volume, to permit limited chain mobility and realignment. This, apparently results in greater

degree of polymer-polymer interaction and molecular order [49]. Gutierrez-Villarreal and coworkers reported this behavior for PMMA films prepared from blends with triacetine and triethylcitrate as plasticizers at concentrations of 10 to 20 wt% and pressed at 200 °C. In their case antiplasticization was explained by the formation of secondary bonds like hydrogen bonds and Van der Waals interactions between the additive and PMMA molecules [49]. Antiplasticization has also been reported for plasticizers that has both a high polarity and a relatively bulky or rigid structure. It may be the case that a plasticizer concentration of 5 wt% permitted lower molecular weight HPC to align in a certain manner such that polymer-polymer interactions increased in order to achieve an equilibrium state. Other researchers such as Repka have used HPC with PEG and PEO as plasticizers (with M_w's of 400 and 1,000,000 g/mol, respectively) for HME at concentrations no lower than 20 wt%, showing plasticization effects on thermal transitions [19].

5.2.4.2 Griseofulvin Concentration

Thermal properties depend on mixing ratios, Flory stated that T_m depression is proportional to the amount of impurity, end-group, or diluents as depicted as in the following equation [47];

$$\left[\frac{1}{T_m} - \frac{1}{T_m^0}\right] \propto (\Phi_s - \Phi_s^2 \chi) \qquad \text{Eq.5- 2}$$

where T_m^0 is the melting temperature of a pure infinite chain length polymer, Φ_s is the volume fraction of the diluent or solvent and χ is the Flory-Huggins interaction parameter between the polymer and the solvent. During melt blending at high shear is possible that the filler migrates into the polymer, which reduce crystallinity and thus T_g decreases [51].

Figures 5.8, 5.9 and 5.10 show T_{mp} as a function of GF concentration at different HPC molecular weights, for each PZ. Figures 5.8 and 5.9 show that when glycerol and d-sorbitol are used as PZ's an increase in T_{mp} is observed when an initial concentration of 5 wt% GF is introduced into the films. But then as GF concentration is increased, T_{mp} starts decreasing in most of the cases. The multiple linear regression coefficient for drug concentration shows a P-value < 0.05, thus, there is a significant decrease in T_{mp} with increasing drug concentration. The addition of GF creates an antiplasticization effect at 5 wt %. As shown by the strengths of interaction calculated in Appendix B, GF have stronger intra molecular interactions with the plasticizers allowing for more polymer-polymer interactions and, therefore, increasing T_{mp}. It seems that the antiplasticization effect is most typical for partially compatible systems. The introduction of small amounts of plasticizers of a particular type, facilitates segmental mobility, and, as the plasticizer concentration increases, leads to structural regrouping which brings the system into a more stable equilibrium (and energetically more favorable) state [52].

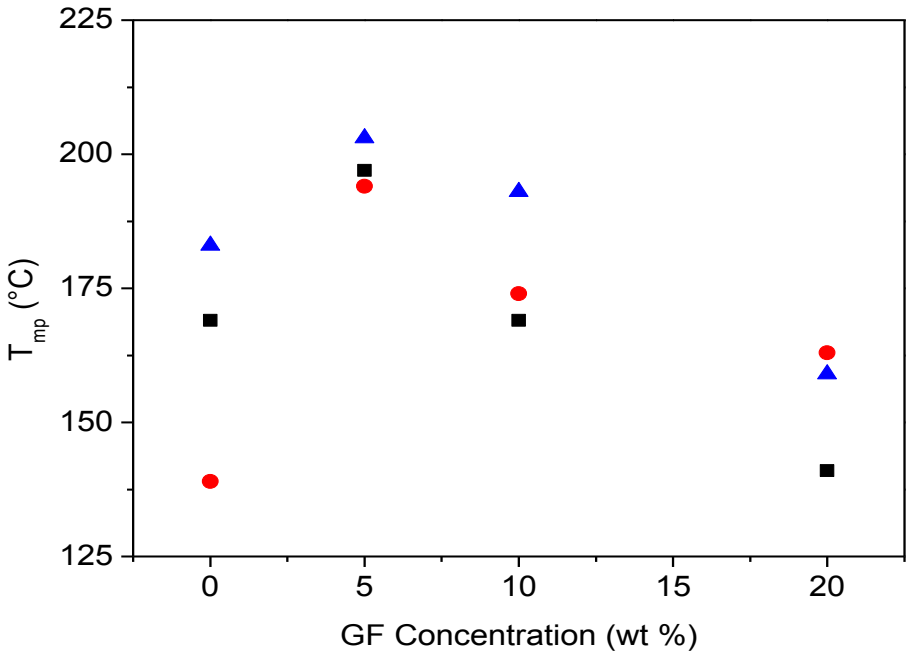

Figure 5:8: Melting point temperature (T_{mp}) as a function of griseofulvin concentration for HPC-glycerol HME films processed at 190°C with 100 (■), 370 (●), or 1,000 kDa (▲) HPC.

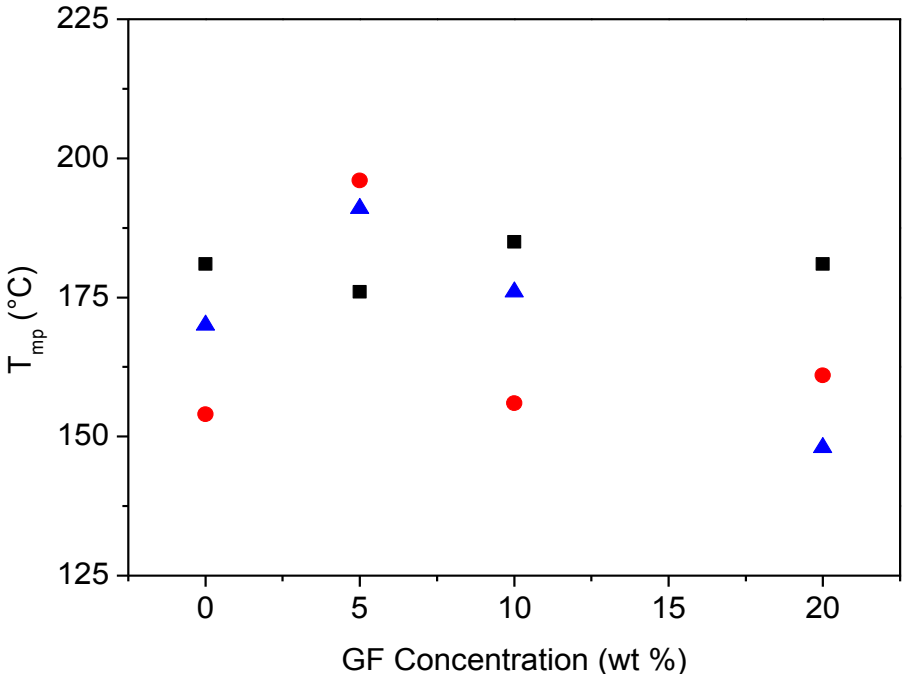

Figure 5:9: Melting point temperature (T_{mp}) as a function of griseofulvin concentration for HPC-d-sorbitol HME films processed at 190°C with 100 (■), 370 (●), or 1,000 kDa (▲) HPC.

Contrary to the other plasticizers, when GF is added to HPC / PEG systems T_{mp} decreases at all GF concentrations as observed in Figure 5.10. In this case GF is more compatible with HPC rather than PEG, hence reducing polymer-polymer interactions at all concentrations. As GF concentration increases there is a tendency for T_{mp} to decrease, this may indicate that GF is dispersed through the polymer matrix. As HPC / PZ / GF mixtures are blended in the extruder, HPC domains can phase separate by GF domains.

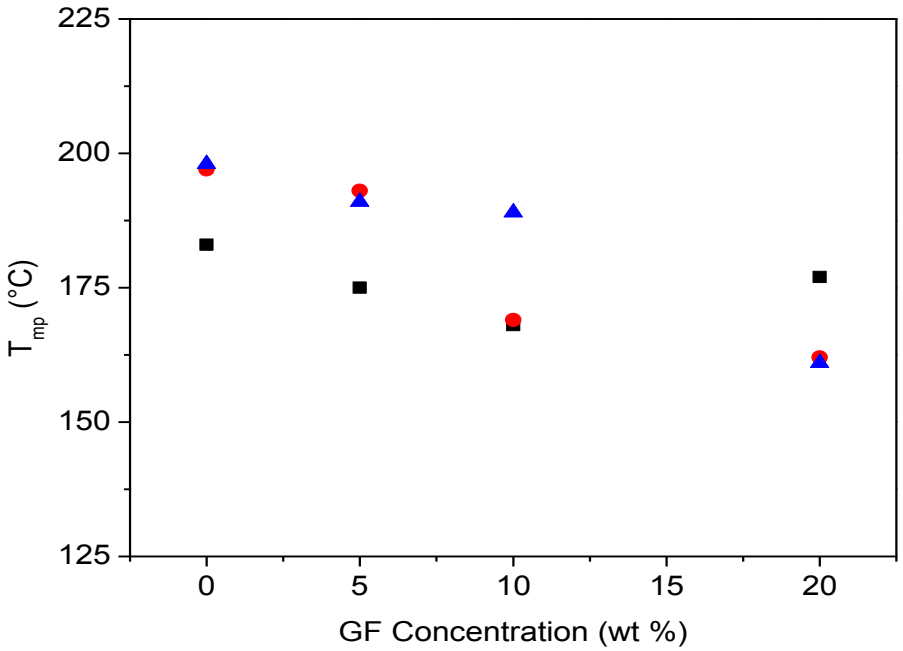

Figure 5:10: Melting point temperature (T_{mp}) as a function of griseofulvin concentration for HPC-PEG HME films processed at 190°C with 100 (■), 370 (●), or 1,000 kDa (▲) HPC.

In previous studies it has been observed that when a drug is added to a polymeric matrix and is hot-melt extruded the obtained film has lower thermal transitions. In the case of Repka when vitamin E TPGS, which is a waxy solid with a polar hydrophilic head and lipophilic tail, and T_m of 38 °C, is used in a HPC / PEO matrix as concentration increases from 1 to 5 wt % the thermal transition decrease by 10 °C. This is attributed to the weakening of the intermolecular attractions within the polymer blends, which increases the polymer free volume [19]. Mididoddi obtained similar results, for PEO / ketoconazole HME films, when 20 wt% ketoconazole was added the melting point of the film decreased by 6 °C. In this case ketaconazole is a solid with a T_m of 148 °C and a difference in solubility parameters of 2.98 $MPa^{1/2}$ between HPC and PEO [21]. Mididoddi states that T_m depresion may be due to transition of extended chain crystallities into folded-chain crystallities, which have lower T_m's or to the drug-polymer interactions [21].

Another way to explain decrease in T_{mp} as additive concentration increases is that low molecular weight substances have a much higher degree of mobility at high temperatures compared with that of macromolecules. It is then evident, that when a mixture is heated thermal energy is taken up by additive molecules first, and then passed on as kinetic energy to the polymer. Apparently, through this mechanism the entire material acquires mobility at low temperatures, and the larger the additive concentration, the lower the temperature at which this mobility becomes possible [52]. It is believed that at low concentrations, the additives are insufficient to cause ordering to take place in the entire volume of the material. As the modifier concentration is increased, structural regrouping takes place under conditions of facilitated mobility and involves the participation of polymer and additive tending towards reduction in the free energy of the system [52]. In our case the heat of fusion (ΔH_f) obtained for the samples are tabulated in Appendix E, Table E-3. It can be observed that for all cases there is a decrease in ΔH_f when increasing griseofulvin concentration from 0 to 20 wt%.

DSC thermograms of the films did not show a peak for griseofulvin after the films were processed. This can be due to the presence of GF in the amorphous state or that GF is dissolving in the HPC / PZ melt during the heating cycle of the DSC studies. Mididoddi and coworkers observed the same behavior in DSC thermograms for HPC / PEO / ketoconazole HME films processes from 150 to 160 °C. The drug should have a peak at 148 °C, and the absence was attributed to the formation of solid solution or to solubilization of the crystalline drug in melted PEO during DSC analysis [21].

5.3 Rheological Properties

5.3.1 Introduction

In order to be able to implement HME for preparing polymer-drug delivery systems, knowledge of the rheological properties of the mixture is required for the formulation and process design. Understanding of the relationships between shear and extensional flows with temperature, processing rate, and polymer/additive systems is advantageous. This information is necessary when conducting process optimization, troubleshooting, or computational fluid dynamic simulations [18].

The applicability of HME has been demonstrated for the development of solid dispersions, transdermal and bioadhesive films, suppositories, pellets, and tablets [18]. In the melt extrusion process, rheology of the polymer melt is an important factor affecting processing conditions and properties of the pharmaceutical product [18]. It is known that carrier properties will influence drug release and correlate with their physicochemical properties [53]. So, physicochemical characterization of the system is essential to ensure efficacy and performance of solid dispersions. Therefore, it is necessary for solid dispersion processing and equipment design, to determine the effects of the polymer molecular weight, plasticizer, drug concentration and processing temperature, as well as extrusion conditions on the melt flow properties of HPC-griseofulvin solid dispersions to identify critical formulation parameters and process parameters of HME.

5.3.2 Capillary Rheometry

Capillary rheometers are used to determine shear properties of the fluid under characteristic shear rates and temperatures of HME processing [18]. The range of shear rates encountered in conventional polymer extrusion processes is between 100 – to 1,000 s^{-1} [18], throughout this work the range of shear rates used was between 36 – to 320 s^{-1}. Extensional properties become important during flow into the die cavity, where melt flow converges and the polymer molecules undergo stretching, alignment and alteration in chain entanglement [18]. Nevertheless, the dominant flow during die or tube extrusion of polymeric melts, is shear flow. Thus, in the case of extrusion of polymeric materials processing properties may be characterized by the shear flow curve [54].

The multiple linear regression model obtained with Minitab indicates that molecular weight, and griseofulvin concentration contribute significantly to the model, as well as the interactions of drug concentration with molecular weight and processing temperature. This empirical model is able to account for 59% of the variability in viscosity response, as shown in Appendix G.

5.3.3 Effect of Molecular Weight

How readily a molecule flow is a function of molecular weight (how much the molecules are entangled), and of molecular structure (how strong intermolecular forces are) among others [26]. Molecular entanglement increases as molecular weight increases, and London forces become increasingly significant as molecular weight increases [26], therefore molecular weight is a critical variable in rheology. More rigid polymers are significantly more viscous, except in the unusual situation where chain conformation results in liquid crystal behavior [26]. The

flexibility of a polymer chain, may be determined by the contribution from the flexibility of individual backbone bonds in terms of both bond stretching and the distortion of the angles between different bonds at a given atom [44]. For most of the molecules the greatest contribution to flexibility stems from rotation about single backbone bonds which enable the chain to take up a wide range of trajectories [44]. Therefore, as molecular weight increases backbone bonds increase resulting in higher flexibility, thus increasing viscosity.

One of the first polymers to exhibit liquid crystalline behavior was a copolyester prepared from terephthalic acid, ethylene glycol and p-hydroxybenzoic acid. It was observed that as p-hydrobenzoic acid concentration was increased, melt viscosity initially increased, which was expected because of the decreased flexibility caused by the incorporation of the "rigid" p-hydroxybenzoate unit [26]. At levels of 30 mol %, the melt viscosity began to decrease reaching a minimum at about 60 to 70 mol %. The viscosity effects result from the rigid polymeric mesophases becoming aligned in the direction of flow, minimizing frictional drag [26].

A power law index (n), of less than one describes the shear thinning character of a polymer melt and is calculated from the slope of a bi-logarithmic shear stress versus shear rate plot. K is the consistency index of the melt and is obtained from the intercept of the shear stress at zero shear rate. The power law index and consistency index of 100, 370 and, 1,000 kDa HPC were calculated at 180 and 190 ℃. Results obtained are summarized in Table 5-3. At 180 ℃ it was unfeasible to extrude the HPC films, and there is no correlation observed between the power law index and molecular weight. On the other hand, at 190 ℃ films extruded, but still there is no correlation between power law index and molecular weight. All the power law indexes obtained are less than one suggesting that the molecular weights of HPC used have a shear thinning behavior. Shear thinning is due to the variation of the rate of chain disentanglement with

increasing shear rate. In previous studies Paradkar and coworkers found that for 65, 131, and 171 kDa HPC, measurements on a capillary rheometer deviated from the power law at shear rates above 1000 s^{-1} and processing temperatures of 140, 145 and 150 °C. The deviations were attributed to departures from the assumptions on which the power law model is based. In the case of Paradkar, power law index showed no correlation to molecular weight and ranged between 0.21 to 0.31, whereas consistency index increased with increasing molecular weight and decreasing temperature [18].

HPC M_W [kDa]	Processing temperature					
	180 °C			190 °C		
	n	log(K)	R^2	n	log(K)	R^2
100	0.38	2.50	0.98	0.51	2.26	0.99
370	0.17	3.63	0.78	0.48	2.33	0.31
1000	0.16	3.71	0.69	0.69	2.39	0.95

Table 5-3: Values of power law (n) and consistency index (K) for different molecular weight HPC powders processed at 180 and 190 °C.

The ranges of viscosity of the different molecular HPC melts at 190 °C are summarized in Table 5-4.

HPC Mw (kDa)	Viscosity (Pa s) at 190 °C
100	33 – 1
370	32 – 7
1,000	86 – 39

Table 5-4: Ranges of viscosities for different molecular weight HPC melts processed at 190 °C, with increasing shear rate.

Figure 5.11 shows the logarithm of viscosity as a function of HPC molecular weight, as expected viscosity increases with increasing molecular weight by one order of magnitude at high shear rates. The multiple linear regressor coefficient for viscosity has a P-value < 0.05. Consequently, the increase in viscosity with increasing molecular weight is significant.

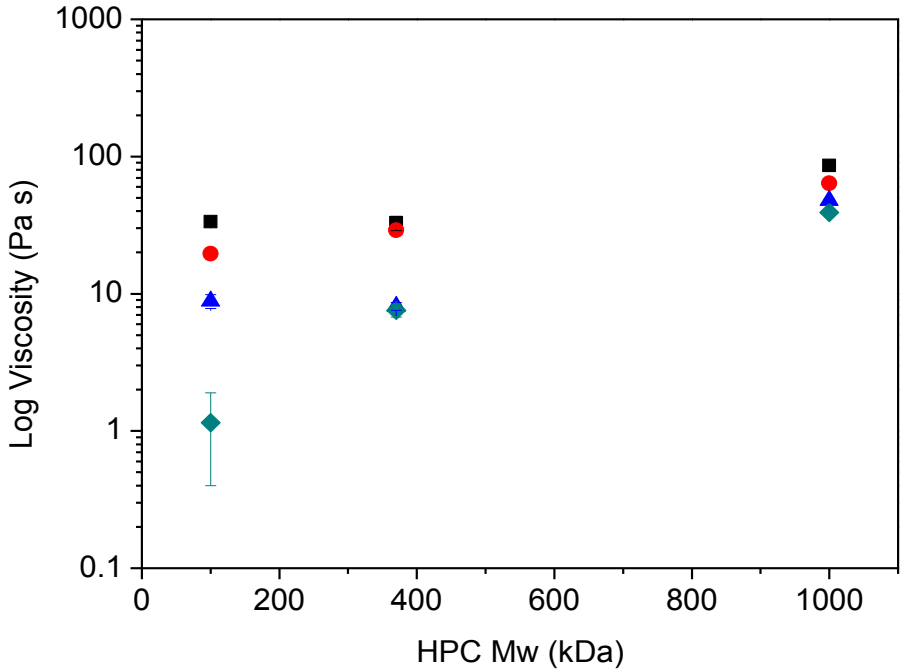

Figure 5:11: Melt viscosity as a function of HPC molecular weight at shear rates of 36 (■), 107 (●), 213 (▲), and 288 (♦) s^{-1} for HPC melts processed at 190 °C. Error bars represent the standard deviation of averaged steady-state values.

5.3.4 Effect of temperature

Viscosity can be related to temperature by the following equation:

$$\eta \propto \frac{1}{T} \qquad \text{Eq. 5-3}$$

It is known that the viscosity of all liquids and polymer melts decreases with increase in temperature because of the increased mobility of the polymer molecules [14]. Sensitivity to temperature varies from polymer to polymer, usually semicrystalline polymers have relatively

low temperature sensitivity [14]. It is also known that the effect of temperature on the viscosity is considerably more pronounced at low shear rates [25].

Rheological data was collected at 180 and 190 °C for all the samples. Figure 5.12 shows shear stress as a function of shear rate for 100 and 1,000 kDa HPC melts. It can be observed that for 100 kDa HPC an increase of 10 °C in processing temperature shows no change in shear stress response, but for 1,000 kDa HPC at low shear rates increasing processing temperature lowers shear stress response. This suggests that as expected the more flexible polymer will be more sensitive to changes in temperature.

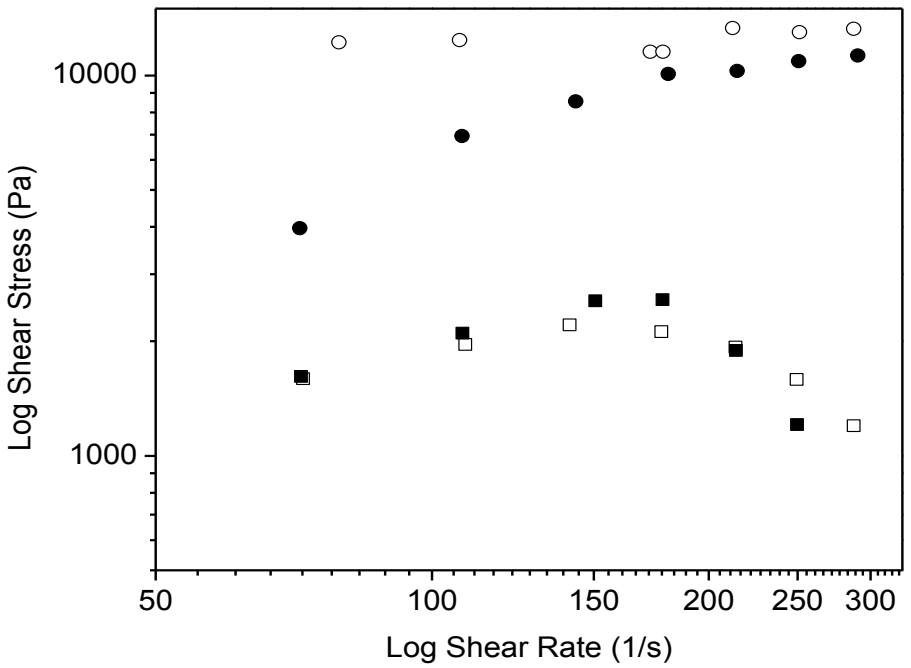

Figure 5:12: Shear stress as a function of shear rate for 100 kDa HPC melts at 180 °C (□), and 190 °C (■) and 1,000 kDa HPC melts at 180 °C (○), and 190 °C (●).

Figure 5-13 shows plots of shear stress as a function of shear rate for 100 kDa HPC melts with each plasticizer at the two processing temperatures. It can be observed that the only plasticizer that does not seem to cause a difference in shear stress with increasing processing

temperature is d-sorbitol. On the other hand, glycerol seems to decrease shear stress with an increase in processing temperature at high shear rates. Whereas PEG shear stress response deviates from the expected behavior at shear rates above 100 s^{-1} and is near the minimum capacity of the extruder. The empirical model obtained shows that viscosity tends to decrease with increasing processing temperature, but the regressor coefficient P-value is greater than 0.05. Thus, there is no statistically significant contribution to viscosity.

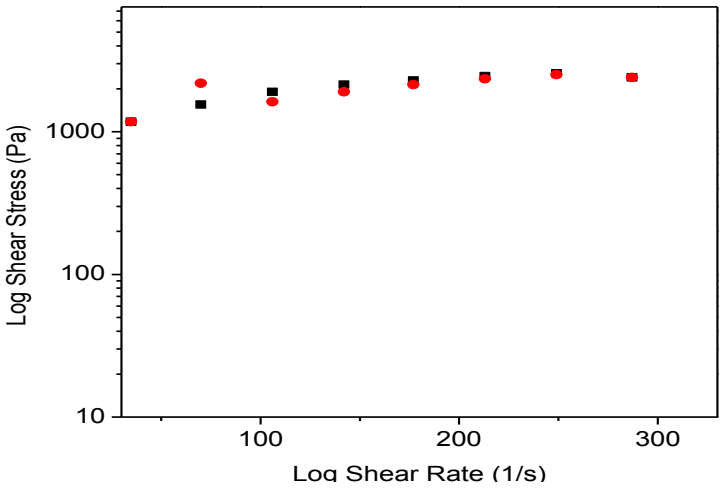

D-sorbitol

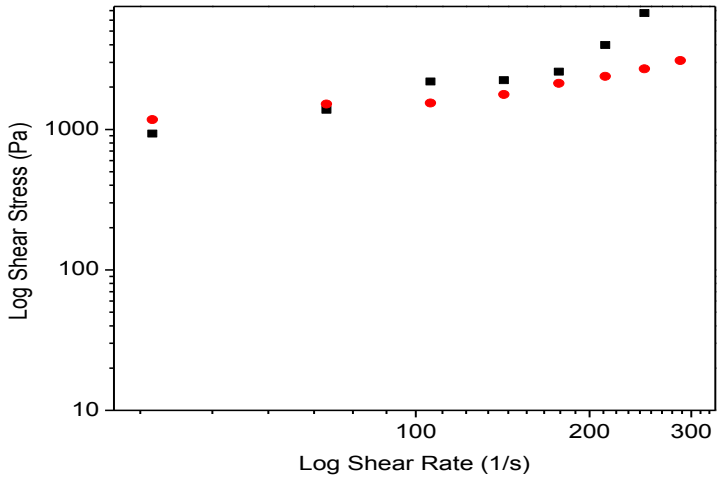

Glycerol

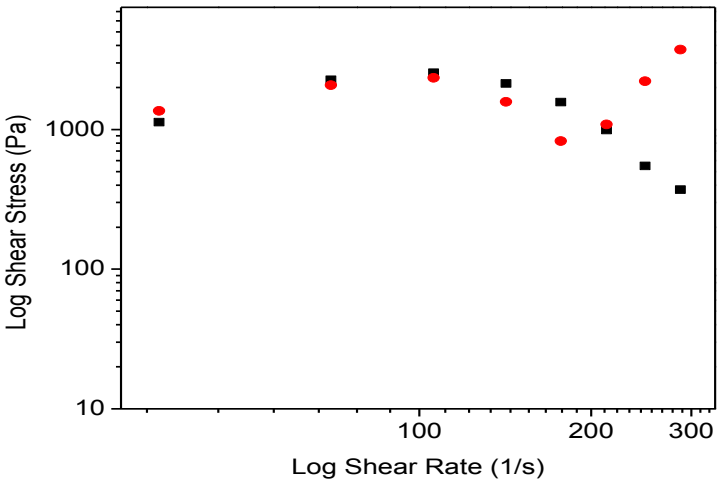

PEG

Figure 5:13: Shear stress as a function of shear rate for 100 kDa HPC melts with the different plasticizers at processing temperatures of 180 °C (■), and 190 °C (●).

5.3.5 Effect of additives

5.3.5.1 Plasticizer

A plasticizer should reduce the viscosity to facilitate extruding. As mentioned before it is believed that the thermal motion of the low molecular weight plasticizers increases the polymer free volume, allowing more "elbow room" for increased long-range segmental motion of the polymer molecules [26].

Solubility factors for polymer solutions apply to plasticizers, but now the polymer is the major constituent of the solution. Flory-Huggins solubility parameters were calculated in Appendix A for the polymer-plasticizer systems. These parameters indicate that our plasticizers are not completely miscible in HPC. Solubility of the plasticizers decrease in the following order: glycerol > d-sorbitol > PEG. It is stated in literature, that a plasticizer having "poor" solubility will reduce the viscosity of a polymer more than one having "good" solubility at equal levels of dilution [26]. In our case Figure 5.14 illustrate viscosity as a function of molecular weight on a bi-logarithmic scale for HPC melts at shear rates of 36, 179 and 288 s^{-1} respectively, with each of the plasticizers. It can be observed that plasticizers have different effect depending on HPC molecular weight and shear rate. For 100 kDa HPC, at low shear rates glycerol and d-sorbitol seem to have a plasticizing effect, but as shear rate is increased all plasticizers point to antiplasticizing effect. For 370 kDa HPC at shear rates above 179 s^{-1} glycerol has the highest plasticizing effect. Whereas for 1,000 kDa HPC, plasticizers illustrate antiplasticizing effect at all shear rates. In this case the multiple liner regression coefficient for viscosity had a P-value > 0.05 and showed no contribution to the model, therefore it was eliminated.

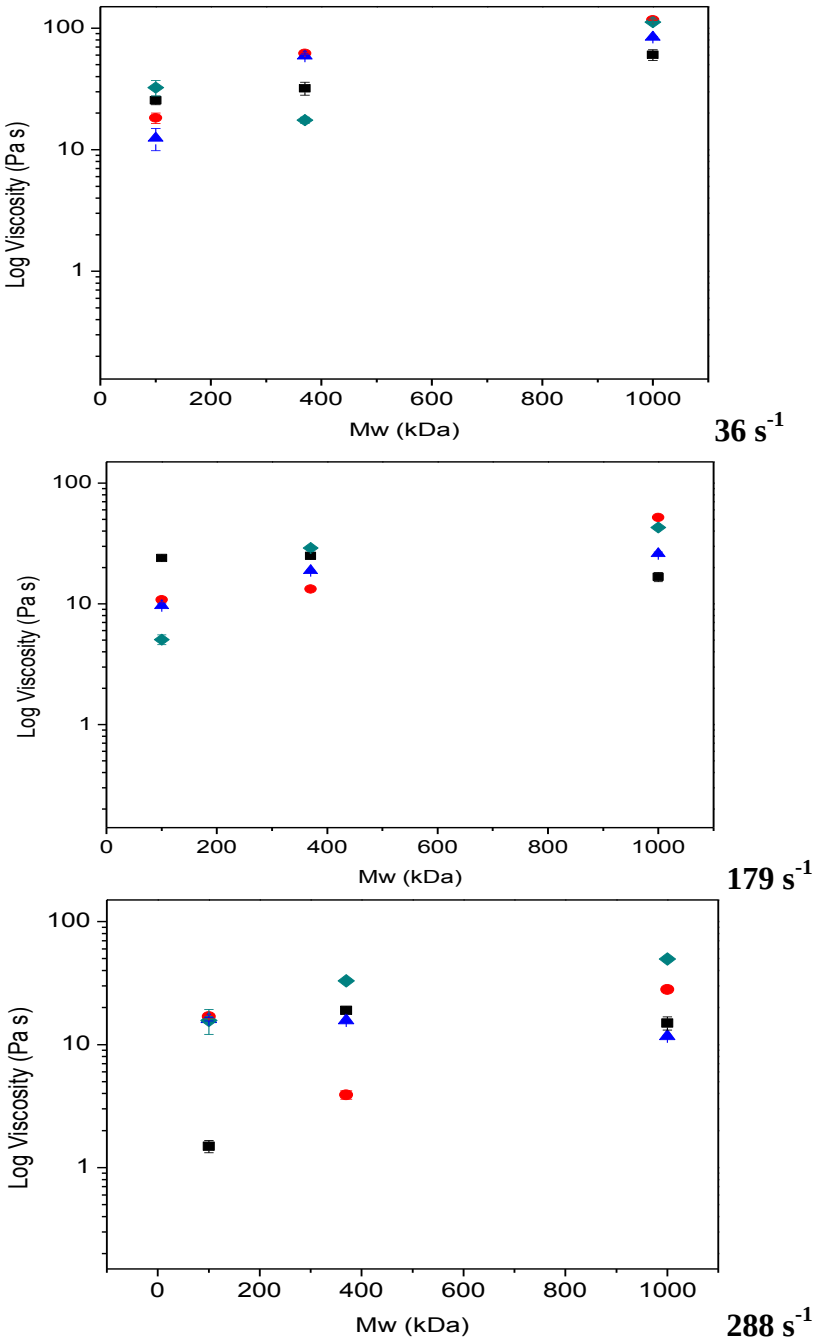

Figure 5:14: Log Viscosity as a function of molecular weight at shear rates of 36, 179 and 288 s^{-1} for HPC melts processed at 190 °C with no plasticizer (■), glycerol (●), d-sorbitol (▲), and PEG (♦).

It is known that viscosity is mainly related to two factors. The first depends upon local features such as free volume, which governs the viscosity of liquids of small molecules [47]. The

second factor depends upon the entanglements of the chains with one another and becomes important once a critical value of molecular weight (i.e. chain length) is reached [47]. The strengths of interaction calculated in Appendix B indicate that inter molecular interactions of HPC-HPC chains and plasticizer-plasticizer molecules are stronger than the intra molecular forces of HPC-PZ. Therefore, HPC and the different plasticizers used will tend to remain separated as illustrated in Figure 5.15.

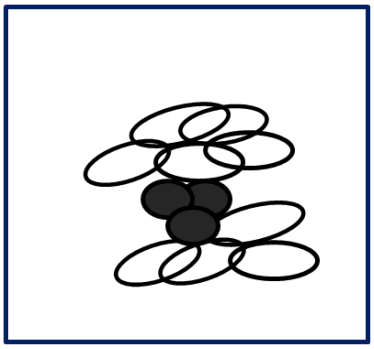

Figure 5:15: Diagram of the interactions between HPC (○) and plasticizer (●) mixtures with hypothetical shape molecules.

It can be imagined that the lower molecular weight plasticizers that are more miscible, will diffuse through the polymeric matrix creating more free volumes and reducing friction and entanglements between polymer chains, thus decreasing viscosity. In our case this behavior was observed at 370 kDa, but not for 100 and 1,000 kDa HPC films where the more miscible plasticizers had an antiplasticizing effect in viscosity. It appears to be that for 100 kDa HPC (more rigid polymer) at high shear rates the inclusion of small molecules disrupts HPC chains alignment.

5.3.5.2 Griseofulvin concentration

As deducted by Einstein the relative viscosity η_r of a very dilute suspension of spheres of volume concentration ϕ could be expressed by [55]:

$$\eta_r = (1 + 2.5\ \emptyset) \qquad \text{Eq. 5-4}$$

Therefore, one would expect that as concentration of the filler increases the η of the mixture ought to increase. Figure 5.16 shows the logarithm of viscosity as a function of griseofulvin volume fraction for 1,000 kDa HPC melts processed at 190 °C. It can be observed that at shear rates below 250 s^{-1} there is a slight increase in η when 0.05 griseofulvin volume fraction is added, but as shear rate increases η is reduced. On the other hand, at 0.20 griseofulvin volume fraction η is reduced by almost one order of magnitude at all shear rates. Consequently, it can be said that griseofulvin has a plasticizing effect on HPC. Since, the viscosity is reduced it does not follow the Einstein's viscosity law assumption of non-interacting particles is not valid.

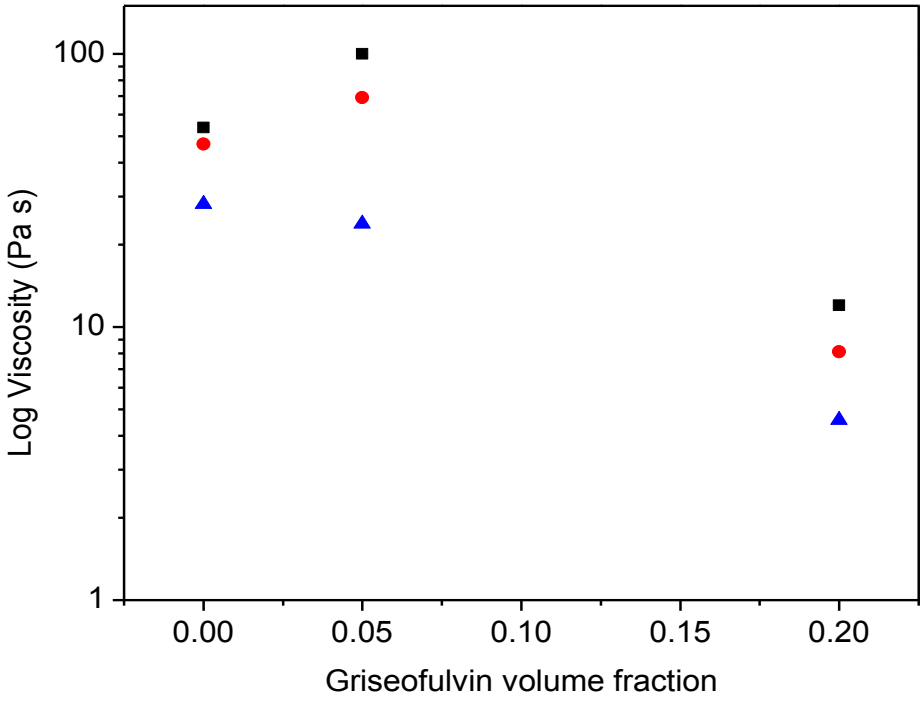

Figure 5:16: Melt viscosity as a function of griseofulvin volume fraction for 1,000 kDa HPC melts processed at 190 °C at shear rates of 71 (■), 143(●), and 250 s^{-1} (▲).

Figure 5.17 illustrates the logarithm of viscosity as a function of griseofulvin volume fraction at different shear rates, for HPC 1,000 kDa with the different plasticizers. The same tendencies were observed at all HPC molecular weights. Contrary to HPC / GF films, when GF is added to HPC / PZ matrix the viscosity increases with increasing GF concentration, as was expected from Einstein equation. In this case Eq. 5-4 over predicts the experimental viscosity especially at higher concentrations. Einstein early studies only considered dilute suspensions consisting of uniform size rigid spherical particles [56], and it may not be applicable to our system.

For most of the cases viscosity decreases with increasing shear rate, indicative of shear thinning behavior. During capillary rheometry, shear thinning usually develops at relatively high shear rates. This phenomenon is believed to stem from disturbances of the equilibrium interparticle distance, so that the time required for the particles to return to the equilibrium position is longer than the reciprocal of the shear rate [3]. When d-sorbitol is used as plasticizer and there is no griseofulvin, the higher shear rate viscosity decrease by one order of magnitude, but as griseofulvin concentration increases viscosity decrease by less than one order of magnitude. Therefore, it can be said that the addition of griseofulvin into the HPC / d-sorbitol matrix reduces the rate of chain disentanglement. For glycerol and PEG the rate of chain disentanglements seem to remain constant, and viscosity seems to remain constant when increasing from 0.10 to 0.20 griseofulvin volume fraction. The standard deviation of the measurements is approximately ± 2.5 Pa s. The multiple linear regression coefficient for griseofulvin concentration has a P-value < 0.05 and, thus, has a significant contribution to viscosity.

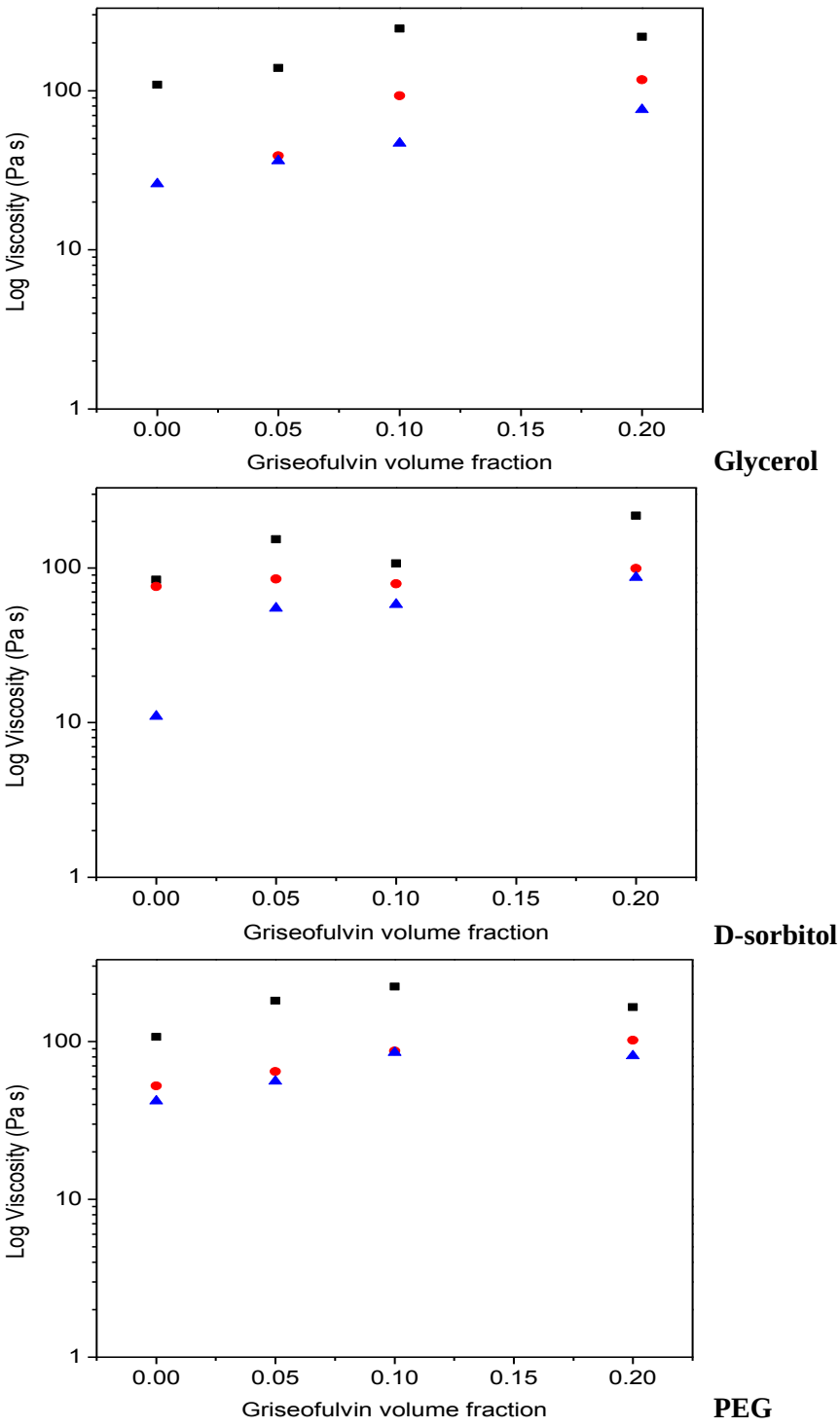

Figure 5:17: Viscosity as a function of griseofulvin volume fraction for 1,000 kDa HPC melts processed at 190 °C with the different plasticizers at shear rates of 36 (■), 143(●), and 250 s^{-1} (▲).

Chokshi and coworkers studied the rheology of HME solid dispersions of poloxamer (T_m = 52 °C) and indomethacin (T_m = 165 °C), which had a difference in solubility parameters of less than 4 $MPa^{1/2}$. They found out that the viscosity of the polymer-drug mixtures was higher compared to the viscosity of the pure polymer melt, indicating immiscibility of the drug in polymer at 60 °C. As the amount of the drug increased in mixtures, the viscosity increased for the binary mixtures. This result suggested that the drug does not show complete miscibility in the polymer and thus the drug imparted higher viscosity to the formulations [3]. They concluded that the binary mixtures containing drug and poloxamer formed a two phase system, thus higher amounts of E_a were required to initiate the flow as a function of the drug concentration [3]. It is also known that when inter molecular forces are strong; these forces encourage agglomeration, which interrupts optimal packing, causing lower packing density. Such low packing density fillers, at a given content, immobilize the matrix fluid, requiring higher shear stresses for flow [56].

In our case Flory-Huggins solubility parameters indicate that griseofulvin is not completely miscible in HPC. The strengths of interaction calculated in Appendix B point out to stronger intra molecular interactions of griseofulvin with glycerol and d-sorbitol. But, independently of the strengths of interaction when there is a plasticizer present griseofulvin increases viscosity. The inclusion of griseofulvin together with the plasticizers must be creating agglomerates that increase as griseofulvin concentration increases, and hinder the macromolecular movement of the HPC chains, increasing flow resistance. This flow resistance, also results in poor crystallization reducing T_{mp} as indicated by DSC results. This is supported by the elimination of the antiplasticization effect of griseofulvin.

6 CONCLUSIONS AND RECOMMENDATIONS

In this research work, the effects of processing temperature, polymer molecular weight, type of plasticizer and drug concentration on solid dispersions formulated via hot-melt extrusion were investigated. Processing temperatures of 180 and 190 °C were used during HME, with HPC molecular weights of 100, 370 and 1,000 kDa, a 5 wt% of glycerol, d-sorbitol or PEG 8000 were used as plasticizers and model drug (griseofulvin) concentrations at either 0, 5, 10, or 20 wt%. The experimental responses of mechanical, thermal and rheological properties of the HME solid dispersions were evaluated. In order to interpret the results the molecular interactions between the polymer, plasticizer and model drug have to be considered. Through an understanding of interactions between polymer, plasticizers and drug particles and their responses on the investigated variables guidelines to predict or optimize the formulations of other systems with similar properties were developed. In this chapter, the conclusions from the previous chapter are summarized and guidelines for the formulation of solid dispersions via HME are presented.

6.1 Mechanical Properties Conclusions

The mechanical tests results obtained using the Anton Paar MCR 301 extensional fixture SER2 had a large uncertainty. This is common for polymers; therefore to reduce the uncertainty a minimum of ten samples must be evaluated. Tests on individual regression coefficients of the multiple linear regression indicates that all factors evaluated have a significant contribution to the Young's moduli response.

Within the temperature range used for the experiments Young's moduli of lower molecular weight HPC showed to be more sensitive to changes in processing temperature. Increasing processing temperature caused a decrease in Young's moduli.

In terms of the effects of molecular weight it was observed that Young's moduli increased from 100 to 370 kDa HPC but decreases at 1,000 kDa HPC. The behavior that we experienced is not the norm, indicating that factors such as polydispersity, chain stiffness, and crystallization are relevant when evaluating the moduli of semirigid polymer HME films.

Addition of 5 wt% plasticizer resulted in an apparent increase in Young's moduli especially when PEG was used as plasticizer. The use of low concentrations of an immiscible high molecular weight plasticizer will result in a stiffer material when hot-melt extruded with a liquid crystal polymer. Films with plasticizers showed Young's moduli in the following ascending order: glycerol, d-sorbitol, and PEG, which is inversely proportional to the miscibility and molar volume of the plasticizers for most of the cases.

The addition of a poorly soluble drug ($\chi_{HPC/GF}$ = 14.2), with a low strength of interaction with the polymeric matrix caused a decrease in Young's moduli as drug concentration was increased for the 100 kDa HPC. When HPC molecular weight is increased the effect of drug loading in Young's moduli disappears.

6.2 Thermal Properties Conclusions

Tests on individual regression coefficients of the multiple linear regression indicate that factors that have a significant contribution to T_{mp} are polymer molecular weight and drug concentration. In general it was observed that as processing temperature is increased from 180 to 190 °C, the melting peak temperature (T_{mp}) of most of the films tend to displace to a higher value, especially for films processed with PEG. The higher processing temperatures allows for higher melting point crystals to grow with an increase in T_{mp} of up to 42 °C.

Melting peak temperature increases with increasing polymer molecular weight. Once that the HPC powder is processed via hot-melt extrusion, without the inclusion of any additive the melting peak temperature decreases.

Addition of 5 wt% plasticizer caused an antiplasticization effect for the lower molecular weight HPC. On the other hand, at higher HPC molecular weights glycerol and d-sorbitol don't show antiplasticizing effect. The lower molecular weight plasticizers whose Flory-Huggins solubility parameters indicate partial miscibility, and have stronger strengths of interaction with HPC are better plasticizers for thermal properties. According to the strength of interactions for each pair of components, griseofulvin will tend to have stronger intermolecular interactions with glycerol and d-sorbitol than the rest of the components including the HPC. Therefore, stronger intra molecular interactions of the drug with the plasticizer will result in an antiplasticization effect at certain threshold concentrations. This was observed for glycerol and d-sorbitol for which addition of 5 wt% griseofulvin increased T_{mp}, but as griseofulvin concentration increased T_{mp} decreased. On the other hand, when griseofulvin was added into the matrices containing PEG, T_{mp} decreased with increasing GF loading.

6.3 Rheological Properties Conclusions

Rhelogical data was collected in the extruder, and the standard deviation obtained is approximately 2.5 Pa s. An empirical model that accounts for 59% of the variability in viscosity was obtained with a multiple linear regression and, therefore, could be used for the approximation of viscosity under the range of conditions used in this work. Molecular weight and drug concentration were found to have a significant contribution to the viscosity of the melts. Increasing processing temperature decreases viscosity, especially to the higher molecular weight HPC films. It was also observed that when glycerol is used as plasticizer with 100 kDa HPC films, increasing processing temperature also causes a reduction in viscosity while the other plasticizers don't.

Viscosity increases with increasing HPC molecular weight to a maximum of one order of magnitude. It was noticed that the effect of the plasticizer on the viscosity depends of HPC molecular weight. For 100 kDa HPC (more rigid polymer), the addition of plasticizer seems to disrupt HPC chains alignment. But for 370 kDa HPC the lower molecular weight, and more miscible plasticizer is more efficient when reducing viscosity. This once again suggests that the lower molecular weight and more miscible plasticizer generate more free volume, resulting in a plasticizing effect.

When griseofulvin is added to an HPC matrix, viscosity decreases as griseofulvin concentration increases showing a plasticizing effect. Therefore, it can be concluded that when a poorly soluble, low molecular weight drug is used and polymer-polymer and drug-drug interactions are preferred, the viscosity of the solid dispersion decreases. On the other hand,

when griseofulvin is added to an HPC matrix with plasticizer viscosity tends to show a slight increase, with was observed for all studied systems. Once a third component, such as a plasticizer, is added to the solid dispersion, independently of the intra drug-plasticizer or polymer-plasticizer interactions, the viscosity increases.

6.4 Recommendations

In this work important parameters for the formulation of solid dispersion were evaluated. In order to design equipment, select processing parameters, and choose the appropriate carrier and additives, an understanding of the behavior of solid dispersions is necessary. The mechanical, thermal, and rheological evaluation helped in determining the effects of miscibility and molecular interactions between the polymer, plasticizers, and model drug.

The miscibility of drug and polymers is an important attribute in establishing the HME process and predicting the performance of the product. Therefore, the first step towards selection of the carrier should be to determine the miscibility parameters and strengths of interaction of the components. A simple pairwise approach to evaluate the interaction parameter between components as that used in this work may be suitable for screening amongst choices. Depending on the properties needed for the solid dispersion the desired mechanical, thermal, rheological, and miscibility performances can be selected. The mechanical properties of the films should be capable of resisting handling. The melting point temperature and rheological properties for any given system are critical to establish the optimum extrusion parameters such as temperature and shear rate.

It is already established in the literature that a miscible system with high T_g is preferred for solubility and bio-enhancement while stabilizing the high-energy form, on the other hand an immiscible system may be sufficient to produce a controlled drug release product [3].

For the formulation of HPC / griseofulvin solid dispersions via hot-melt extrusion, the following recommendations are made based on the results obtained under our experimental conditions. Lower molecular weight HPC grades are recommended, they possess lower viscosities and melting point temperature, therefore procesability of the films will be easier and energy requirements for processing are lower. Another advantage would be that lower molecular weights HPC films can dissolve faster. Since it was determined that griseofulvin reduces the thermal transitions and viscosity of HPC films, the use of an additional plasticizer is not necessary in terms of processing enhancement. Further analysis is needed in order to determine if the addition of plasticizer would have any beneficial effect in the dissolution mechanism of griseofulvin. Processing temperatures no lower than 180 °C should be used to ensure that HPC is melted and dispersion of the drug is promoted.

APPENDIX

Appendix A: Flory-Huggins Solubility Parameters

Flory-Huggins Solubility Parameters were calculated by the group contributions method. Polymer-solvent interaction parameter, χ is considered the sum of two components:

$$\chi = \chi_H + \chi_S \quad \text{Eq. 1}$$

where χ_H is the enthalpic component of polymer-solvent interactions, and χ_S is the entropic component or free-volume dissimilarity [57]. The enthalpic contribution can be calculated with the following equation:

$$\chi_H = \frac{V_S}{RT}(\delta_1 - \delta_2)^2 \quad \text{Eq. 2}$$

where Vs is the solvent molar volume, and δ_i are the solubility parameters of the polymer and solvent respectively [57]. The entropic contribution, χ_S, is usually taken to be a constant of the order 0.35±0.1, therefore the interaction parameter can be calculated as follows:

$$\chi \approx 0.34 + \frac{V_S}{RT}(\delta_P - \delta_S)^2 \quad \text{Eq. 3}$$

The criterion for complete solvent-polymer miscibility is $\chi < 0.5$. This number depends on the solvent molar volume. Molecular mixing of low molar weight liquids is possible for $\chi \leq 2$. Highly crystalline polymers obey the solubility parameter rules at $T \geq 0.9\ T_m$ [57]. A first requirement of mutual solubility is that the solubility parameter of the polymer δ_P, and of the solvent δ_S do not differ too much but this requirement is not sufficient. Mutual solubility only occurs if the degree of hydrogen bonding is about equal [57]. For many liquids and amorphous polymers, however, the cohesive energy is also dependent on the interaction between polar

groups and on hydrogen bonding. Cohesive energy may be divided into three parts, corresponding with the three types of interaction forces

$$E_{coh} = E_d + E_p + E_h \quad \text{Eq. 4}$$

where E_d= contribution of dispersion forces; E_p= contribution of polar forces; E_h= contribution of hydrogen bonding. Cohesive energy represents the total attractive forces within a condensed state material and can be defined as the quantity of energy needed to separate the atoms / molecules of a solid or liquid to a distance where the atoms or molecules possess no potential energy, i.e., no interactions occur between atoms or molecules [58]. Further, cohesive energy density (CED) is the cohesive energy per unit volume. The CED for a material can be used to predict its solubility in other materials; if two components have similar values, they are likely to be soluble in each other, since interactions in one component will be similar to those in the other component. Thus, the overall energy needed to facilitate mixing of the constituents will be small, as the energy required to break the interactions within the components will be equally compensated for by the energy released due to interactions between unlike molecules [58].

Taking into consideration the three types of interaction forces, the corresponding equation for the solubility parameter is

$$\delta^2 = \delta_d^2 + \delta_p^2 + \delta_h^2 \quad \text{Eq. 5}$$

The interaction of different structural groups in producing overall polar and hydrogen-bonding properties is so complicated that it does not obey simple rules so this method will give a rough estimate [57].

Utilizing the method of Hoftyzer and Van Krevelen, the solubility parameter components may be predicted from group contributions, using the following equations:

$$\delta_d = \frac{\sum F_{di}}{V} \quad \text{Eq. 6}$$

$$\delta_p = \frac{\sqrt{\sum F_{pi}^2}}{V} \quad \text{Eq. 7}$$

$$\delta_h = \sqrt{\frac{\sum E_{hi}}{V}} \quad \text{Eq. 8}$$

Table A- 1: Solubility parameter component group contributions (method Hoftyzer – Van Krevelen) [57].

Structural group	F_{di} $(MJ/m^3)^{1/2}$ mol^{-1}	F_{pi} $(MJ/m^3)^{1/2}$ mol^{-1}	E_{hi} J/mol
_CH3	420	0	0
_CH2	270	0	0
_CH	80	0	0
_O_	100	400	3000
_OH	210	500	20000
Phenyl	1430	110	0
_Cl	450	550	400
COO	390	490	7000
_CO	290	770	2000
_COH	470	800	4500

Table A- 2: Molar volume group contributions from Hoy's System (1985) [57].

Structural group	V_i cm^3 / mol
_CH3	21.55
_CH2	15.55
_CH	9.56
_O_	6.45
_OH	10.65
Phenyl	80.52
_Cl	19.5
COO	23.7
_CO	17.3
_COH	23.3

Using equations 5 to 8, and with the values in tables 1 and 2, solubility parameters for our materials were calculated using the Hoftyzer-Van Krevelen group contribution method. The results are summarized in Table A-3. After obtaining the solubility parameters components,

Flory-Huggins solubility parameters can be calculated with equation 3. The results are summarized in Table A-4.

Table A- 3: Molar volumes and solubility parameter components

Compound	V (cm^3/mol)	δ_d	δ_p	δ_h	$\delta(MJ/m^3)^{1/2}$
HPC(100-370- 1,000 kDa)	72458 - 724034	16.14	0.20	16.77	23.28
PEG	9100	12.82	0.59	7.88	15.07
Glycerol	78	16.02	11.10	27.73	33.90
D-sorbitol	144	14.72	8.50	28.86	33.50
GF	316	8.51	3.27	4.13	10.01

Table A- 4: Flory-Huggins solubility parameters.

Polymer/solvent	X
HPC / PEG	153.7
HPC /Glycerol	2.5
HPC / D-sorbitol	4.1
HPC / GF	14.2
PEO / GF	58.5
Glycerol / GF	11.5
D-sorbitol / GF	20.2

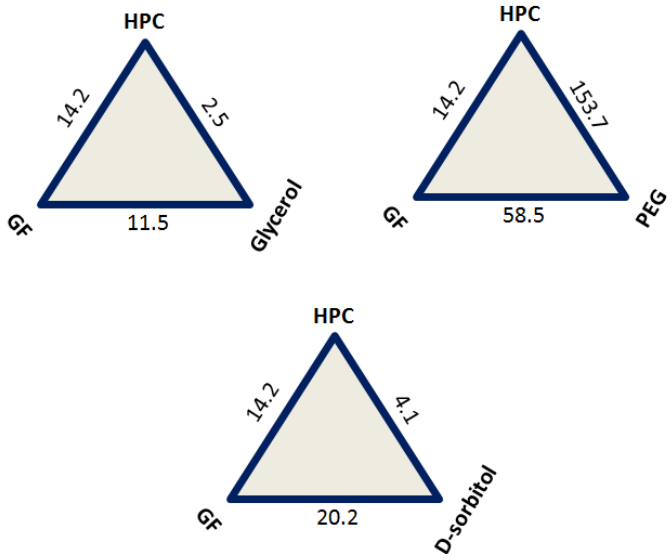

Figure A- 1: Flory-Huggins solubility parameters interactions for ternary mixtures.

Appendix B: Interaction Parameter

Previous studies have demonstrated that, in a binary system involving two materials A and B, there are two types of interactions: inter-(A-A and B-B) and intra-(A-B) interactions. The first type of interaction can be regarded as cohesive, and the second is adhesive. Based on the Lenard Jones pair potential function the strength of interaction (σ MPa) can be related to the solubility parameter (δ) of the two surfaces [59]:

$$^{BB}\sigma = 0.25\ ^{B}\delta^2 \qquad \text{Eq. 1}$$

$$^{AA}\sigma = 0.25\ ^{A}\delta^2 \qquad \text{Eq. 2}$$

$$^{AB}\sigma = 0.25\ ^{AB}\varphi\ ^{A}\delta\ ^{B}\delta \qquad \text{Eq. 3}$$

where $^{AB}\varphi$, the interaction parameter, is defined from the harmonic mean equation proposed by S. Wu :

$$^{AB}\varphi = 2 \cdot \left[\frac{^{A}x_d \cdot\ ^{B}x_d}{^{A}x_d \cdot g_1 + {}^{B}x_d \cdot g_2} + \frac{^{A}x_p \cdot\ ^{B}x_p}{^{A}x_p \cdot g_1 + {}^{B}x_p \cdot g_2}\right] \qquad \text{Eq. 4}$$

The quantities x_d and x_p are the fractional non-polarity and polarity respectively ($x_d + x_p = 1$) for each material, defined by the expressions:

$$x_d = \left(\frac{\delta_d}{\delta}\right)^2 \quad \text{and} \quad x_p = 1 - \left(\frac{\delta_d}{\delta}\right)^2 \qquad \text{Eqs. 5 and 6}$$

where δ_d is the dispersion or non-polar component of the solubility parameters components calculated in Appendix A. Parameters g_1 and g_2 can also be defined in terms of the solubility parameters of the materials:

$$g_1 = \frac{A\delta^2 \cdot AV^{1/3}}{B\delta^2 \cdot BV^{1/3}} \qquad \text{and} \qquad g_2 = \frac{1}{g_1} = \frac{A\delta^2 \cdot AV^{1/3}}{B\delta^2 \cdot BV^{1/3}} \qquad \text{Eqs. 7 and 8}$$

where V is the molar volume of the material [59].

Depending on the value of the strength of interaction a material will coat or not another material as illustrated in the following figure.

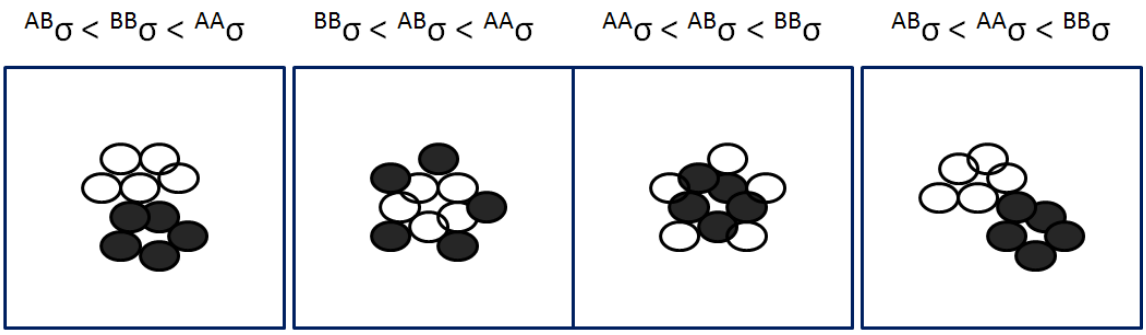

Figure B- 1: Influence of cohesion parameter of two materials A(●) and B(○) on the strength of interaction ($^{AB}\sigma$, $^{BB}\sigma$, $^{AA}\sigma$) [59].

Using equations 5 and 6, factional polarity and non-polarity components were calculated and the results are illustrated in Table B-1. The interaction parameter was calculated using equation 4 and finally the strength for interaction for each pair was calculated using equations 1, 2 and 3, and the results are summarized in Table B-2. To determine the interaction of the different films formulated, the criterion illustrated in Figure B-1 was employed to evaluate each pair.

Table B- 1: Fractional non-polarity and polarity components for each material.

#	Material	V(m^3/mol)	δ_d(MJ/m^3)$^{1/2}$	δ(MJ/m^3)$^{1/2}$	x_d	x_p
1	HPC (100 kDa)	0.07245	16.14	23.28	0.481	0.519
2	HPC (370 kDa)	0.26771	16.14	23.28	0.481	0.519
3	HPC (1000kDa)	0.72403	16.14	23.28	0.481	0.519
4	PEG	0.0091	12.82	15.07	0.724	0.276
5	Glycerol	0.00007	16.02	33.9	0.223	0.777
6	D-sorbitol	0.00014	14.72	33.5	0.193	0.807
7	GF	0.00031	8.51	10.01	0.723	0.277

Table B- 2: Parameters used to calculate the interaction parameters and the strength of interaction.

Compunds	g_1	g_2	Φ	σ (MJ/m^3)
HPC (100 kDa)/PEG	4.765	0.210	0.40	35
HPC (100 kDa)/Glycerol	4.601	0.217	0.41	81
HPC(100 kDa)/d-sorbitol	3.841	0.260	0.48	93
HPC(100 kDa)/GF	33.105	0.030	0.06	4
PEG/GF	8.273	0.121	0.24	9
Glycerol/GF	0.806	1.241	0.74	63
D-sorbitol/GF	0.835	1.198	0.72	60
HPC (370 kDa)/PEG	7.367	0.136	0.27	23
HPC (370 kDa)/Glycerol	7.114	0.141	0.27	54
HPC(370 kDa)/d-sorbitol	5.938	0.168	0.32	63
HPC(370 kDa)/GF	51.179	0.020	0.04	2
HPC (1000 kDa)/PEG	10.264	0.097	0.19	17
HPC (1000 kDa)/Glycerol	9.911	0.101	0.20	39
HPC(1000 kDa)/d-sorbitol	8.273	0.121	0.24	46
HPC(100 kDa)/GF	71.305	0.014	0.03	2
HPC/HPC	-	-	-	135
PEG/PEG	-	-	-	57
Glycerol/glycerol	-	-	-	287
D-sorbitol/d-sorbitol	-	-	-	281
GF/GF	-	-	-	25

Tables B-3, 4 and 5 show the results. According to the strengths of interaction most of the components remain separate except for GF/ glycerol and GF/ d-sorbitol, whose results indicate that griseofulvin will tend to accommodate between the HPC / glycerol and HPC / d-sorbitol interfaces.

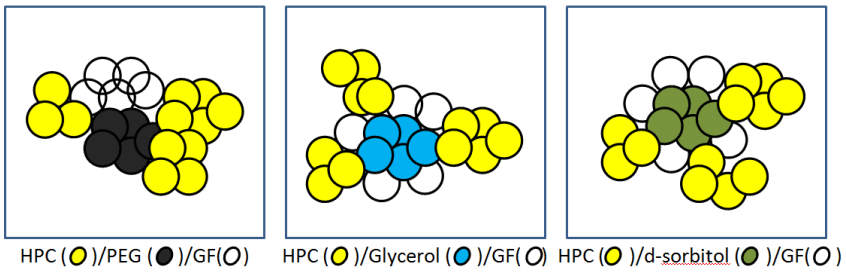

Figure B- 2: Possible interactions between the different films components.

Table B- 3: Strength of interaction for the different components of 100 kDa HPC HME films.

Compounds	Strength of interaction (MJ/m^3)			Interaction
HPC(100 kDa)/ PEG	$^{HPC/PEG}\sigma$	$^{PEG/PEG}\sigma$	$^{HPC/HPC}\sigma$	Separated
	35	57	135	
PEG/GF	$^{PEG/GF}\sigma$	$^{GF/GF}\sigma$	$^{PEG/PEG}\sigma$	Separated
	9	25	57	
GF/HPC(100 kDa)	$^{HPC/GF}\sigma$	$^{GF/GF}\sigma$	$^{HPC/HPC}\sigma$	Separated
	4	25	135	
HPC(100 kDa)/ Glycerol	$^{HPC/Gly}\sigma$	$^{HPC/HPC}\sigma$	$^{Gly/Gly}\sigma$	Separated
	81	135	287	
Glycerol/GF	$^{GF/GF}\sigma$	$^{Gly/GF}\sigma$	$^{Gly/Gly}\sigma$	Glycerol attracts GF
	25	63	287	
GF/HPC(100 kDa)	$^{HPC/GF}\sigma$	$^{GF/GF}\sigma$	$^{HPC/HPC}\sigma$	Separated
	4	25	135	
HPC(100 kDa)/ d-sorbitol	$^{HPC/D\text{-}sorbitol}\sigma$	$^{HPC/HPC}\sigma$	$^{D\text{-}sorb/d\text{-}sorb}\sigma$	Separated
	93	135	281	
D-sorbitol/GF	$^{GF/GF}\sigma$	$^{D\text{-}sorb/GF}\sigma$	$^{D\text{-}sorb/d\text{-}sorb}\sigma$	D-sorbitol attracts GF
	25	60	281	
GF/HPC(100 kDa)	$^{HPC/GF}\sigma$	$^{GF/GF}\sigma$	$^{HPC/HPC}\sigma$	Separated
	4	25	135	

Table B- 4: Strength of interaction for the different components of 370 kDa HPC HME films.

Compounds	Strength of interaction (MJ/m^3)			Interaction
HPC(370 kDa)/ PEG	$^{HPC/PEG}\sigma$	$^{PEG/PEG}\sigma$	$^{HPC/HPC}\sigma$	Separated
	23	57	135	
PEG/GF	$^{PEG/GF}\sigma$	$^{GF/GF}\sigma$	$^{PEG/PEG}\sigma$	Separated
	9	25	57	
GF/HPC(370 kDa)	$^{HPC/GF}\sigma$	$^{GF/GF}\sigma$	$^{HPC/HPC}\sigma$	Separated
	2	25	135	
HPC(370 kDa)/ Glycerol	$^{HPC/Gly}\sigma$	$^{HPC/HPC}\sigma$	$^{Gly/Gly}\sigma$	Separated
	54	135	287	
Glycerol/GF	$^{GF/GF}\sigma$	$^{Gly/GF}\sigma$	$^{Gly/Gly}\sigma$	Glycerol attracts GF
	25	63	287	
GF/HPC(370 kDa)	$^{HPC/GF}\sigma$	$^{GF/GF}\sigma$	$^{HPC/HPC}\sigma$	Separated
	2	25	135	
HPC(370 kDa) / d-sorbitol	$^{HPC/D\text{-}sorbitol}\sigma$	$^{HPC/HPC}\sigma$	$^{D\text{-}sorb/d\text{-}sorb}\sigma$	Separated
	63	135	281	
D-sorbitol/GF	$^{GF/GF}\sigma$	$^{D\text{-}sorb/GF}\sigma$	$^{D\text{-}sorb/d\text{-}sorb}\sigma$	D-sorbitol attracts GF
	25	60	281	
GF/HPC(370 kDa)	$^{HPC/GF}\sigma$	$^{GF/GF}\sigma$	$^{HPC/HPC}\sigma$	Separated
	2	25	135	

Table B- 5: Strength of interaction for the different components of 1,000 kDa HPC HME films.

Compounds	Strength of interaction (MJ/m^3)			Interaction
HPC(1,000 kDa)/ PEG	$^{HPC/PEG}\sigma$	$^{PEG/PEG}\sigma$	$^{HPC/HPC}\sigma$	Separated
	17	57	135	
PEG/GF	$^{PEG/GF}\sigma$	$^{GF/GF}\sigma$	$^{PEG/PEG}\sigma$	Separated
	9	25	57	
GF/HPC(1,000 kDa)	$^{HPC/GF}\sigma$	$^{GF/GF}\sigma$	$^{HPC/HPC}\sigma$	Separated
	2	25	135	
HPC(1,000 kDa)/ Glycerol	$^{HPC/Gly}\sigma$	$^{HPC/HPC}\sigma$	$^{Gly/Gly}\sigma$	Separated
	39	135	287	
Glycerol/GF	$^{GF/GF}\sigma$	$^{Gly/GF}\sigma$	$^{Gly/Gly}\sigma$	Glycerol attracts GF
	25	63	287	
GF/HPC(1,000 kDa)	$^{HPC/GF}\sigma$	$^{GF/GF}\sigma$	$^{HPC/HPC}\sigma$	Separated
	2	25	135	
HPC(1,000)/ d-sorbitol	$^{HPC/D\text{-}sorbitol}\sigma$	$^{HPC/HPC}\sigma$	$^{D\text{-}sorb/d\text{-}sorb}\sigma$	Separated
	46	135	281	
D-sorbitol/GF	$^{GF/GF}\sigma$	$^{D\text{-}sorb/GF}\sigma$	$^{D\text{-}sorb/d\text{-}sorb}\sigma$	D-sorbitol attracts GF
	25	60	281	
GF/HPC(100)	$^{HPC/GF}\sigma$	$^{GF/GF}\sigma$	$^{HPC/HPC}\sigma$	Separated
	2	25	135	

Appendix C: Gel Permeation Chromatography (GPC)

Solutions of 15 mg of HPC standard diluted in 3 mL of THF were prepared and analyzed by gel permeation chromatography (GPC). From the data obtained graphs of intensity as a function of elution volume were used to determine the elution volume at the maximum intensity of the peaks for each standard. The data obtained is summarized in Table C-1.

Table C- 1: GPC data for HPC standards.

HPC standard M_w	Log M_w	Elution Volume	Peak intensity
31,600	4.499687	1.32E+01	1.21E-01
93,000	4.968483	1.26E+01	9.97E+01
205,600	5.313023	1.19E+01	9.94E+01
288,200	5.459694	1.24E+01	4.20E-02
308,000	5.488551	1.18E+01	6.70E-02
486,900	5.68744	1.14E+01	6.41E-02
637,000	5.804139	1.25E+01	4.19E-02
865,000	5.937016	4.74E-02	1.18E+01

A graph of Log M_w as a function of elution volume is used as the calibration curve, such as the ones illustrated in Figure C-1. With a linear regression of the calibration curve the molecular weight of the samples under study can be determined along with the following equations:

$$\log_{10} M_i = solope \cdot Elution\ volume + intercept \quad \text{Eq. 1}$$

$$M_w = \frac{\sum I_i \cdot M_i}{\sum I_i} \quad \text{Eq. 2}$$

$$M_n = \frac{\sum I_i}{\sum \frac{I_i}{M_i}} \quad \text{Eq. 3}$$

$$PDI = \frac{M_w}{M_n} \quad \text{Eq. 4}$$

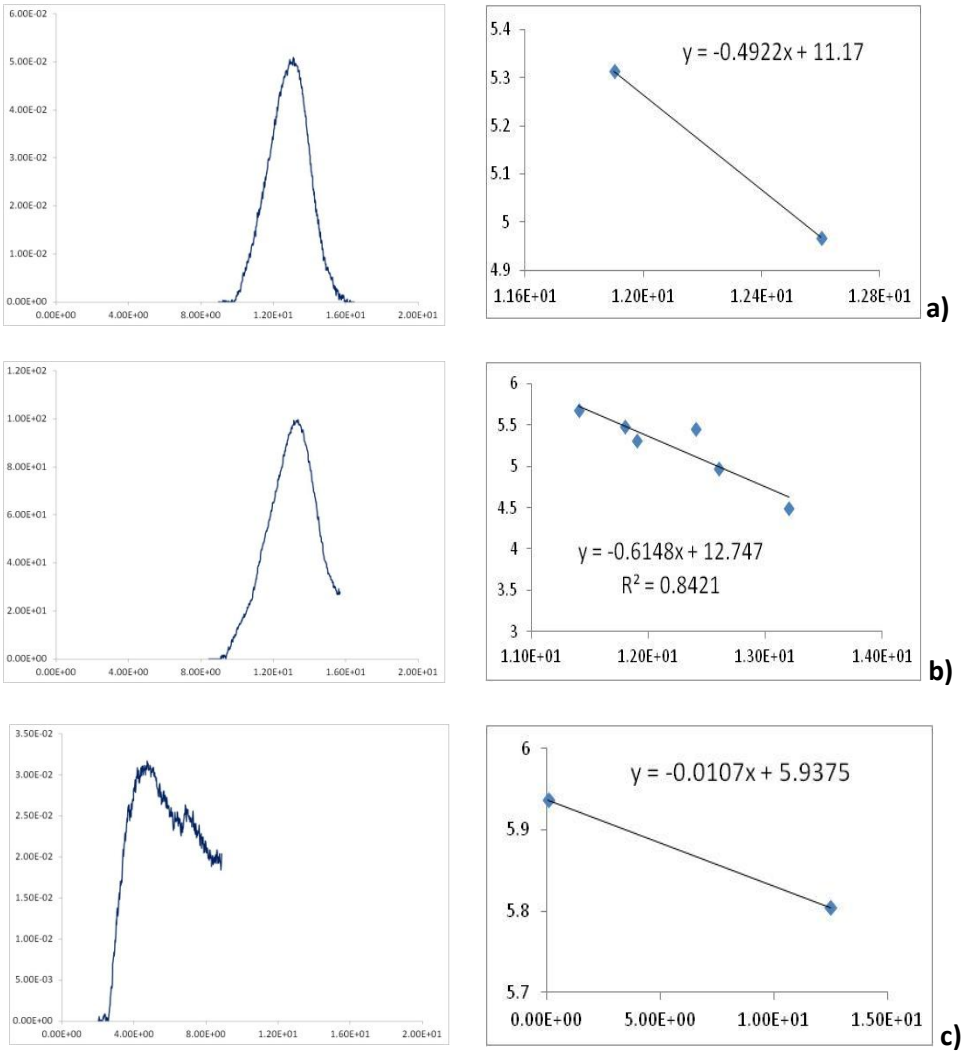

Figure C- 1: Graphs of intensity as a function of elution volume to the left and Log M_w as a function of elution volume to the right for a) 100, b) 370, and c) 1,000 kDa HPC samples.

To determine the average molecular weight M_w, number average weight M_n and PDI's of the HPC samples, equations 1, 2, 3, and 4 were applied to 100, 370, and 1,000 kDa HPC samples data. Results are summarized in Table C-2.

Table C- 2: Average molecular weight, number average molecular weight, and PDI's obtained from GPC for HPC powder samples.

HPC Sample	ΣI_i	Σ Log M_i	ΣM_i	$\Sigma I_i / M_i$	$\Sigma I_i M_i$	M_w	M_n	PDI
100 kDa	8.45E+00	2.16E+03	2.52E+08	2.40E-04	1.28E+06	152,000	35,200	4.31
370 kDa	19811.58	2047.711	6.24E+08	1.415008	6.16E+09	311,000	14,000	22
1,000 kDa	8.84E+00	2.38E+03	3.07E+08	1.18E-05	6.64E+06	751,000	750,000	1

Appendix D: Mechanical Properties

Table D- 1: Average Young's moduli for films processed at 190 °C.

100 kDa Glycerol	Average *E* *[MPa]*	370 kDa Glycerol	Average *E* *[MPa]*	1000 kDa Glycerol	Average *E* *[MPa]*
0	20.0	0	22.5	0	18.6
5	14.8	5	18.6	5	18.3
10	8.9	10	29.4	10	15.2
20	7.4	20	17.2	20	21.0
100 kDa PEG	**Average *E* *[MPa]***	**370 kDa PEG**	**Average *E* *[MPa]***	**1000 kDa PEG**	**Average *E* *[MPa]***
0	37.3	0	46.3	0	10.9
5	26.9	5	31.5	5	28.0
10	25.4	10	41.7	10	25.9
20	39.9	20	28.2	20	28.0
100 kDa D-sorbitol	**Average *E* *[MPa]***	**370 kDa D-sorbitol**	**Average *E* *[MPa]***	**1000 kDa D-sorbitol**	**Average *E* *[MPa]***
0	19.6	0	34.7	0	25.2
5	34.7	5	36.9	5	21.5
10	14.0	10	29.0	10	22.3
20	9.2	20	27.5	20	29.9

Appendix E: Thermal Properties

E.1 Summarized Data

Table E- 1: DSC analysis results for hot-melt extruded films processed at 180 °C.

DSC Analysis Results for films processed at 180 °C						
PZ	**Mw [kDa]**	**wt% GF**	**T_{st} °C**	**T_{mp} °C**	**T_m °C**	**ΔT °C**
PEG	100	0	197	141	217	20
		5	163	150	196	33
		10	157	140	201	44
		20	169	150	187	18
	370	0	172	176	200	28
		5	141	163	212	96
		10	140	158	204	59
		20	146	151	194	25
	1,000	0	109	201	179	70
		5	137	177	188	51
		10	105	170	188	83
		20	120	172	190	70
D-sorbitol	100	0	149	161	206	57
		5	179	181	202	23
		10	185	187	205	20
		20	132	161	195	63
	370	0	213	207	236	23
		5	178	182	203	80
		10	154	170	201	47
		20	133	171	205	12
	1,000	0	152	160	194	42
		5	181	184	209	28
		10	177	185	207	30
		20	147	173	208	25
Glycerol	100	0	120	155	195	75
		5	184	187	203	19
		10	180	180	191	11
		20	106	139	178	72
	370	0	147	166	206	59
		5	136	165	191	55
		10	128	166	214	86
		20	176	177	190	14
	1,000	0	147	166	210	63
		5	171	188	227	54
		10	171	189	211	40
		20	144	151	192	48

* ΔT °C corresponds to the breadth of the melting temperature peak

Table E- 2: DSC analysis results for hot-melt extruded films processed at 190 °C.

DSC Analysis Results for films processed at 190 °C							
PZ	**Mw [kDa]**	**wt% GF**	**T_{st} °C**	**T_{mp} °C**	**T_m °C**	**ΔT °C**	**ΔH_f [J/g]**
None	100	0	153	165	203	50	92.00
None	370	0	145	158	195	50	186.00
None	1000	0	176	183	210	34	90.76
PEG	100	0	197	183	210	13	104.70
		5	187	175	213	26	77.70
		10	187	168	197	10	168.00
		20	156	177	177	21	78.11
	370	0	191	197	207	16	110.00
		5	196	193	210	14	40.00
		10	142	169	209	67	106.00
		20	131	162	193	62	52.00
	1,000	0	181	198	202	21	71.85
		5	169	191	202	33	94.98
		10	161	189	200	39	76.23
		20	175	161	187	12	48.60
D-sorbitol	100	0	160	181	209	27	114.60
		5	159	176	196	17	112.20
		10	183	185	201	18	94.44
		20	179	181	196	17	78.73
	370	0	148	154	175	27	86.36
		5	203	196	215	12	96.00
		10	149	156	195	46	61.21
		20	155	161	197	42	77.66
	1,000	0	145	170	201	56	81.09
		5	187	191	213	26	104.00
		10	175	176	189	14	81.40
		20	142	148	198	56	-
Glycerol	100	0	139	169	202	63	134.10
		5	195	197	210	15	108.50
		10	139	169	202	63	64.54
		20	114	141	181	67	55.47
	370	0	116	139	178	62	123.00
		5	190	194	214	24	95.00
		10	160	174	191	31	79.00
		20	157	163	181	24	72.00
	1,000	0	176	183	209	33	128.90
		5	200	203	213	13	101.30
		10	191	193	204	13	118.60
		20	152	159	186	34	58.74

* ΔT °C corresponds to the breadth of the melting temperature peak

E.3 DSC Thermograms

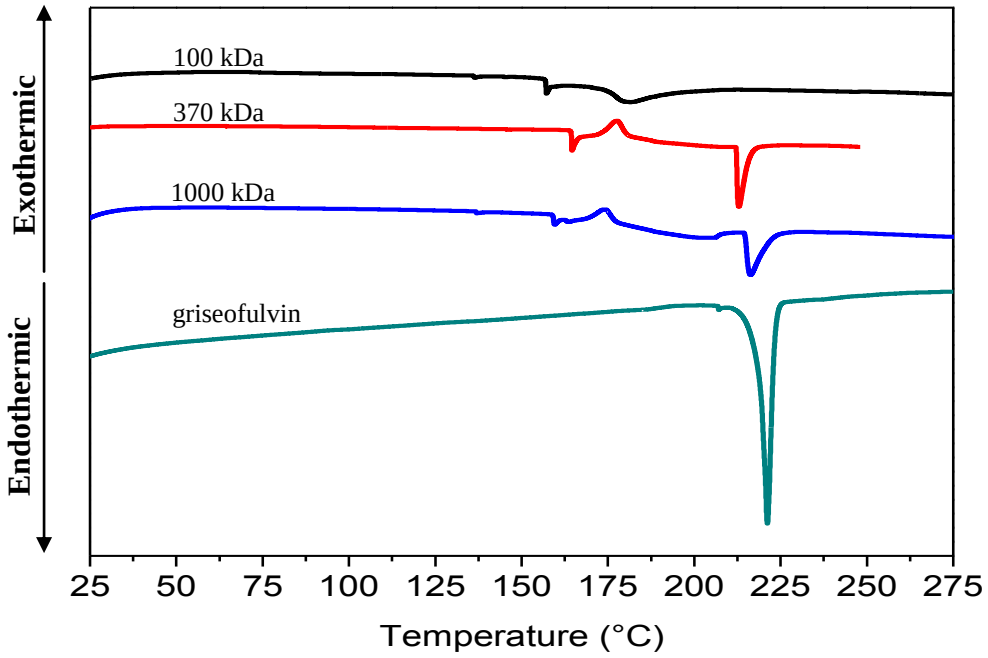

Figure E- 1: DSC thermograms for different molecular weight HPC and griseofulvin powders.

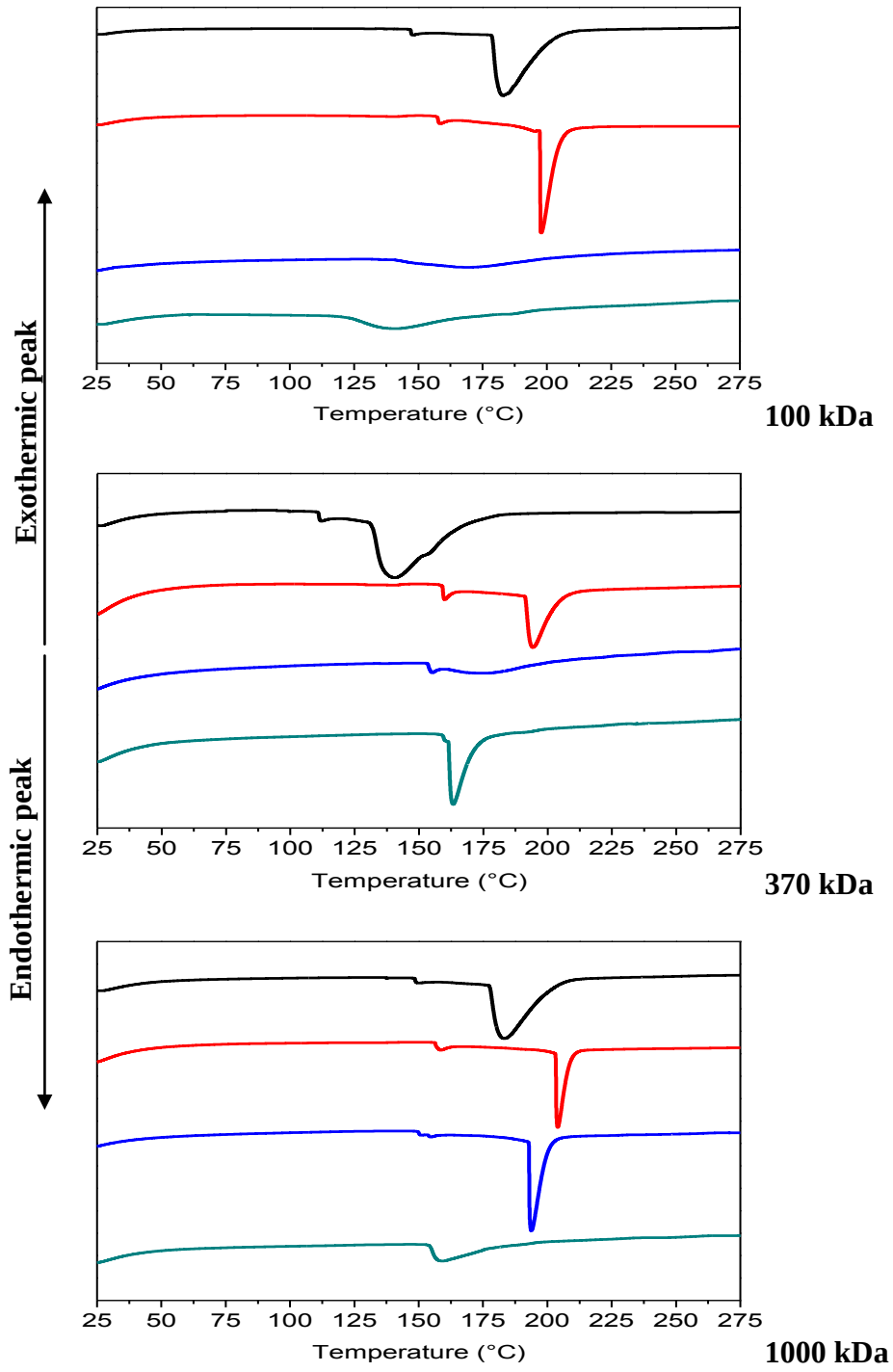

Figure E- 2: DSC thermograms for different molecular weight HPC-glycerol HME films processed at 190 °C with 0, 5, 10, and 20 wt% griseofulvin from top to bottom respectively.

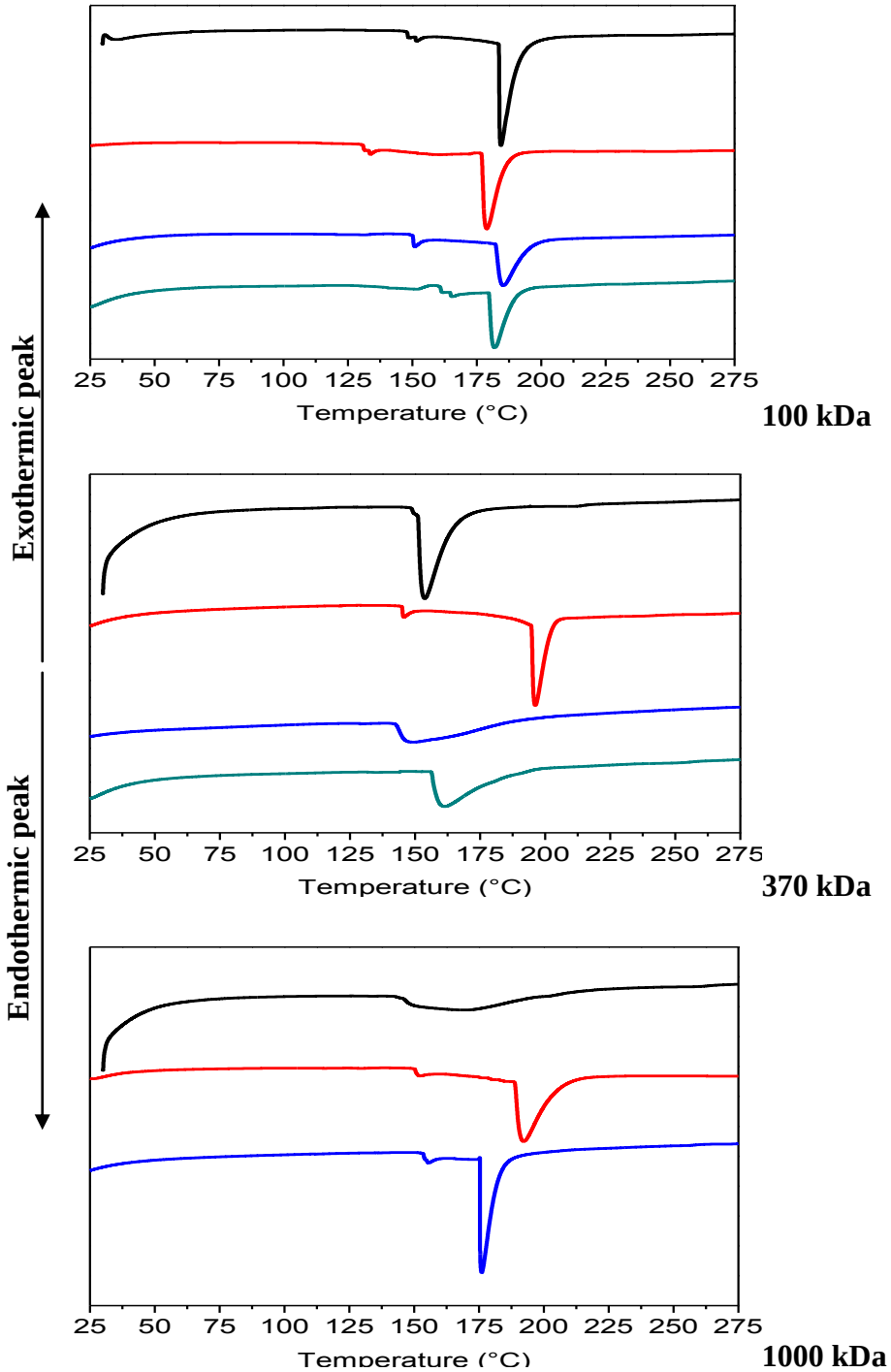

Figure E- 3: DSC thermograms for different molecular weight HPC-d-sorbitol HME films processed at 190 °C with 0, 5, 10, and 20 wt% griseofulvin from top to bottom respectively.

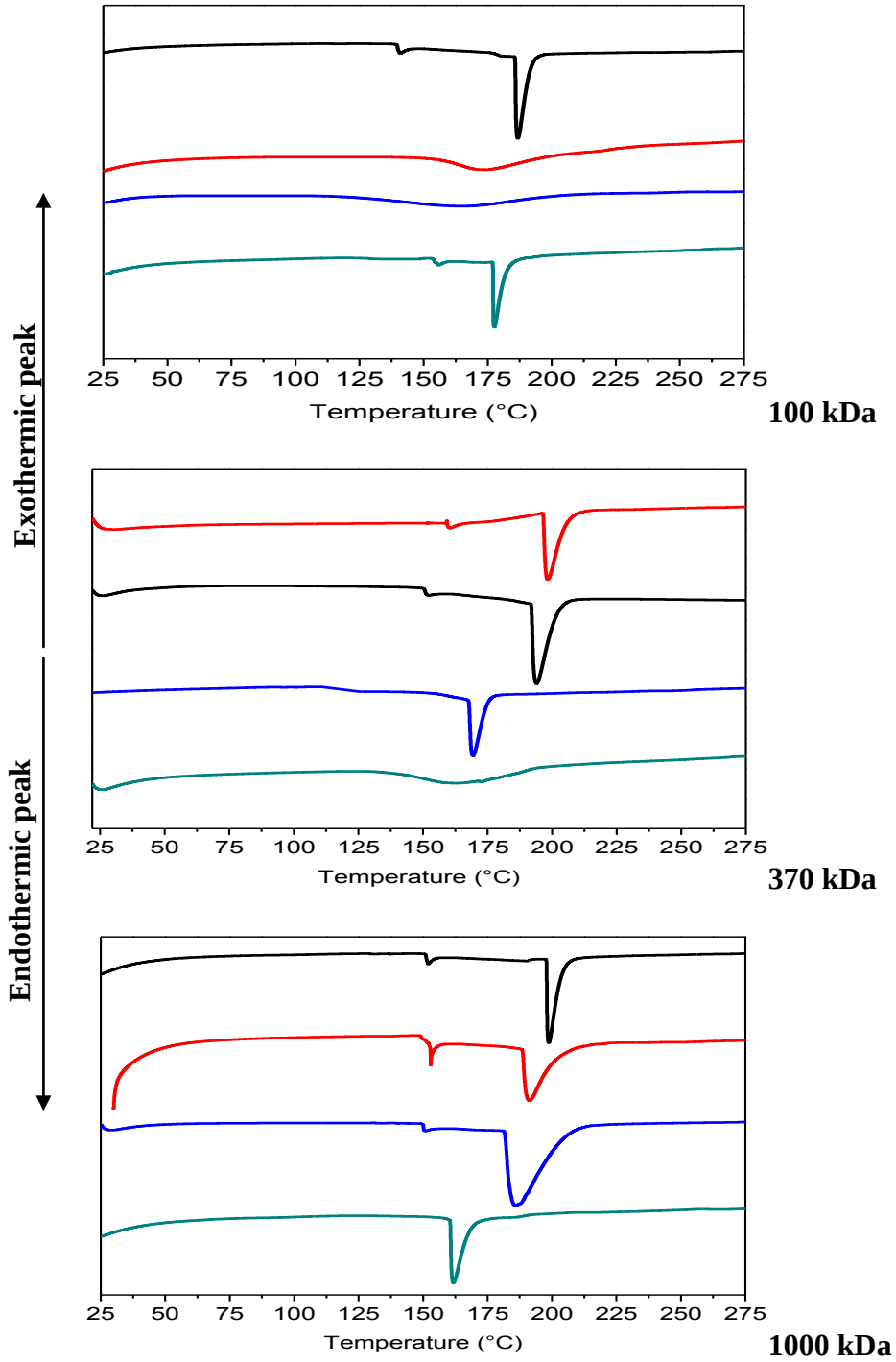

Figure E- 4: DSC thermograms for different molecular weight HPC-PEG HME films processed at 190 °C with 0, 5, 10, and 20 wt% griseofulvin from top to bottom respectively.

Appendix F: Rheological Properties

Table F- 1: 100 kDa HPC melt at 190 °C.

τ (Pa)	$\dot{\gamma}$ (s^{-1})	η (Pa s)	stdv η
1536	37	33.416	6.23
2109	72	21.781	0.93
2490	108	20.636	0.76
3007	145	9.344	0.55
3119	178	30.662	0.78
2404	214	16.899	0.98
1513	250	8.456	0.97
468	289	2.049	1.12

Table F- 2: 370 kDa HPC melt at 190 °C.

τ (Pa)	$\dot{\gamma}$ (s^{-1})	η (Pa s)	stdv η
896	39	32.136	3.91
1845	71	30.051	1.51
3237	107	33.785	1.72
3633	143	-4.280	1.44
2863	169	18.135	1.28
6386	214	9.729	0.53
6488	250	4.773	0.71
6932	289	1.921	0.81

Table F- 3: 1000 kDa HPC melt at 190 °C.

τ (Pa)	$\dot{\gamma}$ (s^{-1})	η (Pa s)	stdv η
3082	37	89.382	6.25
3963	72	59.944	2.5
6929	108	64.479	2.6
8552	143	55.558	1.97
10100	181	56.790	1.45
10278	215	48.410	1.13
10906	251	43.185	1.42
11287	291	39.950	1.85

Table F- 4: Different molecular weight HPC melts with different plasticizers at a shear rate of 36 s^{-1}.

HPC Mw kDa	Viscosity None		Viscosity Glycerol		Viscosity D-sorbitol		Viscosity PEG	
	Pa s	stdv	Pa s	stdv	Pa s	Stdv	Pa s	stdv
100	25.5	2.03	18.21	1.78	12.4	2.58	32.39	4.68
370	32	3.9	61.9	0.85	58.8	1.15	17.5	0.99
1000	60.3	6.25	117	1.27	84	1.2	112	1.21

Table F- 5: Different molecular weight HPC melts with different plasticizers at a shear rate of 179 s^{-1}.

HPC Mw kDa	Viscosity None		Viscosity Glycerol		Viscosity D-sorbitol		Viscosity PEG	
	Pa s	stdv	Pa s	stdv	Pa s	Stdv	Pa s	stdv
100	24	0.7	10.8	0.39	9.63	0.37	5.06	0.47
370	25	1.44	13.27	0.34	18.8	0.19	29	0.6
1000	16.7	1.45	52	0.37	26	0.8	43	0.69

Table F- 6: Different molecular weight HPC melts with different plasticizers at a shear rate of 288 s^{-1}.

HPC Mw kDa	Viscosity None		Viscosity Glycerol		Viscosity D-sorbitol		Viscosity PEG	
	Pa s	stdv	Pa s	stdv	Pa s	Stdv	Pa s	stdv
100	1.49	0.17	16.9	0.37	16.1	0.56	15.7	3.6
370	19	0.81	3.9	0.31	15.7	0.3	33	0.5
1000	14.95	1.85	28	0.4	11.7	0.2	49.7	0.2

Table F- 7: 1,000 kDa HPC melts with different griseofulvin volume fractions at 190 °C.

Griseofulvin volume fraction	71 s^{-1}	143 s^{-1}	250 s^{-1}
	Viscosity	Viscosity	Viscosity
	Pa s	Pa s	Pa s
0	53.7	46.7	28.18
0.05	100	69.18	23.9
0.2	12.02	8.12	4.57

Table F- 8: 1,000 kDa HPC-glycerol melts with different griseofulvin volume fractions at 190.

glycerol	36/s	143/s	250/s
Griseofulvin volume fraction	Viscosity Pa s	Viscosity Pa s	Viscosity Pa s
0	109		26
0.05	139	39	36.3
0.1	245	93	46.77
0.2	218	117	75.85

Table F- 9: 1,000 kDa HPC-d-sorbitol melts with different griseofulvin volume fractions at 190 °C.

d-sorbitol	36/s	143/s	250/s
Griseofulvin volume fraction	Viscosity Pa s	Viscosity Pa s	Viscosity Pa s
0	84	76	11
0.05	153	85	55
0.1	107	79	58
0.2	218	99	87

Table F- 10: 1,000 kDa HPC-PEG melts with different griseofulvin volume fractions at 190 °C.

PEG	36/s	143/s	250/s
Griseofulvin volume fraction	Viscosity Pa s	Viscosity Pa s	Viscosity Pa s
0	107	52.4	42
0.05	181	64.56	56
0.1	223	87	85
0.2	165	102	81

Appendix G: Statistical Analysis: Multiple Linear Regression

A multiple linear regression analysis was used to build empirical models for young's moduli (*E*), melting peak temperature (T_{mp}) and viscosity (η). The influence of processing temperature (temp), polymer molecular weight (Mw), plasticizer (PZ), and drug concentration (wt%) and their interactions was evaluated for each model. The empirical models were obtained using the general regression method found in Minitab 16. The initial model was built including all the variables and the interactions between them and the results are as follows:

Young's moduli (*E*) regression equations:

PZ

None $E = 103.477 - 0.427275\ Temp - 0.192794\ Mw + 1.78167\ wt\ \% + 0.000965708\ Temp*Mw - 0.0124943\ Temp*wt\% + 0.000879703\ Mw*wt\%$

Glycerol $E = 107.441 - 0.427275\ Temp - 0.192794\ Mw + 1.78167\ wt\ \% + 0.000965708\ Temp*Mw - 0.0124943\ Temp*wt\% + 0.000879703 Mw*wt\%$

D-Sorbitol $E = 113.054 - 0.427275\ Temp - 0.192794\ Mw + 1.78167\ wt\ \% + 0.000965708\ Temp*Mw - 0.0124943\ Temp*wt\% + 0.000879703\ Mw*wt\%$

PEG $E = 114.852 - 0.427275\ Temp - 0.192794\ Mw + 1.78167\ wt\ \% + 0.000965708\ Temp*Mw - 0.0124943\ Temp*wt\% + 0.000879703\ Mw*wt\%$

Summary of Model

S = 6.81304 R-Sq = 40.59% **R-Sq(adj) = 32.37%**

PRESS = 3915.65 R-Sq(pred) = 22.90%

Analysis of Variance

Source	DF	Seq SS	Adj SS	Adj MS	F	P
Regression	9	2061.66	2061.66	229.073	4.93505	0.000047
Temp	1	25.38	81.61	81.606	1.75809	0.189504
Mw	1	458.29	286.63	286.626	6.17497	0.015540
PZ	3	848.86	889.66	296.553	6.38882	0.000733

wt %	1	38.37	9.11	9.113	0.19632	0.659179
Temp*Mw	1	218.75	247.75	247.748	5.33739	0.024057
Temp*wt%	1	15.37	15.37	15.367	0.33106	0.567024
Mw*wt%	1	456.64	456.64	456.636	9.83757	0.002568
Error	65	3017.14	3017.14	46.418		
Total	74	5078.79				

Melting peak temperature (T_{mp}) regression equations:

PZ

None T_{mp} = *-90.4868 + 1.32756 Temp + 0.160948 Mw + 6.60944 wt % - 0.000772806 Temp*Mw - 0.0379683 Temp*wt% -0.000722858 Mw*wt%*

Glycerol T_{mp} = *-76.3062 + 1.32756 Temp + 0.160948 Mw + 6.60944 wt % - 0.000772806 Temp*Mw - 0.0379683 Temp*wt% - 0.000722858Mw*wt%*

D-Sorbitol T_{mp} = *-72.8062 + 1.32756 Temp + 0.160948 Mw + 6.60944 wt % - 0.000772806 Temp*Mw - 0.0379683 Temp*wt% - 0.000722858Mw*wt%*

PEG T_{mp} = *-76.3479 + 1.32756 Temp + 0.160948 Mw + 6.60944 wt % - 0.000772806 Temp*Mw- 0.0379683 Temp*wt% - 0.000722858 Mw*wt%*

Summary of Model

S = 15.2392 R-Sq = 26.05% **R-Sq(adj) = 15.81%**

PRESS = 19902.8 R-Sq(pred) = 2.49%

Analysis of Variance

Source	DF	Seq SS	Adj SS	Adj MS	F	P
Regression	9	5316.5	5316.5	590.720	2.54367	0.014408
Temp	1	593.9	787.8	787.804	3.39232	0.070064
Mw	1	1473.1	199.8	199.757	0.86016	0.357125
PZ	3	331.9	786.1	262.046	1.12838	0.344170
wt %	1	2327.8	125.4	125.407	0.54001	0.465073
Temp*Mw	1	139.6	158.7	158.657	0.68318	0.411516
Temp*wt%	1	141.9	141.9	141.906	0.61105	0.437229
Mw*wt%	1	308.3	308.3	308.321	1.32764	0.253445

Error	65	15095.1	15095.1	232.232
Total	74	20411.5		

Viscosity (η) regression equations:

PZ

None $\eta = 118.866 - 0.57966\ Temp - 0.0380024\ Mw - 19.5956\ wt\ \% + 0.000303161\ Temp*Mw + 0.109587\ Temp*wt\% + 0.0016483\ Mw*wt\%$

Glycerol $\eta = 120.043 - 0.57966\ Temp - 0.0380024\ Mw - 19.5956\ wt\ \% + 0.000303161\ Temp*Mw + 0.109587\ Temp*wt\% + 0.0016483\ Mw*wt\%$

D-Sorbitol $\eta = 121.21 - 0.57966\ Temp - 0.0380024\ Mw - 19.5956\ wt\ \% + 0.000303161\ Temp*Mw + 0.109587\ Temp*wt\% + 0.0016483\ Mw*wt\%$

PEG $\eta = 129.877 - 0.57966\ Temp - 0.0380024\ Mw - 19.5956\ wt\ \% + 0.000303161\ Temp*Mw + 0.109587\ Temp*wt\% + 0.0016483\ Mw*wt\%$

Summary of Model

S = 15.2417 R-Sq = 62.75% **R-Sq(adj) = 57.59%**

PRESS = 20764.9 R-Sq(pred) = 48.78%

Analysis of Variance

Source	DF	Seq SS	Adj SS	Adj MS	F	P
Regression	9	25438.6	25438.6	2826.51	12.1670	0.000000
Temp	1	234.1	150.2	150.19	0.6465	0.424287
Mw	1	10913.3	11.1	11.14	0.0479	0.827376
PZ	3	2804.6	1444.0	481.33	2.0720	0.112520
wt %	1	8691.4	1102.3	1102.33	4.7451	0.033015
Temp*Mw	1	9.8	24.4	24.42	0.1051	0.746835
Temp*wt%	1	1182.2	1182.2	1182.17	5.0888	0.027453
Mw*wt%	1	1603.1	1603.1	1603.14	6.9009	0.010734
Error	65	15100.1	15100.1	232.31		
Total	74	40538.7				

The adequacy of the models can be assessed with a probability plot, which is a graphical method for determining whether sample data conformed to a hypothesized distribution based on a subjective visual examination of the data. If the hypothesized distribution adequately describes

the data, the plotted points will fall approximately along a straight line. Figures G-1, 2, and 3 show the normal probability plots of our models. In this case the standardized residuals fall within the straight lines, therefore no serious deviations from normality are observed within the models.

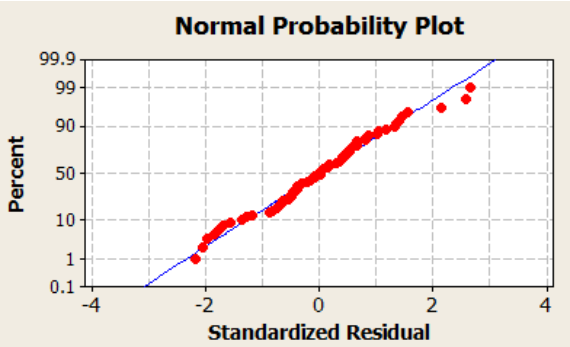

Figure G- 1: Young's moduli normal probability plot.

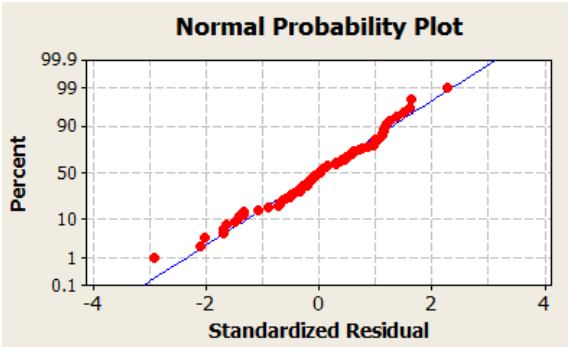

Figure G-2: Melting peak temperature normal probability plot.

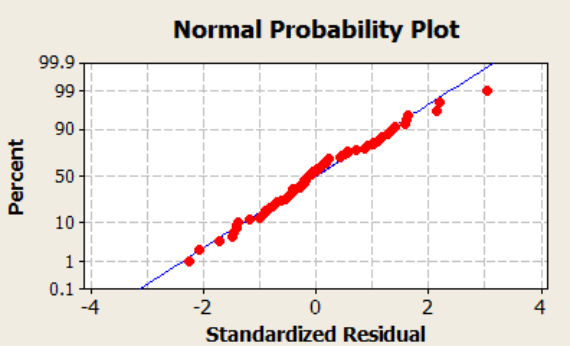

Figure G- 3: Viscosity normal probability plot.

It is known that adding unimportant variables to a model can actually increase the error mean square, indicating that adding such a variable has actually made the model a poorer fit to the data. In order to determine the potential value of each of the regressor variables in the regression model the following test statistic can be employed;

H_0: $\beta_j = 0$

H_1: $\beta_j \neq 0$

If the P-value is $>$ 0.05 the variable does not contribute to the model, if H_0 is not rejected, this indicates that the regressor x_j can be deleted from the model. This does not necessarily imply that the relationship found is an appropriate model for predicting y as a function of x but it provides a good estimate.

Another statistic that can be used to assess the fit of the model is the R^2 value. The R^2 accounts for the variability in the y response. From all the R^2's provided by Minitab 16 only the R^2 adjusted will increase when a variable is added to the model if the new variable reduces the error mean square. Thus, it is useful for variable selection and prevent overfitting (including regressors that are not useful). The model that maximizes R^2_{adj} is considered a good candidate for the best regression equation and it also minimizes the mean square error, so this is a very attractive criterion. In the same manner models with small values of Prediction Error Sum of Squares (PRESS) are preferred. PRESS provides a measure of how well the model is likely to perform when predicting a new data. Therefore all this criteria was use to evaluate the initial models obtained including all the variables and their interactions. After applying the criterions described above the best models obtained are the following:

Young's moduli

Regressors that initially showed no contribution to the model were processing temperature, drug concentration and the interaction between temperature and drug concentration. It was observed that only when the interaction between processing temperature and drug concentration was eliminated a model with increased R^2_{adj} and decreased PRESS is obtained, as desired. In the new model all the regressors make a contribution to the model and it accounts for 40% of the variability in young's moduli response.

PZ

None $E = 124.249 - 0.5366\ Temp - 0.192794\ Mw - 0.529774\ wt\ \% + 0.000879703\ Mw*wt\% + 0.000965708\ Temp*Mw$

Glycerol $E = 127.667 - 0.5366\ Temp - 0.192794\ Mw - 0.529774\ wt\ \% + 0.000879703\ Mw*wt\% + 0.000965708\ Temp*Mw$

D-Sorbitol $E = 133.279 - 0.5366\ Temp - 0.192794\ Mw - 0.529774\ wt\ \% + 0.000879703\ Mw*wt\% + 0.000965708\ Temp*Mw$

PEG $E = 135.077 - 0.5366\ Temp - 0.192794\ Mw - 0.529774\ wt\ \% + 0.000879703\ Mw*wt\% + 0.000965708\ Temp*Mw$

Summary of Model

S = 6.77842 R-Sq = 40.29% **R-Sq(adj) = 33.05%**

PRESS = 3801.82 R-Sq(pred) = 25.14%

Analysis of Variance

Source	DF	Seq SS	Adj SS	Adj MS	F	P
Regression	8	2046.29	2046.29	255.786	5.56698	0.0000217
Temp	1	25.38	197.31	197.306	4.29419	0.0421532
Mw	1	458.29	286.63	286.626	6.23819	0.0150032

wt %	1	11.84	424.68	424.680	9.24281	0.0033880
Mw*wt%	1	427.63	456.64	456.636	9.93830	0.0024354
PZ	3	875.40	875.40	291.799	6.35076	0.0007546
Temp*Mw	1	247.75	247.75	247.748	5.39204	0.0233238
Error	66	3032.50	3032.50	45.947		
Total	74	5078.79				

Melting peak temperature

In this case none of the variables seemed to make a contribution to the model, even though that the normal probability plot showed no deviation from normality of the standardized residuals. The best R^2_{adj} and PRESS values were obtained when the regressors for the interactions were eliminated from the model. Final model shows dependence to molecular weight of the polymer and drug concentration. The best model obtained accounts for only 23% of the variability in melting peak temperature of the solid dispersions.

PZ

None $T_{mp} = 45.7413 + 0.616667\ Temp + 0.0117525\ Mw - 0.768889\ wt\ \%$

Glycerol $T_{mp} = 58.2607 + 0.616667\ Temp + 0.0117525\ Mw - 0.768889\ wt\ \%$

D-Sorbitol $T_{mp} = 61.7607 + 0.616667\ Temp + 0.0117525\ Mw - 0.768889\ wt\ \%$

PEG $T_{mp} = 58.2191 + 0.616667\ Temp + 0.0117525\ Mw - 0.768889\ wt\ \%$

Summary of Model

S = 15.1875 R-Sq = 23.16% **R-Sq(adj) = 16.38%**

PRESS = 18868.8 R-Sq(pred) = 7.56%

Analysis of Variance

Source	DF	Seq SS	Adj SS	Adj MS	F	P
Regression	6	4726.7	4726.7	787.78	3.4153	0.005260
Temp	1	593.9	684.5	684.50	2.9676	0.089495
Mw	1	1473.1	1473.1	1473.05	6.3863	0.013831
PZ	3	331.9	689.6	229.85	0.9965	0.399873
wt %	1	2327.8	2327.8	2327.81	10.0920	0.002240

Error	68	15684.9	15684.9	230.66
Total	74	20411.5		

Viscosity

The regressors that didn't contributed to the initial viscosity model were: processing temperature, molecular weight, type of plasticizer and the interaction between molecular weight and processing temperature. When eliminating the regressors for type of plasticizer and the interaction of processing temperature and molecular weight from the model, the R^2_{adj} decreases by approximately 1% but on the other hand PRESS decreased as well. In this case it is not clear what model would be a better fit for viscosity. The models account for an average of 61% of the variability in viscosity, therefore this empirical model could be used for the approximation of viscosity under the range of conditions used in this work.

Regression Equation

$$\eta = 110.694 - 0.511852\,Temp + 0.0182202\,Mw - 20.56\,wt\,\% + 0.11497\,Temp*wt\% + 0.00163912\,Mw*wt\%$$

Summary of Model

S = 15.4959 R-Sq = 59.13% **R-Sq(adj) = 56.17%**

PRESS = 19824.2 R-Sq(pred) = 51.10%

Analysis of Variance

Source	DF	Seq SS	Adj SS	Adj MS	F	P
Regression	5	23970.2	23970.2	4794.03	19.9649	0.000000
Temp	1	234.1	214.4	214.36	0.8927	0.348044
Mw	1	10913.3	1557.8	1557.83	6.4876	0.013096
wt %	1	9866.6	1271.9	1271.92	5.2969	0.024388
Temp*wt%	1	1367.6	1367.6	1367.64	5.6956	0.019755
Mw*wt%	1	1588.6	1588.6	1588.56	6.6156	0.012265
Error	69	16568.5	16568.5	240.12		
Lack-of-Fit	18	5726.7	5726.7	318.15	1.4966	0.130370
Pure Error	51	10841.8	10841.8	212.58		
Total	74	40538.7				

Appendix H: Results Summary

Table H- 1: Additive effect in Young's moduli.

Plasticizer / GF wt %	HPC 100 kDa				HPC 370 kDa				HPC 1,000 kDa			
	0	*5*	*10*	*20*	*0*	*5*	*10*	*20*	*0*	*5*	*10*	*20*
Glycerol	+	-	-	-	+	-	+	-	+	=	=	=
D-sorbitol	+	+	-	-	+	+	-	=	+	=	=	+
PEG	+	-	-	+	+	-	+	-	-	+	=	=

Table H- 2: Additive effect in melting peak temperature.

Plasticizer / GF wt %	HPC 100 kDa				HPC 370 kDa				HPC 1,000 kDa			
	0	*5*	*10*	*20*	*0*	*5*	*10*	*20*	*0*	*5*	*10*	*20*
Glycerol	+	+	-	-	-	+	-	-	=	+	-	-
D-sorbitol	+	+	-	-	-	+	-	-	-	+	-	-
PEG	+	-	-	+	+	-	-	-	+	-	-	-

Table H- 3: Additive effect in viscosity.

Plasticizer / GF wt %	HPC 100 kDa				HPC 370 kDa				HPC 1,000 kDa			
	0	*5*	*10*	*20*	*0*	*5*	*10*	*20*	*0*	*5*	*10*	*20*
Glycerol	+	+	+	+	-	+	+	+	+	+	+	+
D-sorbitol	+	+	+	+	-	+	+	+	-	+	+	+
PEG	+	+	+	+	+	+	+	+	+	+	+	+

*Effect at 5, 10 and 20 wt% griseofulvin is a comparison with the previous sample (not with the HPC film with no additive).

REFERENCES

[1] G. P. Andrews and D. Jones, "Hot-melt extrusion: an emerging drug delivery technology," *Pharmaceutical Technology Europe*, vol. 21, no. 1, 2009.

[2] M. M. Crowley, F. Zhang, M. A. Repka, S. Thumma, S. B. Upadhye, S. Kumar Battu, J. W. McGinity, and C. Martin, "Pharmaceutical Applications of Hot-Melt Extrusion: Part I," *Drug Development and Industrial Pharmacy*, vol. 33, no. 9, pp. 909–926, 2007.

[3] R. J. Chokshi, H. K. Sandhu, R. M. Iyer, N. H. Shah, A. W. Malick, and H. Zia, "Characterization of physico-mechanical properties of indomethacin and polymers to assess their suitability for hot-melt extrusion process as a means to manufacture solid dispersion/solution.," *J. Pharm. Sci*, vol. 94, pp. 2463–2474.

[4] M. A. Repka and J. W. McGinity, "Physical-mechanical, moisture absorption and bioadhesive properties of hydroxypropylcellulose hot-melt extruded films," *Biomaterials*, vol. 21, no. 14, pp. 1509–1517, 2000.

[5] Y. Rane, R. Mashru, M. Sankalia, and J. Sankalia, "Effect of Hydrophilic Swellable Polymers on Dissolution Enhancement of Carbamazepine Solid Dispersions Studied Using Response Surface Methodology," *PharmSciTech*, vol. 8 (2) Article 27, 2007.

[6] L. Mapelli, J.-W. Lai, L. Boltri, G. Venkatesh, F. Flabiani, and I. Colombo, "Drug Delivery Systems Comprising Solid Solutions of Weakly Basic Drugs," U.S. Patent 2008006987820-Mar-2008.

[7] A. Funke, T. Wagner, and R. Lipp, "Stabilised supersaturated solid solutions of steroidal drugs," U.S. Patent 20878832009.

[8] F. A. Maulvi, S. J. Dalwadi, V. T. Thakkar, T. G. Soni, M. C. Gohel, and T. R. Gandhi, "Improvement of dissolution rate of aceclofenac by solid dispersion technique," *Powder Technology*, vol. 207, no. 1–3, pp. 47–54, 2011.

[9] X. Liu and S. Tallavajhala, "Solid state solutions and dispersions of poorly water soluble drugs," U.S. Patent 99642903-May-2000.

[10] E. Mehuys, C. Vervaet, and J. P. Remon, "Hot-melt extruded ethylcellulose cylinders containing a HPMC-Gelucire® core for sustained drug delivery," *Journal of Controlled Release*, vol. 94, no. 2–3, pp. 273–280, 2004.

[11] J. Knoblauch and I. Zimmermann, "Studies of Dispersions of (2S,6R)-7-Chloro-2,4,6-trimethoxy- 6-methyl-3H, 4H-spiro[1-benzofuran-2,1-cyclohex[2]ene]-3, 4-dione in Poly(ethane-1,2-diol)," *Journal of Chemical and Engineering Data*, vol. 55, no. 3, pp. 1300–1309, 2010.

[12] X. Zhou and Z. Li, "Characterizing rheology of fresh short fiber reinforced cementitious composite through capillary extrusion," *Journal of Materials in Civil Engineering*, vol. 17, no. 1, pp. 28–35, 2005.

[13] R. Dangtungee, J. Yun, and P. Supaphol, "Melt rheology and extrudate swell of calcium carbonate nanoparticle-filled isotactic polypropylene," *Polymer Testing*, vol. 24, no. 1, pp. 2–11, 2005.

[14] C. Rauwendaal, *Polymer Extrusion*, 4th ed. Hanser Gardner Publications.

[15] J. M. Dealy and R. G. Larson, *Structure and Rheology of Molten Polymers*. Cincinnati: Hanser Gardner Publications.

[16] F. A. Morrison, *Understanding Rheology*, vol. 1. New York: Oxford University Press.

[17] R. O'Connell, H. Hanson, and G. D. J. Phillies, "Neutral polymer slow mode and its rheological correlate," *J. Polym. Sci. B Polym. Phys.*, vol. 43, no. 3, pp. 323–333, 2005.

[18] A. Paradkar, A. Kelly, P. Coates, and P. York, "Shear and extensional rheology of hydroxypropyl cellulose melt using capillary rheometry," *Journal of Pharmaceutical and Biomedical Analysis*, vol. 49, no. 2, pp. 304–310, Feb. 2009.

[19] M. A. Repka and J. W. McGinity, "Influence of Vitamin E TGPS on the properties of hydrophilic films produced by hot-melt extrusion," *International Journal of Pharmaceutics*, no. 202, pp. 63–70, 2000.

[20] J. McGinity and F. Zhang, "Hot-melt extrudable pharmaceutical formulation," U.S. Patent 101494101-Apr-2009.

[21] P. K. Mididoddi and M. A. Repka, "Characterization of hot-melt extruded drug delivery systems for onychomycosis," *European Journal of Pharmaceutics and Biopharmaceutics*, vol. 66, no. 1, pp. 95–105, Apr. 2007.

[22] M. A. Repka, K. Gutta, S. Prodduturi, M. Munjal, and S. P. Stodghill, "Characterization of cellulosic hot-melt extruded films containing lidocaine," *European Journal of Pharmaceutics and Biopharmaceutics*, vol. 59, no. 1, pp. 189–196, Jan. 2005.

[23] M. M. Crowley, F. Zhang, J. J. Koleng, and J. W. McGinity, "Stability of polyethylene oxide in matrix tablets prepared by hot-melt extrusion," *Biomaterials*, vol. 23, no. 21, pp. 4241–4248, 2002.

[24] S. Radl, T. Tritthart, and J. G. Khinast, "A novel design for hot-melt extrusion pelletizers," *Chemical Engineering Science*, vol. 65, no. 6, pp. 1976–1988, 2010.

[25] W. Michaeli, *Extrusion dies for plastics and rubber design and engineering computations*, 3rd revised ed. Hanser.

[26] M. P. Stevens, *Polymer Chemistry an Intruduction*, Third ed. Oxford University Press.

[27] James E. Mark, *Polymer Data Handbook*. Oxford University Press, 1999.

[28] M. A. Aden, "Mesophase formation and chain rigidity in cellulose and derivatives. 2. (Hydroxypropyl)cellulose in dichloroacetic acid," *Macromolecules*, vol. 17, no. 10, pp. 2010–2015, 1984.

[29] "http://dod.chemnetbase.com." .

[30] Y. Corvis, W. Barzyk, G. Brezesinski, N. Mrabet, M. Badis, S. Hecht, and E. Rogalska, "Interactions of a fungistatic antibiotic, griseofulvin, with phospholipid monolayers used as models of biological membranes," *Langmuir*, vol. 22, no. 18, pp. 7701–7711, 2006.

[31] L. Zhiyi, J. Jingzhi, L. Xuewu, Z. Shunxuan, X. Yuanjing, and W. Jian, "Preparation of griseofulvin microparticles by supercritical fluid expansion depressurization process," *Powder Technology*, vol. 182, no. 3, pp. 459–465, 2008.

[32] R. Thakur and R. B. Gupta, "Rapid expansion of supercritical solution with solid cosolvent (Ress-Sc) process for particle formation: Pharmaceutical nanoparticles," in *05AIChE: 2005 AIChE Annual Meeting and Fall Showcase, October 30, 2005 - November 4, 2005*, Cincinnati, OH, United states, 2005, p. 3251.

[33] H.-W. Leung, "Polyethylene Glycol," in *Encyclopedia of Toxicology (Second Edition)*, New York: Elsevier, 2005, pp. 515–516.

[34] "Physical properties of glycerine and its solution." .

[35] G. Rocha Plácido Moore, S. Maria Martelli, C. Gandolfo, P. José do Amaral Sobral, and J. Borges Laurindo, "Influence of the glycerol concentration on some physical properties of feather keratin films," *Food Hydrocolloids*, vol. 20, no. 7, pp. 975–982, Oct. 2006.

[36] L. H. Cheng, A. A. Karim, and C. C. Seow, "Effects of Water-Glycerol and Water-Sorbitol Interactions on the Physical Properties of Konjac Glucomannan Films," *Journal of Food Science*, vol. 71, no. 2, p. E62–E67, 2006.

[37] I. Mellan, *Handbook of solvents.* New York: Reinhold Pub. Corp., 1957.

[38] J. D. Menczel and R. B. Prime, *Thermal Analysis of Polymers Fundamentals and Applications*. John Wiley & Sons.

[39] N. Espinoza Herrera, "Thermal, Mechanical and Microstructures Properties of Cellulose Derivatives Films: A Comparative Study," *Food biophysics*, vol. 6, no. 1, pp. 106–114, 2011.

[40] M. P. Stevens, *Polymer Chemistry an Introduction*, Third ed. Oxford University Press.

[41] P. F. Popescu, "Dynamics of Semi-Flexible Polymers," *Rowland Institute at Harvard*.

[42] N. Yanagida, “Morphology and mechanical properties of hydroxypropyl cellulose cast films crosslinked in solution,” *Polymer*, vol. 33, no. 5, pp. 996–1005, 1992.

[43] M. Matsuo and N. Yanagida, “Molecular-weight dependence of morphology and mechanical properties of hydroxypropyl cellulose films cast from water,” *Polymer*, vol. 32, no. 14, pp. 2561–2576, 1991.

[44] A. Donald, A. Windle, and S. Hanna, *Liquid Crystalline Polymers*, Second. Cambridge University Press.

[45] W. Weiwei, “Effect of carboxyl on vulcanization and mechanical properties of carboxylated acrylic rubber prepared by 60Co-γ-ray-induced polymerization,” *Journal of applied polymer science*, vol. 102, no. 6, p. 5587–94, 2006.

[46] S. Yano, “Physical properties and structure of organic-inorganic hybrid materials produced by sol-gel process,” *Materials science & engineering. C, Biomimetic materials, sensors and systems*, vol. 6, no. 2–3, pp. 75–90, 1998.

[47] P. C. Painter and M. M. Coleman, *Fundamentals of Polymer Science*, Second. CRC Press.

[48] B. Ghanbarzadeh, A. R. Oromiehie, M. Musavi, Z. E. D-Jomeh, E. R. Rad, and J. Milani, “Effect of plasticizing sugars on rheological and thermal properties of zein resins and mechanical properties of zein films,” *Food Research International*, vol. 39, no. 8, pp. 882–890, 2006.

[49] M. H. Gutierrez-Villarreal and J. Rodriguez-Velazquez, “The effect of citrate esters as plasticizers on the thermal and mechanical properties of poly(methyl methacrylate),” *Journal of Applied Polymer Science*, vol. 105, no. 4, pp. 2370–2375, 2007.

[50] R. C. Rowe, “Microindentation - a method for measuring the elastic properties and hardness of films on conventionally coated tablets,” *Journal of Pharmacy and Pharmacology*, vol. 28, no. 4, pp. 310–311, 1976.

[51] A. Jha, B. Dutta, and A. K. Bhowmick, “Effect of fillers and plasticizers on the performance of novel heat and oil-resistant thermoplastic elastomers from nylon-6 and acrylate rubber blends,” *Journal of Applied Polymer Science*, vol. 74, no. 6, pp. 1490–1501, 1999.

[52] Y. Zvonkova, V. Zvonkov, and M. Kerber, “On the reasons for extrema in the mechanical properties of amorphous polycarbonate-plasticizer systems,” *Polymer Science U.S.S.R.*, vol. 27, no. 3, pp. 666–677, 1985.

[53] B. Saša, P. Odon, S. Stane, and K. Julijana, “Analysis of surface properties of cellulose ethers and drug release from their matrix tablets,” *European Journal of Pharmaceutical Sciences*, vol. 27, no. 4, pp. 375–383, Mar. 2006.

[54] J.-Z. Liang, “Melt Rheology during Extrusion of Polypropylene Composites Filled with Diatomite Particles.,” *Journal of thermoplastic composite materials*, vol. 23, no. 2, p. 265, 2010.

[55] Hughes, A. J, “The Einstein relation between relative viscosity and volume concentration of suspensions of spheres,” *Nature*, vol. 173, no. 4414, pp. 1089–1090, 1954.

[56] T. Kaully, A. Siegmann, and D. Shacham, “Rheology of highly filled natural CaCO3 composites. II. Effects of solid loading and particle size distribution on rotational rheometry,” *Polym Compos*, vol. 28, no. 4, pp. 524–533, 2007.

[57] D. W. van Krevelen and K. te Nijenhuis, *Properties of Polymers*, Fourth ed. Oxford University Press.

[58] D. J. Greenhalgh, “Solubility parameters as predictors of miscibility in solid dispersions,” *Journal of pharmaceutical sciences*, vol. 88, no. 11, pp. 1182–1190, 1999.

[59] J. Barra, “Influence of surface free energies and cohesion parameters on pharmaceutical material interaction parameters-theoretical simulations,” *Pharmaceutical research*, vol. 13, no. 11, pp. 1746–1751, 1996.